Vol. 121 Nos. 1-6

July-August 1958

PROCEEDINGS OF THE ACADEMY OF SCIENCES

OF THE USSR

(DOKLADY AKADEMII NAUK SSSR)

Physical Chemistry Section

A publication of the Academy of Sciences of the USSR

IN ENGLISH TRANSLATION

Year and issue of first translation:
Vol. 112, Nos. 1-6 Jan.-Feb. 1957

Annual subscription	*$160.00*
Single issue	*35.00*

Copyright 1959

CONSULTANTS BUREAU INC.
227 W. 17th ST., NEW YORK 11, N. Y.

A complete copy of any paper in this issue may be purchased from the publisher for $5.00

Note: The sale of photostatic copies of any portion of this copyright translation is expressly prohibited by the copyright owners.

Printed in the United States of America

PROCEEDINGS OF THE ACADEMY OF SCIENCES OF THE USSR

Volume 121, Numbers 1-6 July-August 1958

CONTENTS

	PAGE	ISSUE	RUSS. PAGE
Spectral Study of Dye Interactions in Solution. Kh. L. Arvan	485	1	123
Electrochemical Behavior of Zirconium in Sulfuric Acid. N. A. Balashova and B. N. Kabanov	489	1	126
On the Adsorption of Cs^+ Ion at the Surface of Mercury Electrode. B. B. Damaskin, N. V. Nikolaieva-Fedorovich and A. N. Frumkin	493	1	129
On the Photographic Activity of Gelatin. A. L. Karpova, A. A. Mikhailova, and K. B. Chibisov	497	1	133
Wetting Heats of Etherified Cellulose. E. F. Nekriach and A. V. Dumanskii	501	1	136
Optical Sensitization of the Photoeffect in Silver and Thallium Bromides by Organic Dyes. I. A. Akimov	503	2	311
Influence of the Structure of Organic Molecules on the Probability of Transition to a Metastable State. V. V. Zelinskii, V. P. Kolobkov and I. I. Reznikova	507	2	315
The Influence of the Intensity of the Radiation from S^{35} on the Rate of Isotopic Exchange of Sulfur in the System K_2SO_4-SO_3. Vikt. I. Spitsyn and I. E. Mikhailenko	511	2	319
The Influence of Cation Radius on the Properties of the Boundary Layers of Electrolyte Solutions in the Flat Areas Between Quartz Surfaces. G. I. Fuks and N. I. Kaverina	515	2	322
An Investigation of the Structures of Liquid Bi–Sn Alloys. N. V. Alekseev and Ia. I. Gerasimov	521	3	488
The Action of the γ-Radiation of Co^{60} on $Ca(NO_3)_2 \cdot 4H_2O$. A. S. Baberkin and M. A. Proskurnin	527	3	492
Radioactive Catalysts. The Dehydration of Cyclohexanol on Magnesium and Sodium Sulfates. A. A. Balandin, Vikt. I. Spitsyn, N. P. Dobrosel'skaia and I. E. Mikhailenko	531	3	495
A Spectroscopic Study of the Adsorption and Catalytic Reaction of Cyclohexadiene on Transparent Films of Palladium. V. M. Griaznov, V. D. Iagodovskii, A. M. Bogomol'nyi and Huo Tiu-ok	535	3	499
The Diffusional Electrical Potential of a Falling Droplet with an Adsorbed Layer. S. S. Dukhin and B. V. Deriagin	539	3	503
Two Types of Manganese Luminescence Centers in the Cadmium–Lithium Orthosilicate Phase. V. V. Osiko	545	3	507
Formal Kinetic Laws for the Thermal Decomposition of Explosives in the Liquid Phase. F. I. Dubovitskii, G. B. Manelis and A. G. Merzhanov	549	4	668

CONTENTS (continued)

	PAGE	RUSS. ISSUE	RUSS. PAGE
The Use of Water as a Sensitizer for the Radiation Initiation of the Oxidation of Benzene. M. A. Proskurnin, E. V. Barelko and L. I. Kartasheva	553	4	671
The Catalytic Synthesis of Unsaturated Hydrocarbons of the C^4 Series Labeled with Radioactive Carbon C^{14}, Using Vapor-Phase Distribution Radiochromatography. G. M. Zhabrova, O. M. Vinogradova, B. M. Kadenatsi and Z. A. Markova	557	4	674
The Equation for Isothermal Diffusion in the Critical Region. L. A. Rott	561	4	678
The Coefficients for the Equilibrium Distribution of Deuterium in the Isotopic Exchange Between Water and Certain Thiols. K. I. Sakodynskii, S. I. Babkov and N. M. Zhavoronkov	565	4	681
Equilibrium Potentials of Titanium in Chloride Melts. M. V. Smirnov, L. E. Ivanovskii and N. A. Loginov	569	4	685
The Kinetic Isotopic Effect in the Reaction of Hydrogen and Tritium with the Oxides of Certain Metals. V. A. Shushunov and B. Ia. Andreev	573	4	689
The Electrochemical Properties and Corrosion Behavior of Titanium in Sulfuric Acid Solutions. V. V. Andreeva and V. I. Kazarin	577	5	873
The Electron Theory of the Adhesion of Metals Which are Joined by a Semiconducting Film. B. V. Deriagin and V. P. Smilga	581	5	877
Concerning Calculations on Electrochemical Reactions with an Intermediate Reagent. M. A. Loshkarev and I. P. Chernobaev	587	5	881
The Anodic Protection of Titanium in Sulfuric Acid. N. D. Tomashov, R. M. Al'tovskii and A. G. Arakelov.	593	5	885
The Rate of Absorption of Ethylene and Propylene by Sulfuric Acid of Different Concentrations. G. V. Korovina, S. G. Entelis and N. M. Chirkov	597	6	1038
The Influence of Pressure on the Solubility of Molecular Hydrogen in Niobium and Tantalum. P. S. Perminov	601	6	1041
A Contribution to the Theory of the Temperature Dependence of the Coordination Numbers of Ions in Aqueous Solutions. O. Ia. Samoilov	603	6	1043
A Contribution to the Diffusion Theory of the Kinetics of Bimolecular Reactions in Solution. B. Ia. Sveshnikov and L. A. Kuznetsova	607	6	1045
The Dipole Moments of the Hemioxanines of the Derivatives of 3-Ethylrhodanine and 1,3-Indandione. E. A. Shott-L'vova, Ia. K. Syrkin, I. I. Levkoev and M. V. Deichmeister	611	6	1048

SPECTRAL STUDY OF DYE INTERACTIONS IN SOLUTION

Kh. L. Arvan

(Presented by Academician A. N. Terenin, March 3, 1958)

It is known that in solutions of many dyes an aggregation and partial dimerization process takes place. This results in the union of two or more ions. One of the most sensitive methods of detecting this process is spectroscopic, and is based on the fact that a change in the state of the dye in solution is accompanied by a change in the absorption spectrum.

Studying the absorption spectra of solutions containing two diazo dyes, Lemin and Vickerstaff [1], as well as Derbyshire and Peters [2], were able to establish that bimolecular compounds, made up of both dyes, are probably formed.

A similar phenomenon was observed by us in solutions containing a mixture of thiazine and acridine group dyes. The thiazine dyes studied were thionin, methylene blue, and toluidine blue. The acridine dyes were trypaflavine, acridine yellow, rhoduline orange, and also unsubstituted acridine (as the hydrochloride). Measurements were conducted on a SF-4 spectrophotometer.

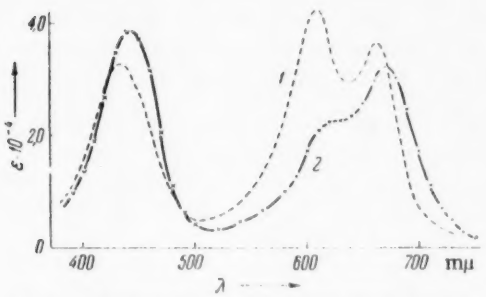

Fig. 1. Absorption of a methylene blue ($C = 2.8 \cdot 10^{-4}$ moles/liter) and acridine yellow ($C = 2.8 \cdot 10^{-4}$ moles/liter) mixture in aqueous solution. 1) Curve calculated on the basis of additive absorptions; 2) measured absorption of the mixture.

In Fig. 1 are given the absorption spectra of two dyes (methylene blue and acridine yellow) in aqueous solution. Curve 1 is calculated assuming that the absorptions of the two dyes are additive; Curve 2 represents the experimentally determined absorptions of the mixture. As is apparent from the figure, the dye interaction produces a change in the shape of the curve and a shift in the absorption band of each dye toward a longer wavelength. This can best be explained by a change in each spectrum resulting from their binding, and also a change in the state of aggregation of each dye. To eliminate the latter case we studied the effects of various quantities of acridine yellow on solutions of methylene blue; these were made dilute enough to make the concentration of homogeneous dimers small (see Fig. 2).

The presence of a common intersection point among some curves indicates that the absorption in that region of the spectrum is determined only by two kinds of absorbing centers – methylene blue and methylene blue bound to acridine yellow.

On the basis of the law of mass action we calculated the share of methylene blue bound with acridine yellow and its derivatives (α) at varying concentrations of the latter in solution, as well as absorption curves for methylene blue completely bound with those dyes (dotted curve in Fig. 2). • Similar data were obtained for thionin and toluidine blue bound with acridine yellow.

•Calculations were done using a method analogous to the one used previously for the case of homogeneous dimerization of methylene blue [3].

The dissociation constants for these complexes were calculated according to the formula:

$$K = \frac{[(1-\alpha)C_{syn}][\alpha_{acr}C_{acr} - \alpha \cdot C_{syn}]}{[\alpha C_{syn}]}$$

where C_{syn} is the concentration of the thiazine dye, C_{acr} the concentration of the acridine dye, $1-\alpha$ is the fraction of free thiazine dye, α_{acr} fraction of monomeric acridine dye (this factor is introduced to calculate the independent aggregation of acridine dye). The results of these calculations are listed in Table 1.•

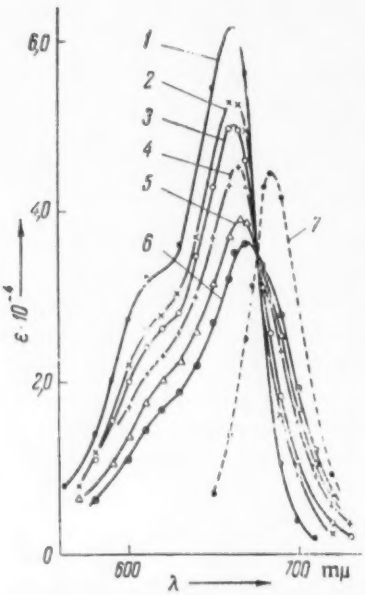

Fig. 2. The effect of various quantities of acridine yellow on the absorption of methylene blue ($C = 1.41 \cdot 11^{-5}$ moles/liter) in aqueous solutions. 1) Methylene blue without acridine yellow; 2) with acridine yellow ($C = 1.78 \cdot 10^{-5}$ moles/liter); 3) with acridine yellow ($C = 3.55 \cdot 10^{-5}$ moles/liter); 4) with acridine yellow ($C = 7.1 \cdot 10^{-5}$ moles/liter); 5) with acridine yellow ($C = 1.42 \cdot 10^{-4}$ moles/liter); 6) with acridine yellow ($C = 2.84 \cdot 10^{-4}$ moles/liter); 7) methylene blue completely bound to acridine yellow.

According to our data, the increase in independent aggregation in the acridine group proceeds in the order: acridine–trypaflavine–acridine yellow–rhoduline orange; in the thiazine group: thionin–methylene blue–toluidine blue. Thus it appears that the binding activity of two dyes with each other is directly proportional to their tendency to form homogeneous dimers. Only rhoduline orange constitutes an exception; its ability to form homogeneous aggregates is greater than that of the remaining acridine dyes; however, the ability to complex with methylene blue is approximately the same as that of acridine orange.

The investigation on the effect of solvent, temperature, and length of time during which the solutions were preserved showed that the properties of these complexes are analogous to those of common dimers:

1) As with dimers, heterogeneous complexes arise mainly in aqueous solutions. In organic solvents complex formation was only observed at lower temperatures.

2) Both are decomposed when temperature is raised. Warming also decreases the deviation of the actual absorption curve from that of the calculated one.

3) Complex formation, as with homogeneous aggregates (by increasing the concentration or introducing an electrolyte into solution), somehow stabilizes the absorption magnitude of dilute solutions which have a tendency to decolorize [4].

As was already pointed out, the absorption curve of each of the interacting dyes undergoes a change in shape along with a shift (Fig. 1). The presence of a second dye causes a decrease in the relative size of the adjoining short wavelength maximum, which indicates a decrease in the quantity of the dimer in solution. It shows that the complex formation is accompanied by a weakening of the state of aggregation among the individual interacting dyes. Maximum disaggregation was observed, of course, under the action of the most active (in the binding sense) second component. Thus, the effect of acridine is much smaller in this respect, than that of its derivatives.

We calculated the complex-formation energy before starting the temperature-dependence study of the process. For the union of methylene blue with acridine yellow it came out to approximately 9 kcal/mole. It exceeds the homogeneous dimerization energy of methylene blue by one and a half times,•• which is in full accord with the fact that homogeneous dimers are decomposed during complex formation.

•The values calculated for α, K, and the absorption curves will be slightly inexact as the original solution of methylene blue contains some quantity of homogeneous dimers. Work with even more dilute solutions is made difficult because of fast discoloration [4].

••Dimerization energy of methylene blue amounts to 6 kcal/mole. The difference between this figure and that given by us previously [3], is due to a refinement in our calculations.

TABLE 1

Dissociation Constants of Two-Dye Complexes

Acridine dye	Thiazine dye		
	thionin	methylene blue	toluidine blue
Acridine	–	$11.8 \cdot 10^{-4}$	–
Trypaflavine	–	$1.4 \cdot 10^{-4}$	–
Acridine yellow	$1.2 \cdot 10^{-4}$	$0.8 \cdot 10^{-4}$	$0.4 \cdot 10^{-4}$
Rhoduline orange	–	$0.8 \cdot 10^{-4}$	–

LITERATURE CITED

[1] D. K. Lemin and T. Vickerstaff, Trans. Farad. Soc. 43, 491 (1947).

[2] A. N. Derbyshire and R. H. Peters, J. Soc. Dyers and Colour, 72, 268 (1956).

[3] L. Pes'kina and E. V. Zhidkova, Bull. Acad. Sci. USSR, phys. series, 14, 493 (1950).

[4] Kh. L. Arvan, Collected papers: Some Problems in the Synthesis and Application of Dyestuffs, Leningrad, 1956, p. 127.

Received March 4, 1958

ELECTROCHEMICAL BEHAVIOR OF ZIRCONIUM IN SULFURIC ACID

N. A. Balashova and B. N. Kabanov

(Presented by Academician A. N. Frumkin, March 11, 1958)

The scant literature data available at the present time points to a strong dependence of the electrochemical behavior of zirconium on solvent composition. According to chemical literature, zirconium is extremely inert towards hydrochloric acid, sodium chloride, and alkaline solutions [1]. The investigation of anodic solubility of zirconium in nitric acid showed that it becomes passive in this solution, while the properties of the oxide coating that is formed (consisting of monoclinic ZrO_2) depend on the solution concentration [2]. In neutral solutions of sodium chloride [3], zirconium does not become passive on anodic polarization – on the contrary, its complete decomposition was observed. The H_2 overvoltage curve has two crests, the upper of which (current density $3 \cdot 10^{-4} - 10^{-5}$ amps/cm^2) is explained by oxygen ionization. In a neutral sodium sulfate solution zirconium becomes slightly passive on anodic polarization (current density $10^{-4} - 10^{-5}$ amps/cm^2).

In the present work the cathodic and anodic behavior of zirconium was studied, as well as the change in its potential in 1 N H_2SO_4 solution at 25° with time, in the absence of current.

Experiments were conducted with a 99.9% pure zirconium rod in a hermetically sealed glass apparatus. Before each experiment the electrode was cleaned with moist quartz powder; after a quick rinsing with twice-distilled water it was lowered into solution, while the solution was constantly stirred with nitrogen passed over a cupric catalyst to remove any hydrogen present. After a constant potential was reached, hydrogen overvoltage on zirconium was measured by starting with a large current density, in order to reduce any soluble oxides that might be present on the surface. The magnitude of the current density was varied every 1-2 minutes in the interval between $1\text{-}3 \cdot 10^{-3}$ and $5\text{-}6 \cdot 10^{-7}$ amp/cm^2, as computed on the observable surface. After a potential close to the stationary was reached, anodic polarization would immediately set in and curves were plotted in the same fashion, first with the increase in current density, later with decrease. After this, curves for the hydrogen overvoltage on the anodically oxidized electrode were recorded, going from small current density to large.

Results obtained showed that the oxide film formed on the zirconium surface, after prolonged exposure to air, displaced the stationary potential in the positive direction. Thus, the potential on zirconium exposed for a long time to air and uncleaned before the experiment had a magnitude of -0.17 to -0.19 v (with reference to a standard hydrogen electrode), and -0.2 to -0.3 v on zirconium cleaned in air. In sulfuric acid zirconium potential slowly levels off with time, as shown in Fig. 1.

As shown in the figure, the change in potential is particularly large for an electrode that has long been exposed to the air (Fig. 1, Curve 1); the terminal potential on such an electrode equals 0.12 v, i.e., 0.3 v more positive than the initial value. For an electrode that has been cleaned the change in the positive direction amounts to $0.10 - 0.16$ v (Fig. 1, 3). An electrode oxidized in air, placed in sulfuric acid, and then re-exposed to air, acquires the most positive potential in 1 N H_2SO_4; this potential quickly levels off with time (Fig. 1, 2). The change in the potential of cleaned and uncleaned electrodes with time in 1 N H_2SO_4 in a positive direction indicates that in this solution an oxidation process (passivation) of zirconium takes place.

During cathodic and anodic polarization of zirconium in 1 N H_2SO_4, regularities appear which would indicate a great effect of the oxide film on polarization. In Fig. 2 the curves for anodic and cathodic polarizations of cleaned zirconium are drawn. The deviation between corresponding curves from different experiments attained -0.1 v in the cathode region, and a few tenths of a volt in the region of anodic passivity. An inflection

point on the cathodic curve was observed in the region between −0.6 and −0.2 v. On both sides of the inflection point the hydrogen overvoltage curve obeys Tafel's equation.

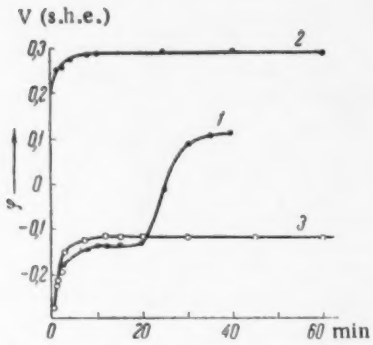

Fig. 1. Change in zirconium potential with time. 1) after exposure to air; 2) after being kept in a sulfuric acid solution; 3) cleaned electrode.

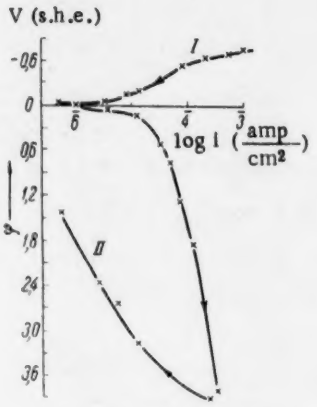

Fig. 2. Cathodic (I) and anodic (II) polarization curves of zirconium in 1 N H_2SO_4.

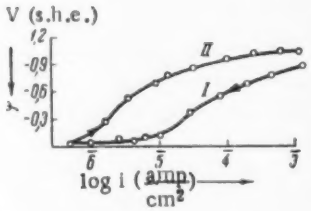

Fig. 3. Hydrogen overvoltage on cleaned (I) and anode-oxidized (II) zirconium.

The inflections, as is well known, were observed on the curves of hydrogen overvoltage on several metals [4], provided the curve was slowly recorded. These inflections are explained by assuming that when the potential goes through a point located slightly to the negative side of the point of zero charge of the metal (zero electrode potential) its adsorption properties change; in the presence of anion adsorption hydrogen overvoltage is lower than in its absence. There is no literature data on the zero point of zirconium. From the work on electron discharge one would expect it to lie close to −1v; therefore the inflection point observed by us probably has to be explained by an approach to zero point strongly displaced in the positive direction due to the action of adsorbed oxygen.

Zirconium becomes strongly passive during anodic polarization in sulfuric acid starting at very low current densities ($1\text{-}2 \cdot 10^{-5}$ amp/cm^2). With current densities in excess of 10^{-4} amp/cm^2, a film was formed with an effective d.c. resistance of the order of tens of ohms (the experiment was conducted using direct current). This film had a golden tinge. A large hysteresis was observed in the reverse direction of the anodic polarization curve. Apparently, as the anodic polarization is decreased, an activation process takes place which is caused by solution of phase oxides of zirconium in sulfuric acid accompanied by a decrease in their rate of formation on the electrode surface; this is analogous to the case of an iron electrode [5]. By extrapolating cathodic and anodic current density curves to less than 10^{-5} amp/cm^2, the value for current produced when zirconium freely dissolves in 1 N H_2SO_4 may be obtained; it is equal to $2 \cdot 10^{-6}$ amp/cm^2.

The oxide film, obtained when zirconium undergoes anodic oxidation, decreases the rate of hydrogen evolution on zirconium. The increase in hydrogen overvoltage caused by an oxide layer on the metallic surface has previously been observed in iron [6], and magnesium [7] only in alkaline solutions. In Fig. 3 hydrogen overvoltage curves are shown for cleaned (Curve 1), and anode-oxidized (Curve 2) zirconium. It is obvious that the rate of hydrogen evolution on the oxidized zirconium is about $^1/_{10}$ as high as on the cleaned one. The inflection point on Curve 2 of the hydrogen overvoltage is also displaced in the direction of lower current density. At high current densities the separation between the curves diminishes, apparently on account of increased rate of oxide solubility and retarded formation.

LITERATURE CITED

[1] A. F. Joffe, J. Metals, No. 7, 6 (1949); E. I. Kerg, J. Appl. Chem. 10, No. 10-11, 1931 (1937); Donald Taylor, Ind. and Eng. Chem. 42, 639 (1950); A. E. Gola and Goldon, Ind. and Eng. Chem. 41, 1668 (1949).

[2] R. D. Heish and W. E. Ratter, J. Electrochem. Soc. 100, No. 12, 531 (1953).

[3] H. Hackerman and B. C. Olin, J. Electrochem. Soc. 101, No. 8, 419 (1954).

[4] Z. Iofa, B. Kabanov, E. Kuchinskii and F. Chistiakov, J. Phys. Chem. 13, 1105 (1939); Ia. M. Kolotyrkin and N. Ia. Bune, J. Phys. Chem. 21, 581 (1947).

[5] K. F. Bonhöffer and U. F. Franck, Zs. Electrochem. 55, 180 (1951).

[6] S. A. Rosentsveig and B. N. Kabanov, J. Phys. Chem. 22, 513 (1948).

[7] E. V. Barelko and B. N. Kabanov, Proc. Acad. Sci. USSR 90, 1059 (1953).

Electrochemical Institute
USSR Academy of Sciences

Received March 7, 1958

ON THE ADSORPTION OF Cs^+ ION AT THE SURFACE OF MERCURY ELECTRODE

B. B. Damaskin, N. V. Nikolaeva - Fedorovich and Academician A. N. Frumkin

In our previous work [1], we described how a superequivalent adsorption of Cs^+ and La^{+++} cations was observed on the surface of a negatively charged mercury electrode. We brought as evidence the change in the differential capacity at the electrocapillary zero (e.z. – point of zero charge) in going from Li^+ to Cs^+, 0.01 N chloride solutions of these metals and also the difference between the potentials at which the separation between capacity values disappears in corresponding 0.1 N solutions of NaCl–NaI and CsCl–CsI. But, as we already noticed, the experimental data was complicated by the specific adsorption of Cl^- and I^- anions, which affects the cation adsorption on the mercury electrode surface. In order to avoid the complications connected with the specific adsorption of the anions, while investigating the super-equivalent adsorption of the cations, we ran the measurements in solutions of sodium and cesium fluorides; according to Grahame's data [2, 3], the F^- anion has no specific adsorption (chemisorption) on mercury.

The experiments were conducted using an impedance bridge, the design of which did not differ in principle from that described in the works of D. G. Grahame [4] and V. I. Melik-Gaikazian [5]. The electrode potentials given in this work are with reference to a normal calomel electrode). The cesium fluoride used was obtained in the following fashion. Decomposition of cesium amalgam in a "fluoroplast"* container gave cesium hydroxide, which was then neutralized with hydrofluoric acid; the acid was previously distilled twice in a palladium apparatus. The solution obtained was depolarized over a mercury cathode in a fluoroplast container, and after evaporation the residual CsF was baked in a platinum crucible. We also utilized a sample of commercial cesium fluoride; after adding twice-distilled hydrofluoric acid to remove CO_3^{2-} ion, we depolarized it in a fluoroplast container and baked-out in a platinum crucible. Under these conditions both samples gave similar results.

We measured the differential capacity on a mercury-drop electrode suspended in NaF and CsF solutions of the following concentrations: 0.9, 0.1 and 0.01 N, and also 0.9 and 0.1 N solutions of sodium and cesium iodides. The data obtained with 0.9 and 0.01 N solutions are reproduced in Figs. 1 and 2. The capacity values measured in NaF solutions are in good agreement with those of D. Grahame [6], with the exception of extreme positive potentials where, unlike D. Grahame, we did not detect any sharp rise in the differential capacity curve even down at $\varphi = +0.25$ v. Such a rise was only observed in solutions kept for a long time in glass containers, and evidently must be connected with solution contamination by traces of surface-active anions. As shown in Fig. 1, the capacity values of an electrical double layer in solutions of cesium fluoride lie higher than the corresponding values for sodium chloride within the interval plotted. In 0.1 N solutions results were obtained that were analogous to those given for 0.9 N NaF and CsF solutions. In the case of the 0.01 N solutions of sodium and cesium fluorides the separation between capacity values remains to a potential of approximately $\varphi = 0.0$. At more positive potentials the capacity values in these solutions become of the same order of magnitude as experimental errors. One can conclude from this data that the cesium cation is adsorbed on the surface of mercury (on which fluoride anion is already adsorbed) to a greater extent than sodium cation, and since the fluoride ion is not adsorbed in superequivalent quantity, i.e., the presence of fluoride ion does not cause overcharge of the mercury surface, and the adsorption of cesium ion cannot be interpreted in any other way except as specific.

It is possible to arrive at the same conclusion about superequivalent adsorption of Cs^+ by comparing corresponding capacity curves for fluorides and iodides and sodium and cesium. Actually, as can be seen in Fig. 1,

*Russian name for "Teflon."

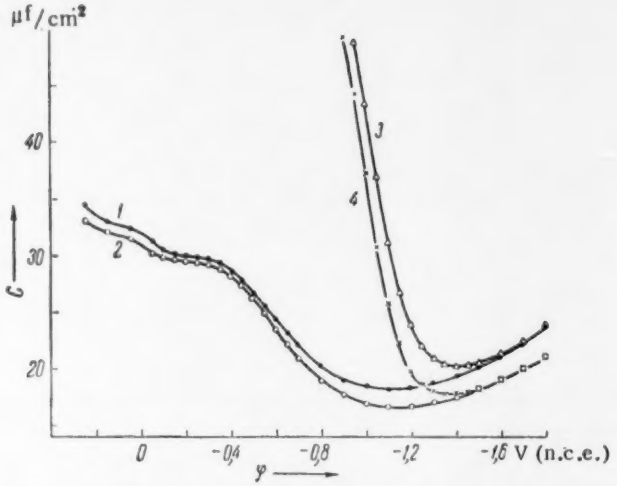

Fig. 1. Differential capacity curves in 0.9 N solutions. 1000 kc, 25 ± 0.1°.
1) CsF; 2) NaF; 3) CsI; 4) NaI.

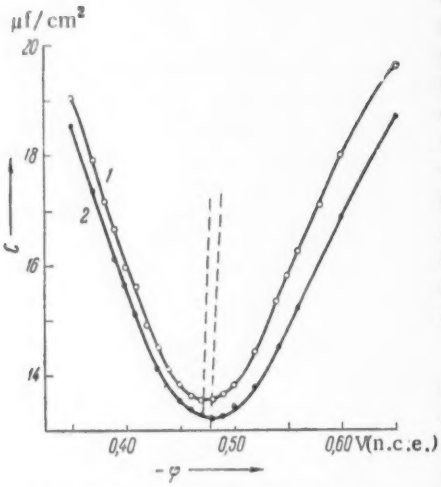

Fig. 2. Differential capacity curves in 0.01 N solutions. 400 kc, 25 ± 0.1°.
1) CsF; 2) NaF.

the iodide ion ceases to have any effect on the capacity at sufficiently negative potentials, and the differential capacity values for corresponding iodides and fluorides converge. However, the potentials at which the capacity curves converge are not identical but depend on the nature of the cation. Within the limits of our experimental errors and accuracy, the action of the iodide ion in 0.9 N solutions of NaF and NaI is evident up to the potential $\varphi = -1.5$ v and in 0.9 N solutions of CsF and CsI up to $\varphi = -1.7$ v; this can only be explained by superequivalent adsorption of cesium, as its adsorption pushes the iodide adsorption towards more negative potentials than does that of sodium cation. Analogous results were obtained for the corresponding 0.1 N solutions of sodium and cesium fluorides and iodides.

The presence of superequivalent adsorption of cesium cation can also be deduced from the magnitudes of the e.z. (point of zero charge) measured by us on an interrupted streaming mercury electrode; the solutions were cleaned by prolonged polarization on a mercury electrode. With the help of Henderson's equation and using ionic mobilities at infinite dilution, we converted the values obtained into diffusion potentials (see Table 1).

As may be seen in Table 1, the fluoride solutions show a small displacement of e.z. in the direction of positive potentials in going from Na^+ to Cs^+, this points out to some superequivalent adsorption of cesium cation.* Displacement of e.z. in going from 0.1 N LiCl solution to 0.1 N CsCl was first observed by D. Grahame in his investigations [7]; however, the presence of specifically adsorbed chloride anions led the author to a different explanation for the observed effect [8]. It must be noted that the location of the e.z. in 0.9 N fluoride solutions depends on the pH of the medium; with increase in the basic strength of solution the e.z. moves towards more negative

*In 0.01 N solutions of NaF and CsF the e.z. values measured on the streaming mercury electrode fall within the range of experimental errors, but the minimum in the conductance curve is displaced 6 mv in the positive direction when going from NaF to CsF (Fig. 2).

TABLE 1

Solution	NaF			CsF			NaI		CsI	
	0,9 *N*	0,1 *N*	0,01 *N*	0,9 *N*	0,1 *N*	0,01 *N*	0,9 *N*	0,1 *N*	0,9 *N*	0,1 *N*
—φe.z.	0,4724	0,4733	0,473	0,4694	0,4723	0,473	0,799	0,726	0,812	0,732
The same according to D. Grahame	0,4716	0,4736	0,4735							

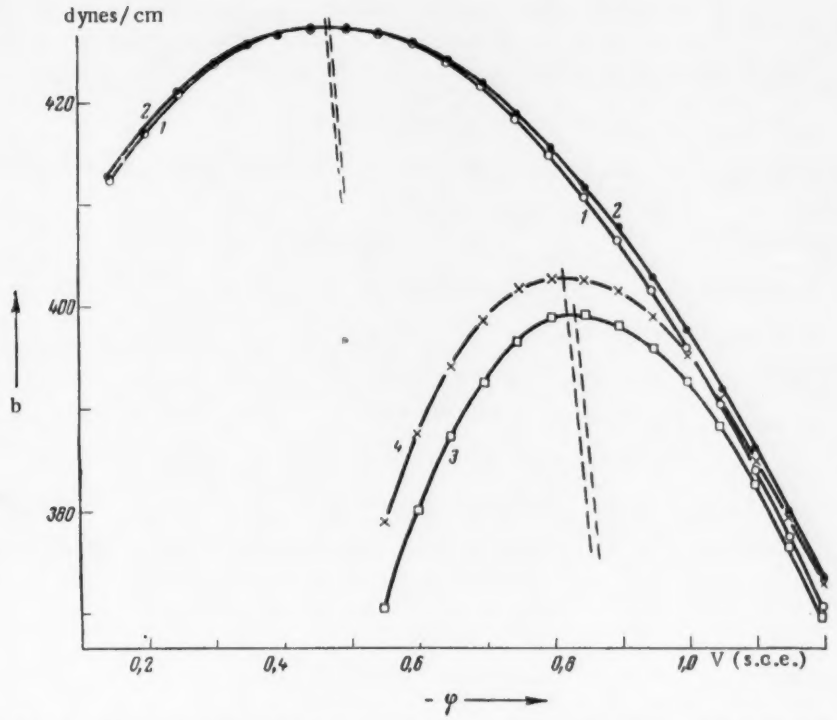

Fig. 3. Mercury interfacial tensions in 0.9 N solutions. 22 ± 0.5°. 1) CsF; 2) NaF; 3) CsI; 4) NaI.

potentials. Thus, in the case of NaF the e.z. falls at the applied potential of −0.4724 v at pH = 7.0; −0.4732 v at pH = 7.5, and −0.4740 v at pH = 8.5. We were unable to elucidate the cause of this phenomenon. The values listed in Table 1 for 0.9 N solutions of NaF and CsF are at pH = 7.0.

In the case where the anion is strongly adsorbed, as it happens in iodide solutions, the resulting cation adsorption gives rise to an additional anion adsorption causing a shift of the e.z. towards more negative potentials in going from NaI to CsI [9].

Electrocapillary measurements in 0.9 N solutions of NaF, NaI, CsF, and CsI, confirmed our results on the superequivalent adsorption of cesium. The final results of these determinations are shown in Fig. 3. As may be seen from the graph, the CsF curve is slightly below that of NaF, while the CsI curve is noticeably lower than that of NaI. The difference between the interfacial tensions of mercury in NaF and CsF solutions amounts to 0.1 dynes/cm at the maximum of the electrocapillary curve and gradually increases with increase in either the positive or negative potential. Thus at $\varphi = -0.145$ v the difference is 0.3 dynes/cm while at $\varphi = -1.195$ v

it already becomes 2.9 dynes/cm. The lowering in the interfacial tension of mercury is caused in this case by the greater adsorption of Cs^+ as compared to Na^+. In the case of the iodide salts the specific adsorption of cesium increases the iodide anion adsorption, and the interfacial tension is lowered to a greater extent. The lowering is particularly large on the rising branch of the electrocapillary curve, on which the mercury surface in the presence of iodide ions by acquiring a negative charge makes the cesium adsorption easier. Thus, at the maximum, the difference for the NaI and CsI solutions reaches the value of 3.4 dynes/cm and increases to 8.0 dynes/ cm at $\varphi = -0.55$ v. It is interesting to compare $\Delta\sigma$ for NaF – NaI and CsF – CsI solutions at some particular, sufficiently negative potential (for example at $\varphi = -1.195$ v). These differences are equal to 0.4 and 0.9 dynes/cm respectively, and their relative magnitudes indicate that since the cesium cation is comparatively more adsorbed than the sodium cation, iodine must be pulled into the electrical double layer. Finally, an important result of the electrocapillary measurements was the detection of a shift in the maximum , from −0.471 v for NaF to −0.468 v for CsF, and from −0.815 v for NaI to −0.833 v for CsI. The results for the fluoride solutions agree well with the data which we obtained in measuring the e.z. by the streaming electrode method. For the iodides, however, the e.z. values obtained using the streaming electrode are slightly more positive than the corresponding electrocapillary maxima; the difference could possibly be connected with an incomplete removal of traces of free iodine from these solutions – iodine acts as a depolarizer; however, the shift in e.z. in going from NaI to CsI appears identical when determined by both methods.

LITERATURE CITED

[1] A. N. Frumkin, B. B. Damaskin and N. V. Nikolaeva-Fedorovich, Proc. Acad. Sci. USSR 115, 751 (1957).

[2] D. C. Grahame and B. A. Soderberg, J. Chem. Phys. 22, 449 (1954).

[3] D. C. Grahame, Zs. Electrochem. 59, 773 (1955).

[4] D. C. Grahame, J. Am. Chem. Soc. 68, 301 (1946).

[5] V. I. Melik-Gaikazian, J. Phys. Chem. 26, 560 (1952).

[6] D. C. Grahame, J. Am. Chem. Soc. 76, 4819 (1954).

[7] D. C. Grahame, J. Electrochem. Soc. 98, 343 (1951).

[8] D. C. Grahame, E. M. Coffin, J. I. Cummings and M. A. Poth, J. Am. Chem. Soc. 74, 1207 (1952).

[9] A. N. Frumkin and V. N. Nikolaeva-Fedorovich, Vestn. MGU, mech., astr., math., phys., chem. series, No. 4, 169 (1957).

Received May 8, 1958

ON THE PHOTOGRAPHIC ACTIVITY OF GELATIN

A. L. Karpova, A. A. Mikhailova and Corresponding Member AN SSSR

K. B. Chibisov

It is known that the source of the photographic activity in gelatin lies in certain contaminating substances which possess an affinity towards silver and interact with the solid phase of the emulsion. Most conclusive evidence for this appears when gelatine binding of Ag^+ is studied, or during experiments on the action of certain ion-exchange resins on gelatin solutions.

Investigation of the silver nitrate–gelatin interaction kinetics leads to the conclusion that three types of substances enter into the composition of the active impurities: substances forming thermally stable silver complexes, compounds with labile sulfur, and reducing agents [1]. The dependence of tied-up Ag^+ on its concentration in solution was studied and revealed [2, 3] that there are two groups of complex-forming substances in gelatin: one is composed of compounds with the greatest affinity towards Ag^+ ions, with which they form thermally stable and irreversible complexes; the second contains compounds with a smaller affinity, forming thermally stable but reversible complexes (possessing solubility products larger than AgI). Center-forming substances present in gelatin (composed of labile sulfur and reducing agents) possess an even smaller affinity towards Ag^+ ions; therefore, it is natural to expect that the rate of the chemical ripening be directly connected with the magnitude of the ratio between the quantities of the first and second type of complex-forming substances (activity coefficient), but not directly related to the composition of the sulfur-containing compounds and reducing agents, see Table 1.

TABLE 1

Nos. of gelatin sample KZhZ	Quantity of impurities (g-equiv · 10^7 per 1 g of gelatin)				Activity coefficient $\frac{a}{k\ b}$	Time needed to achieve S_{max} τ_0 (min)	Constant quantity $H = k\tau_0$	Calculated value τ_0 (av. H = 88)
	compounds with labile sulfur	reducing agents	complex-forming compounds-accelerators (a)	complex-forming compounds-inhibitors (b)				
463	60	3	13	20	0,65	150	98	135
6768	76	5	10	20	0,50	180	90	175
6769	61	23	10	20	0,50	180	90	175
1101	33	22	16	35	0,46	180	83	190
7166	80	33	4	10	0,40	210	84	220
7188	32	34	8	25	0,32	270	86	275
479	42	29	5	18	0,28	300	84	315

In order to learn the function of extraneous materials in the process of chemical ripening, experiments were set up to remove them from gelatin with the help of adsorbents or through separation by use of electro-dialysis Various adsorbents possess a selective action, and only certain ion-exchange resins ("Vofatit M+", AN-1) proved capable of removing almost completely all the active impurities. As a result different samples of gelatin acquired the same properties; they changed into a slow-acting (in the phase of chemical ripening) inert

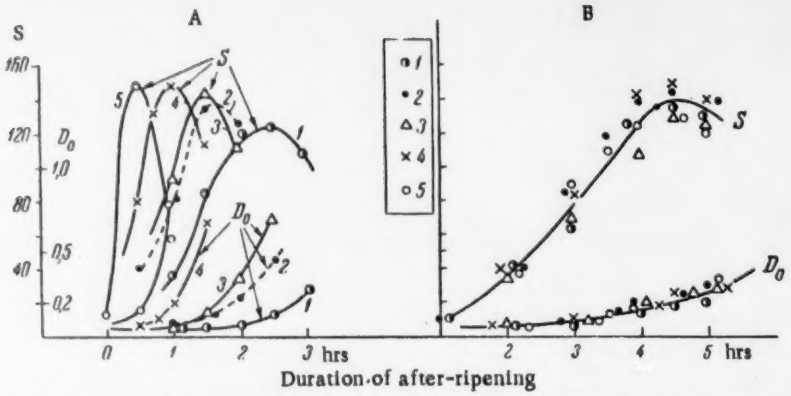

Fig. 1. Chemical-ripening kinetics of photographic emulsion. A – before purification, B – after purification.

1) Sample No. 418; 2) No. 7174; 3) No. 3516; 4) No. 456; 5) No. 1856.

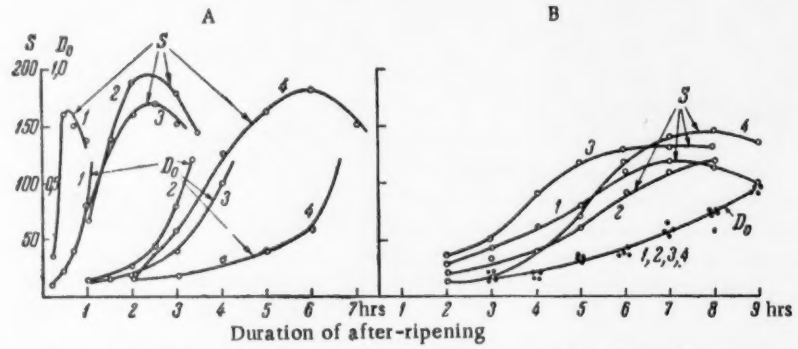

Fig. 2. Chemical-ripening kinetics of photographic emulsion. A– before electrodialysis, B – after electrodialysis.

1) Sample No. 12240; 2) No. 418; 3) No. 443; 4) No. 482.

TABLE 2

The Amount of Impurities (in g-equiv. $\times 10^7$ per 1 g of gelatin)

No. No. of gelatin sample	In gelatin before electrodialysis				In the anode fraction			
	overall	compounds with labile sulfur	reducing agents	complex-forming compounds	overall	compounds with labile sulfur	reducing agents	complex-forming compounds
KZhZ482	39	20	19	0	17	6	11	—
KZhZ443	70	56	6	8	24	13	11	—
American 12 240	60	50	25	15	45	17	17	11

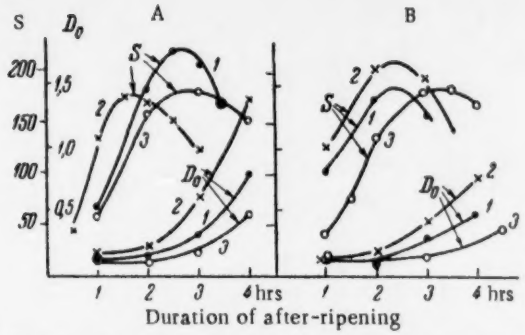

Fig. 3. The effect of cathodic and anodic fractions, extracted from fast (A) and slow (B) gelatins, on the kinetics of chemical ripening of photographic emulsions.
1) Control emulsion; 2) emulsion with admixture of anode fraction; 3) emulsion with admixture of cathode fraction.

gelatin (see Fig. 1). Analysis showed that after such a purification only insignificant quantities of reducing agents could be detected in gelatin ($\sim 4.0 \cdot 10^{-7}$ g-equiv per 1 g of gelatin).

Electrodialysis also produces a removal of active impurities making the gelatin inert (see Fig. 2). With a five-chamber apparatus, electrodialysis permits a separation of the impurities into cathode and anode fractions. After studying these solutions we were able to conclude that the substances in the cathode fraction do not enter into irreversible reactions with the silver ions, whereas the anode fraction contained compounds with labile sulfur and complex-forming substances of the first type. The analytical results for the anode fraction are given in Fig. 2.

Photographic tests showed that the solution of the cathode fraction has a retarding function in the chemical ripening and the solution of the anode fraction – an accelerating function. Figure 3 shows kinetic curves for the change in light-sensitivity and growth of fogging when one or the other fraction, isolated from a slow or fast gelatin, is introduced into gelatin at the stage of chemical ripening. It is obvious from the curve displacement that in the first case gelatin accelerators prevail, while in the second case inhibitors of ripening prevail. These results are in full accord with the inference that the rate of chemical ripening depends on the ratio between the complex-forming substances of the first and second type, both of which have the greatest affinity towards Ag^+ ions.

Thus it is possible to make a general conclusion that the photographic activity of gelatin during ripening is caused by two of its components: macrocomponents (albuminous substances in gelatin, possessing protective properties and some reducing function), and microcomponents, whose basic role is to regulate the rate of chemical ripening.

LITERATURE CITED

[1] A. A. Titov and I. M. Ratner, Trans. Sci. Res. Inst. Cinephot. 8, 20 (1948).

[2] A. A. Titov, ibid, 8, 41 (1948).

[3] A. L. Karpova and Iu. Sh. Moshkovskii, J. Phys. Chem. (in Russian) 28, 1746 (1954).

All-Union Scientific Research Institute
of Cinephotography

Received March 18, 1958

WETTING HEATS OF ETHERIFIED CELLULOSE

E. F. Nekriach and Corresponding Member AN SSSR A. V. Dumanskii

It is possible to rupture and re-form again hydrogenous agents present in cellulose; these determine a number of important properties in cellulose materials: hygroscopic nature, solution rates, and many others. Bond rupture may be achieved through mechanical or chemical dispersion, solvation, or etherification of hydroxyl groups.

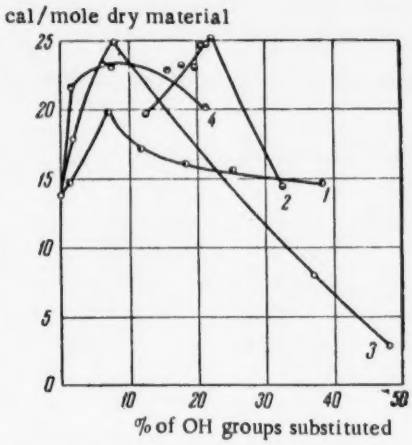

Fig. 1. Wetting heats of dry samples. 1) Methylcellulose from cotton linters; 2) methylcellulose from viscose silk; 3) ethylcellulose from cotton linters; 4) hydroxyethylcellulose from cotton linters.

Some very interesting results, obtained during investigation of low-substitution cellulose ethers, could only be explained by considering the possibility that new, free hydroxyl groups are formed from the rupture of hydrogen bonds between cellulose macromolecules.

In recent years it has been established that when a small number of acetyl [1], methoxy or ethoxy [2] groups all of which are less hydrophilic than hydroxyl groups are introduced into cellulose molecules the hygroscopic nature of the materials is not reduced – on the contrary, it increases. This unexpected result could only be explained by assuming that introduction of ether groups increases the distance between the macromolecules of cellulose till rupture of hydrogen bonds takes place; whereupon the number of hydroxyl groups formed and capable of binding with water exceeds the number etherified. On further etherification the hydrophilic nature of cellulose materials, having attained a specific maximum, decreases, and products with a high degree of etherification become hydrophobic.

The number of papers devoted to the study of hydrophilic properties of low-substitution cellulose ethers is very small, and the investigating methods used were often very satisfactory. For this reason, it seemed interesting to carry out such an investigation; in order to get a quantitative estimate of the hydrophilic nature of cellulose and its derivatives, wetting heats were measured since they appear most fundamental from the theoretical point of view [3].

In the present work the effects of the substituents and of preliminary treatment on the hydrophilic nature of cellulose were investigated as well as the effect of the degree of substitution.

Many samples of methyl, ethyl, and hydroxyethyl cellulose obtained from cotton linters and methylcellulose from viscose silk, were studied. The method of determining heats in an adiabatic calorimeter has been previously described [4]. Results obtained are shown graphically in Fig. 1. As may be seen from the drawing, the type of change in wetting heats with change in degree of etherification is similar for all the investigated cellulose samples: wetting heats increase at first, attain a maximum at a specific degree of etherification, and then decrease.

The absolute values of wetting heats of the ethers depend on two factors: the chemical nature of the ether

group and the structure of the original cellulose. A comparison of curves Q = f (γ) for methyl, ethyl, and hydroxyethyl cellulose obtained from cotton linters, showed that the introduction of a radical with a large number of carbon atoms into the cellulose macromolecule made the product more hydrophilic. It is very interesting that the maximum wetting heat of those samples was observed at one and the same degree of etherification—8%.

Treatment before etherification has a great influence on the hydrophilic nature of the cellulose ethers. Curves 1 and 2 refer to methylated cellulose: first to methylcellulose from cotton linters, second to that from viscose silk. According to the available literature data the wetting heat of viscose silk is considerably higher than that of cotton, ranging between 20 and 22.5 cal/g. As a result of this, the maximum hydrophilic state of methyl cellulose obtained from it is higher than that for methyl cellulose from cotton; however, the differences between the maxima of etherified and original materials are sufficiently close to each other (6.9 cal/g and 6 cal/g). Besides the differences in the absolute values of the heat maxima, there is a displacement in the location of the maximum for different samples of methylcellulose; the largest values for wetting heats of methylcellulose from viscose silk are observed at a considerably higher degree of substitution (about 22%).

LITERATURE CITED

[1] J. C. Bletzinger, Ind. and Eng. Chem. 35, 474 (1943); W. H. Aicken, Ind. and Eng. Chem. 35, 1206 (1943); N. I. Nikitin, Paper Indust. No. 1-5 (1947).

[2] N. I. Nikitin and N. I. Klenkova, Coll. Investigation in the Field of High-Molecular Compounds, Izd. AN SSSR, 1949, p. 138; N. I. Klenkova and N. I. Nikitin, J. Appl. Chem. 27, 171 (1954).*

[3] A. G. Pasynskii, Colloid J. 8, 53 (1946); A. Tager, Solutions of High-Molecular Compounds, Moscow – Leningrad, 1951, p. 147 [in Russian].

[4] A. V. Dumanskii and E. F. Nekriach, Colloid J. 15, 91 (1953);* E. F. Nekriach, Factory Labs. 21, 12448 (1955).

[5] H. J. White and H. Eyring, Text. Res. J. 17, 529 (1947); M. Wahba, J. Phys. and Coll. Chem. 52, 1197 (1948).

Institute of General and Inorganic Chemistry
Academy of Sciences,
Ukrainian SSR

Received March 27, 1958

*Original Russian pagination. See C. B. Translation.

OPTICAL SENSITIZATION OF THE PHOTOEFFECT IN SILVER AND THALLIUM BROMIDES BY ORGANIC DYES

I. A. Akimov

(Presented by Academician A. N. Terenin, March 24, 1958)

A number of papers have been devoted to a study of the optical sensitization of the internal photoeffect in inorganic semiconductors by organic dyes. However, the results of various authors who studied the sensitization of the photoeffect in AgBr are contradictory, and the possibility of sensitizing the photoeffect in silver bromide free of impurities remains unanswered. As early as 1940, using AgBr electrodes, obtained by the electrolytic bromination of silver plates and then dyed with thiacarbocyanine dyes, Sheppard and co-workers [1] observed a sensitization of the photovoltaic effect. However, Noddack and co-workers [2], who recently studied the photovoltaic effect on similar electrodes, failed to reveal sensitization. In a brief communication by Kameyama and co-workers [3], the conditions under which they observed a sensitization of the photoconductivity of fused silver bromide layers by dyes are not described. Later West and Carroll [4] established and investigated the optical sensitization of the photoconductivity of brominated gelatin emulsions. In the studies of Terenin, Putseiko and Akimov [5-7], who investigated the photoeffect in powdered, sublimed and fused layers of silver and thallium halides by the capacitor and photoconductivity methods, it was shown that whereas a substantial sensitization is observed for the iodides, the same is practically absent in the case of the silver and thallium bromides. Amsler [8] found that silver bromide photocells, prepared by the electrolytic bromination of silver plates, can be sensitized by dyes.

The purpose of the present study was to determine the conditions under which it is possible to observe a sensitization of the inner photoeffect in silver and thallium bromides by dyes. The capacitor method, described in [9, 10], was used to study the photoeffect. The photo-e.m.f., induced in the capacitor using modulated illumination, is measured with this method. The use of this method permitted us to run the experiments on powder layers, which had a composition close to the stoichiometric, and possessed a large surface area. In addition, this method makes it possible to run the measurements on layers that possess a variable dark-conductivity, which was essential for our experiments on the adsorption of bromine vapors, since the conductivity of AgBr changes greatly under the influence of bromine [11]. The dyes were adsorbed on the powder from alcohol solutions with a concentration of 10^{-4} mole/liter. The spectral distribution of the photoeffect was measured in the region from 390 to 1000 mμ using an UM-2 glass monochromator. The spectral curves of the photoeffect depicted below represent the value of the photo-e.m.f., referred to the same values of a falling monochromatic energy, measured at the discharge side of the amplifier.

In the spectral distribution of the photoeffect, measured either by the photoconductivity method or by the capacitor method, a maximum at about 430 mμ [12, 13] is usually observed for AgBr in the visible region, while for TlBr maxima are observed at about 410 and 430-440 mμ [14]. The positions of the photo-e.m.f. maxima of the powders investigated by us coincided with those indicated above. In both bromides the long-wave boundary of the photo e.m.f. was found to be at about 500 mμ.

By means of numerous experiments it was established that powder layers of AgBr and TlBr, in contrast to AgI and TlI, fail to show a sensitization of the photoeffect after being dyed with various dyes. The striking influence of adsorbed vapors and gases on the sensitization effect, discovered earlier in our laboratory [15, 6, 7], revealed that an important role in the phenomenon of sensitization is played by the surface electron levels,

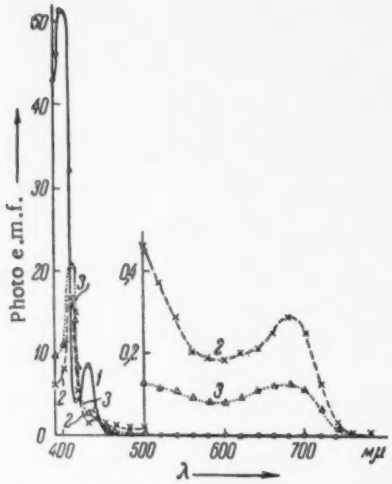

Fig. 1. Spectral distribution of the photo-e.m.f. in a layer of TlBr dyed with malachite green: 1) prior to adsorption; 2) after adsorption of bromine vapors, P ~ 0.1 mm Hg; 3) after partial bromine desorption.

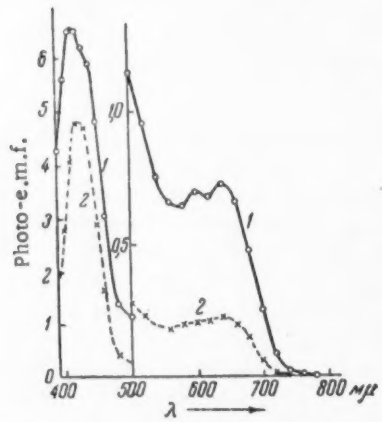

Fig. 2. Spectral distribution of the photo-e.m.f. in a layer of AgBr dyed with malachite green: 1) after adsorption of bromine vapors, P ~ 0.1 mm Hg; 2) after partial bromine desorption.

created in the adsorption of molecules with electron-acceptor properties. The purpose of the present study was to investigate the influence exerted by the adsorption of bromine molecules on the photoelectric sensitivity of undyed and dyed layers of AgBr and TlBr. In these experiments only the dyes resistant to the action of bromine vapors could be used as sensitizer, as for example malachite green, crystal violet, methylene blue and thionine.

Experiments revealed that the admittance of bromine vapors at a vapor pressure of about 0.1 mm Hg exerts a large effect on both the magnitude and the spectral distribution of the photoeffect. After bromine adsorption the photoelectric sensitivity in the 400-450 mμ region increased for AgBr, and decreased somewhat for TlBr. Simultaneously with this there appeared in both the visible and near-infrared regions a slight sensitivity with weakly expressed maxima at about 500 and 900 mμ. Removal of the adsorbed bromine by either freezing or heating the layer restored the original sensitivity.

Especially pronounced changes in the spectral distribution of the photoeffect were manifested when bromine vapors were adsorbed on dyed layers of AgBr and TlBr. The curves for the spectral distribution of the photo-e.m.f. in TlBr powder, dyed with malachite green, are shown in Fig. 1. Whereas no photoelectric sensitivity was observed in the region of dye absorption (600-700 mμ) prior to the adsorption of bromine vapors (Curve 1), after bromine adsorption there appeared on this layer a distinct sensitized photoeffect maximum at about 680 mμ (Curve 2).

The position of this photoeffect maximum coincides with the absorption maximum of the dye adsorbed on the TlBr powder, and is shifted toward longer waves when compared with a solution of the dye in ethanol. Partial desorption of the bromine molecules led to a substantial reduction in the sensitized photoeffect (Curve 3), while when all of the adsorbed bromine was removed the layer again lost its photoelectric sensitivity to light of long wavelength. It should be mentioned that the adsorbed bromine molecules are held more tenaciously on the dyed layers than on the undyed. The adsorption of bromine vapors on dyed silver bromide also led to the appearance of a sensitized photoeffect (Fig. 2), which after desorption of the bromine molecules decreased. A similar picture was observed in the adsorption and desorption of bromine on silver and thallium bromides dyed with other dyes (thionine, crystal violet). The positions of the maxima of the photoeffect, sensitized by the same dye, differed somewhat for AgBr and TlBr.

In the case of layers dyed with methylene blue the adsorption of bromine vapors not only changed the magnitude of the sensitized photoeffect, but it also led to a substantial change in the spectral distribution of the photoeffect in the absorption region of the dye. When the bromine was adsorbed at low vapor pressures (about 0.01 mm) the photoeffect, sensitized by methylene blue, showed a maximum at about 680-700 mμ (Fig. 3, Curve 1). After additional adsorption of bromine vapors the indicated band of the photoeffect diminished substantially and there simultaneously appeared a second distinct band with a maximum at 780-800 mμ (Fig 3,

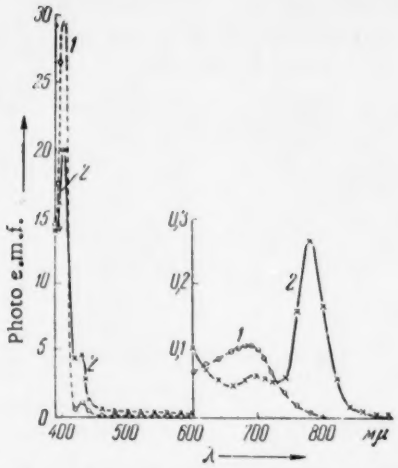

Fig. 3. Spectral distribution of the photo-e.m.f. in a layer of TlBr dyed with methylene blue: 1) after adsorption of bromine vapors, P ~ 0.01 mm Hg; 2) after the additional adsorption of bromine vapors, P ~ ~ 0.1 mm Hg.

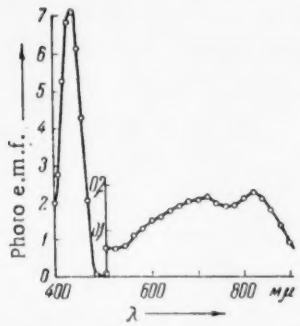

Fig. 4. Spectral distribution of the photo-e.m.f. in a layer of AgBr dyed with methylene blue, after the adsorption of bromine vapors P ~ 0.1 mm Hg.

Curve 2). The spectral distribution of the photo-e.m.f. for the AgBr layer, dyed with the same dye, after its exposure to bromine vapors, is shown in Fig. 4. The desorption of bromine from these layers was accompanied by the disappearance first of the photoeffect maximum at 800 mμ, and then of the maximum at 700 mμ. In the case of the other dyes the bromine vapors exerted an influence only on the magnitude of the sensitized photoeffect. It should be mentioned that the effectiveness of the sensitization, estimated as the ratio of the photoeffect value in the absorption region of the adsorbed dye to the photoeffect in the absorption region of the semiconductor itself, reached in these experiments for the case of AgBr and TlBr, even in the presence of bromine vapors, was much smaller than in the case of ZnO, TlI and AgI [5-7].

Using the capacitor method and a synchronous detector at the discharge side of the amplifier [15] we determined the sign of the photocurrent carriers in the investigated layers. Holes were the photocurrent carriers both in the absorption region of the semiconductor itself and in the absorption region of the dye.

The results obtained in the present study are in full agreement with the earlier studies [15, 6, 7] on the influence of gases and vapors on the sensitization of the photoeffect in semiconductors by dyes. An increase in the sensitized photoeffect for AgBr and TlBr when bromine vapors are adsorbed is similar to the earlier shown [6] effect of iodine vapors on the photoeffect in dyed silver and thallium iodides. The mechanism of the sensitization by dyes of the photoeffect in silver and thallium bromides, the same as in the iodides [7], apparently consists in the transmission of the energy of a photon by the absorbed dye to the semiconductor and the transfer under the influence of this energy of an electron in the semiconductor to a local level, formed by the adsorbed bromine molecule. The hole that is freed here in the main zone is the photocurrent carrier. In accordance with such a postulate for the mechanism of the examined phenomenon a necessary condition for making the sensitization of the photoeffect by dyes possible is the existence of acceptors, creating local electron levels on the surface of the semiconductor. In our case such levels were created by the adsorbed bromine molecules. The energy of the photon, adsorbed by the dye molecule, is apparently sufficient to effect the transfer of an electron in the semiconductor to this acceptor level.

In conclusion I take this opportunity to gratefully thank Academician A. N. Terenin and E. K. Putseiko for their constant interest in the work and for their valuable advice.

LITERATURE CITED

[1] S. Sheppard, W. Vanselow and G. Happ, J. Phys. Chem. 44, 411 (1940).

[2] W. Noddack and G. Eckert and H. Meier, Zs. Elektrochem. 56, 735 (1952).

[3] N. Kameyama and Hukumoto, J. Soc. Chem. Ind. (Japan) 42, 244 (1939); N. Kameyama and K. Mizuta, J. Soc. Chem. Ind. (Japan) 42, 426 (1939).

[4] W. West and B. H. Carroll, J. Chem. Phys. 15, 529 (1947); 19, 417 (1951).

[5] E. K. Putseiko and A. N. Terenin, J. Phys. Chem. (USSR) 23, 676 (1949); Proc. Acad. Sci. USSR 70, 401 (1950); Advances in Scientific Photography [in Russian] 3, 101 (1955); E. K. Putseiko, Bull. Acad. Sci. USSR, Phys. Ser. 13, 224 (1949); A. G. Gol'dman and I. A. Akimov, J. Phys. Chem. (USSR) 27, 355 (1953).

[6] I. A. Akimov and E. K. Putseiko, Proc. Acad. Sci. USSR 102, 481 (1955); I. A. Akimov, J. Phys. Chem. (USSR) 30, 1007 (1956); J. Scientific and Applied Photography and Cinematography [in Russian] 1, 254 (1956).

[7] A. Terenin, E. Putseiko and I. Akimov, J. chim. phys. 54, 716 (1957).

[8] H. Amsler, Zs. Elektrochem. 56, 733 (1952); 57, 801 (1953).

[9] L. Bergmann, Physik. Z. 33, 209 (1932).

[10] E. K. Putseiko, Proc. Acad. Sci. USSR 67, 1009 (1949).

[11] L. M. Shamovskii, A. A. Dunina and M. I. Gosteva, J. Exptl. and Theoretical Physics [in Russian] 30, 640 (1956); G. W. Luckey and W. West, J. Chem. Phys. 24, 879 (1956).

[12] E. A. Kirillov and A. S. Fomenko, Trans. Odessa State Univ. 13, 7 (1951); B. A. Barshchevskii, J. Exptl. and Theoretical Physics 16, 815 (1946); 20, 795 (1950).

[13] P. V. Meikliar and E. K. Putseiko, Proc. Acad. Sci. USSR 73, 63 (1950).

[14] E. K. Putseiko, Proc. Acad. Sci. USSR 78, 453 (1951).

[15] E. K. Putseiko, Proc. Acad. Sci. USSR 19, 1071 (1953); Radio Engineering and Electronics [in Russian] 1, 1364 (1956).

[16] U. Kh. Nymm and L. Ia. Uibo, Trans. Inst. Physics and Astronomy, Acad. Sci. Estonian SSR 1956, No. 4, 124.

Received March 3, 1958

INFLUENCE OF THE STRUCTURE OF ORGANIC MOLECULES ON THE PROBABILITY OF TRANSITION TO A METASTABLE STATE

V. V. Zelinskii, V. P. Kolobkov and I. I. Reznikova

(Presented by Academician A. N. Terenin, March 31, 1958)

It has been shown [1, 2, 3] that at 196° the ratio of quantum yields of phosphoresence and fluorescence, which we shall designate as δ, for substances whose fluorescence spectra occupy different positions in different media, is determined primarily by the frequency of the maximum of the fluorescence spectrum ν_{fe}^{max}. In this communication we shall consider the influence of some structural characteristics on the quantity δ and, thus, also on the probability of transition to a metastable state. It can be concluded [4, 5] that for a series of phthalimide derivatives, the ability to phosphoresce, in general, decreases with the shift of the fluorescence spectrum in the direction of smaller frequencies.

The fact that δ is determined not only by the position of the fluorescence spectrum, but also by the structural characteristics of fluorescent molecules, can best be demonstrated by comparing δ for 3- and 4-acetylamino-N-methylphthalimides, and 3- and 4-hydroxy-N-methylphthalimides (Fig. 1). Thus, at $\nu_{fe}^{max} = 24{,}000$ cm^{-1} δ for 3-acetylamino-N-methylphthalimide is 20 times as large as δ for its isomer at the same position of the fluorescence spectrum. At the same ν_{fe}^{max}, δ for 3-hydroxy-N-methylphthalimide is approximately 10 times as large as δ for 4-hydroxy-N-methylphthalimide.

It has been shown [1, 2, 3] that δ depends only slightly on the chemical nature and the state of the medium, but is primarily determined by the position of the spectral fluorescence band. Therefore it is clear that the relative phosphorescence ability of different substances should be compared not in the same solvent, but at the same ν_{fe}^{max}, even if for the substances being compared this ν_{fe}^{max} is obtained in different solvents.

Let us consider several cases of the effect of the introduction of the methyl group in a molecule on the quantity δ. In Fig. 1 the dependence of δ on ν_{fe}^{max} is given for 3-acetylamino- and 3-methylacetylamino-N-methylphthalimide (Curves III and V, respectively). The curve for the methyl derivative is shifted in the direction of smaller frequencies as compared to the curve for 3-acetylamino-N-methylphthalimide. For the same ν_{fe}^{max}, the values of δ for the first substance are considerably larger.

The effect of the methyl group on δ is particularly pronounced in the case of 3,6-derivatives of N-methylphthalimide (Fig. 2). For 3-acetylamino-6-amino-N-methylphthalimide (I), δ does not exceed 0.02; at $\nu_{fe}^{max} = 20{,}500$ cm^{-1} at smaller values of ν_{fe}^{max}, phosphorescence does not occur at all. The dependence of δ on for ν_{fe}^{max} 3-acetylamino-6-dimethylamino-N-methylphthalimide (II) is given in the same figure. When ν_{fe}^{max} is smaller than in the previous case, a very weak, but definite phosphorescence is observed for this substance; $\delta = 0.02$ at $\nu_{fe}^{max} = 19{,}000$ cm^{-1}. (in isopropyl formate and chloroform, ν_{fe}^{max} is approximately 25,500 cm^{-1}, the corresponding δ being ~ 3; it is difficult to determine an exact position of the fluorescence spectrum due to to the large magnitude of δ). Curve III represents the dependence of δ on ν_{fe}^{max} for 3-methylacetylamino-6-dimethylamino-N-methylphthalimide which is a derivative of a phthalimide that already contains 3 methyl groups. This curve is even further displaced in the direction of smaller frequencies as compared to Curves I and II. The values of δ for 3-methylacetylamino-6-dimethylamino-N-methylphthalimide reach 0.15. In Fig. 2 the dependence of the quantity δ on ν_{fe}^{max} is given schematically for 3,6-diacetylamino- and 3-methylacetylamino-6-acetylamino-N-methylphthalimides in different solvents. At the same ν_{fe}^{max}, values of δ are larger for the second compound. Thus, at $\nu_{fe}^{max} = 22{,}000$ cm^{-1}, $\delta \simeq 0.15$ for 3,6-diacetylamino-N-methyl-

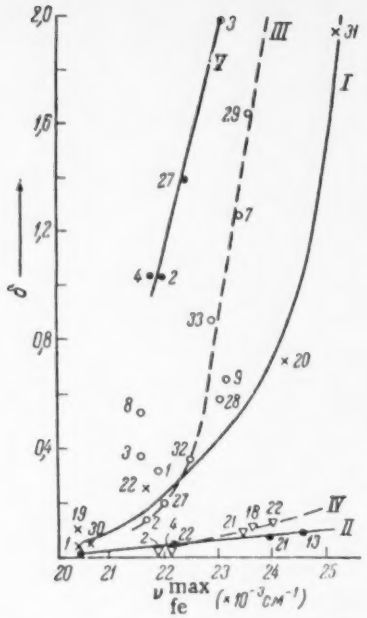

Fig. 1. Dependence of δ on ν_{fe}^{max} for derivatives of N-methylphthalimide: 3-hydroxy- (I), 4-hydroxy- (II), 3-acetylamino- (III), 4-acetylamino- (IV), 3-methylacetylamino (V). The numbers in Fig. 1-5 correspond to the following solvents: 1) crystalline state; 2) water; 3) benzene; 4) carbon tetrachloride; 5) menthene; 6) α-chloronaphthalene; 7) acetic acid; 8) anisole; 9) nitromethane; 10) dioxane; 11) triethylamine; 12) formamide; 13) propyl acetate; 14) ethyl acetate; 15) ethyl orthoformate; 16) acetone; 17) tertiary butyl alcohol; 18) acetic anhydride; 19) methyl alcohol; 20) glycerol; 21) chloroform; 22) ethyl alcohol; 23) diisopropyl ether; 24) diisobutyl ether; 25) diisoamyl ether; 26) toluene; 27)isooctane; 28) cumene; 29) m-xylene; 30) pyridine; 31) butyl alcohol; 32) n-hexane; 33) o-xylene; 34) isobutyl alcohol; 35) isopropyl alcohol; 36) glue # 235; 37) diethyl ether; 38) n-octane; 39) propyl formate; 40) chlorobenzene; 41) isoamyl formate.

phthalimide. This is also true for 3- and 4-methoxy-N-methoxy-N-methylphthalimides as compared to corresponding 3- and 4-hydroxy- derivatives. In the case of 3-amino-6-nitro- and 3-dimethylamino-6-nitro-N-methylphthalimides (Fig. 3) the curve showing the dependence of δ on ν_{fe}^{max} for the second compound (I) is displaced in the direction of long wavelengths as compared to the curve for the first compound (II); thus, in this case also, at the same ν_{fe}^{max} the values of δ are larger for the methylated compound.

In such a way, the methylation of various compounds invariably leads to an increase in δ, although the fluorescence spectrum is nearly always simultaneously displaced towards smaller frequencies. On the other hand, replacement of hydrogen in the imide group by the methyl group does not change the dependence of δ on ν_{fe}^{max} Thus, in ethyl alcohol and carbon tetrachloride δ's for 3-hydroxyphthalimide fall on the same curve as obtained for 3-hydroxy-N-methylphthalimide. The values of δ for 3-acetylaminophthalimide fall on the δ vs. ν_{fe}^{max} curve obtained for 3-acetylamino-N-methylphthalimide.

For the examples of 3-diphenylamino-N-methylphthalimide, phenylanthranilic acid, and phenyl-β-naphthylamine, one concludes that introduction of the phenyl group into the compound likewise increases δ. Upon comparing 3-diphenylamino-N-methylphthalimide (Figure 2, IV) and 3-amino-N-methylphthalimide (Fig. 3, IV), one sees that although ν_{fe}^{max} for 3-amino-N-methylphthalimide in ethyl alcohol, chloroform, toluene and a number of other solvents is greater (21,800 cm^{-1}) than ν_{fe}^{max} for 3-diphenylamino-N-methylphthalimide in ethyl alcohol and isopropyl formate (ν_{fe}^{max} = 18,600 cm^{-1}), nevertheless in the case of 3-amino-N-methylphthalimide phosphorescence is completely absent but it is present in the case of 3-diphenylamino-N-methylphthalimide in the above-mentioned solvents, with δ = 0.13-0.16.

In the case of phenyl-β-naphthylamine (Fig. 4, III) δ = 0.4 corresponds to ν_{fe}^{max} = 24,600 cm^{-1}, but for β-naphthylamine the same value of δ is observed only at ν_{fe}^{max} = = 26,000 cm^{-1} (Fig. 4, IV). From Fig. 4 it is also apparent that the curve δ vs. ν_{fe}^{max} for phenylanthranilic acid is shifted to the left on the frequency axis with respect to the analogous curve for anthranilic acid (II).

In contrast to the methyl group which, when substituted for hydrogen in the imide group, does not change δ, a phenyl group in this position greatly increases δ. For 4-acetylamino-N-methylphthalimide in ethyl alcohol δ is equal to 1.2 at ν_{fe}^{max} = 21,000 cm^{-1}; for 4-acetylamino-N-methylphthalimide at considerably greater values of ν_{fe}^{max}, δ does not exceed 0.15.

Comparing the values of δ for 3-amino and 3-dimethylamino-N-methylphthalimides with those for 3-amino-6-nitro- and 3-dimethylamino-6-nitro-N-methylphthalimides (Fig. 3), it becomes apparent that the nitro group also promotes the transition of molecules to the metastable state. Thus, for 3-amino-N-methylphthalimide (IV) in ethyl alcohol ν_{fe}^{max} = 21,800 cm^{-1} and phosphorescence is absent, for 3-amino-6-nitro-

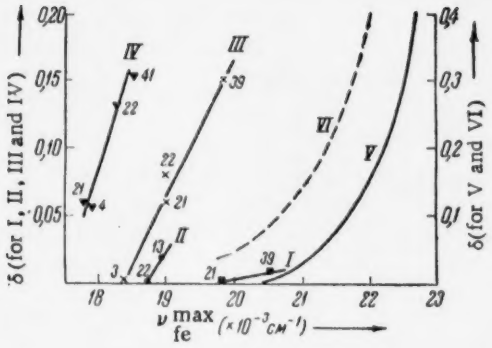

Fig. 2. Dependence of δ on ν_{fe}^{max} for derivatives of N-methylphthalimide: 3-acetylamino-6- (I); 3-acetylamino-6-dimethylamino (II); 3-methylacetylamino-6-dimethylamino- (III); 3-diphenylamino (IV); 3,6-diacetylamino- (V); 3-methylacetylamino-6-acetylamino- (VI).

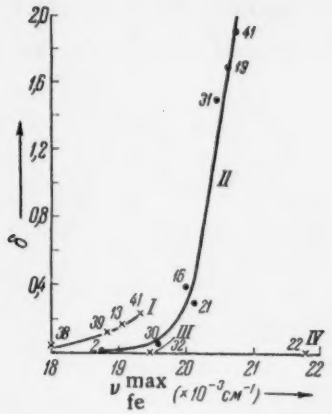

Fig. 3. Dependence of δ on ν_{fe}^{max} for derivatives of N-methylphthalimide: 3-dimethylamino-6-nitro- (I); 3-amino-6-nitro- (II); 3-dimethylamino- (III); 3-amino- (IV).

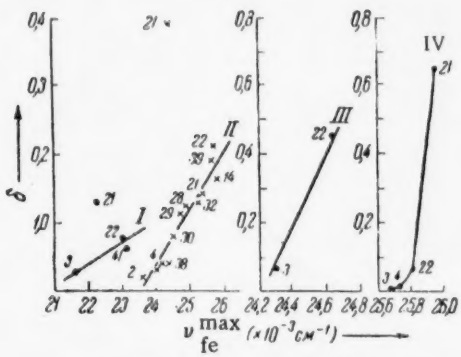

Fig. 4. Dependence of δ on ν_{fe}^{max} for phenylanthranilic acid (I), anthranilic acid (II), phenyl-β-naphthylamine (III), and β-naphthylamine (IV).

N-methylphthalimide (II) in alcohols ν_{fe}^{max} = 21,800 cm^{-1} and phosphorescence is absent, and for 3-amino-6-nitro-N-methylphthalimide (II) in alcohols ν_{fe}^{max} = = 20,800 cm^{-1} and δ 's are of the order of 2. Similarly, for 3-dimethylamino-N-methylphthalimide (III) in ethyl alcohol at ν_{fe}^{max} = 19,500 cm^{-1} phosphorescence is absent, but for the compound which differs from 3-dimethylamino-N-methylphthalimide by the presence of a nitro group (I) δ ≅ 0.2 at the same ν_{fe}^{max}.

Thus, it has been shown that certain structural changes in luminescing molecules lead to a greater probability of transition to the metastable state. The considerable similarity of action by the structural factors should be particularly noted.

The methylation of a molecule leads to an increase in δ regardless of whether the amino or the hydroxy group is being methylated; this is true for rather different substances. Similarly, introduction of a phenyl group into various organic compounds leads to an increase in δ.

It should be noted that sometimes the position of the substituted group is more important than the nature of the group. For example, at corresponding ν_{fe}^{max} greater δ 's are observed for 3-acetylamino- and 3-hydroxy-N-methylphthalimides than for 4-acetylamino- and 4-hydroxy-N-methylphthalimides, respectively.

LITERATURE CITED

[1] V. V. Zelinskii and V. P. Kolobkov, Proc. Acad. Sci. USSR 119, No. 5 (1958).*

[2] V. V. Zelinskii, V. P. Kolobkov and I. I. Reznikova, Bulletin Acad. Sci. USSR, physics series (in print).

*Original Russian pagination. See C. B. Translation.

[3] L. E. Golikova, V. V. Zelinskii and V. P. Kolobkov, Optics and Spectroscopy (in the press).

[4] B. S. Neporent and A. I. Iniushin, Proc. Acad. Sci. USSR 98, 197 (1945).

[5] V. V. Zelinskii and V. P. Kolobkov, Proc. Acad. Sci. USSR 101, 241 (1955).

Received March 18, 1958

THE INFLUENCE OF THE INTENSITY OF THE RADIATION FROM S^{35} ON THE RATE OF ISOTOPIC EXCHANGE OF SULFUR IN THE SYSTEM $K_2\overset{*}{S}O_4 - SO_3$

Corresponding Member AN SSSR Vict. I. Spitsyn and I. E. Mikhailenko

During the study of the isotopic exchange of sulfur between solid alkali metal sulfates and gaseous sulfur trioxide at high temperatures [1] the authors observed that the level of radioactivity of the specimens under study has an influence on the rate of the isotopic exchange processes. A more detailed study has been made of this phenomenon.

We have studied the influence of the beta-radiation from S^{35} on the degree of isotopic exchange of sulfur between solid potassium sulfate labeled with S^{35} and gaseous sulfur trioxide. The experiments were carried out under the same conditions at a temperature of 840° using samples of $K_2\overset{*}{S}O_4$ with different specific activity values. Figure 1 gives a diagram illustrating the apparatus used. The round-bottomed flask (1), the condenser (2), the tube (4) with ground stopper and gas tubes, and the bottles (7), (8) and (9) were made of molybdenum glass, while the tube (6) and the boat inside it were made of quartz glass. 60% "chemically pure" oleum was placed in the flask and the SO_3 distilled off at a temperature of 60-70°. The two-way tap (5) was closed and the sulfur trioxide passed through the condenser and three-way tap (3) into the measuring tube (4), on which each scale division corresponded to 0.05 ml. The measured quantity of SO_3 was drawn by a current of dry air through the tap (5) into the reaction space of the quartz tube (6). After passing over the material, the sulfur trioxide was trapped in the bottles containing concentrated H_2SO_4 (7) and 0.1 N NaOH solution (8) and (9). A definite weight of the radioactive specimen of potassium sulfate was placed in the quartz boat. Before and after each experiment, dry air was blown through the whole apparatus via the branch piece of the three-way tap (3). The temperature of the furnace (10) was measured using a platinum–platinorhodium thermocouple. During the experiments the temperature was maintained at 840° with an accuracy of ±5°. In each experiment the weight of sulfate amounted to 0.3-0.4 g; the quantity of SO_3 amounted to 0.3 ml or 0.6 g. The rate of flow of the dry air used to draw the sulfur trioxide through the apparatus was 37 liters/hour. The time taken for the SO_3 to pass over the specimen under study was 10 minutes. The sample of sulfate was kept in the heated zone of the furnace for 20 minutes. The K_2SO_4 specimens with labeled sulfur were prepared by adding a small quantity of active sodium sulfate to solutions of K_2SO_4. The solutions were then evaporated to dryness and the residue ignited at 800°. Identical values for the specific surfaces of the K_2SO_4 specimens were ensured by grinding them carefully to a fine powder and dividing them into fractions using sieves. The particle size varied between 0.17 and 0.10 mm.

After each experiment the sample of active sulfate was dissolved in a graduated flask. A definite volume of the solution was evaporated on a sheet of filter paper placed in a round aluminum dish. The activity of the specimen was measured each time under identical geometrical conditions relative to an end-window counter. The highly active specimen solutions, obtained after the experiments, were diluted in such a way that the value of the impulse count in all the specimens was of approximately the same order of magnitude (1500-2000 impulses/minute). 4-6 isotopic exchange experiments were carried out with each K_2SO_4 specimen of a given specific activity. Examples of the changes which took place in the activity of the potassium sulfate are given in Table 1, while the mean results of the measurements are given in Table 2 and Fig. 2. The degree of exchange was calculated according to the formula .

$$W = (A_0 - A_1)/B,$$

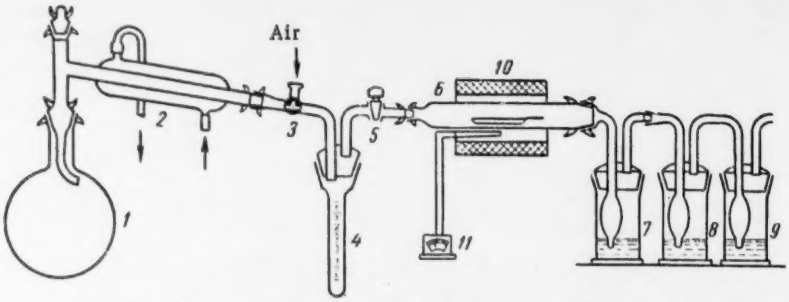

Fig. 1. Diagram of the apparatus used to study isotopic exchange in the system $K_2SO_4 - SO_3$.

TABLE 1

Examples of the Change in Activity of Potassium Sulfate in Experiments on Isotopic Exchange with SO_3

K_2SO_4 Specimen	K_2SO_4 Sample, g	Wt. of K_2SO_4 after the experiment, g	Change in weight		Original activity, impulses/minute	Activity of K_2SO_4 after the expt.		Degree of exchange %
			g	%		impulses/minute	%	
1	0,3362	0,3362	—	—	$2164 \cdot 10^2$	$1942 \cdot 10^2$	89,8	11,7
2	0,4034	0,4039	+0,0005	+0,1	$4625 \cdot 10^2$	$4160 \cdot 10^2$	90,0	12,0
3	0,3780	0,3785	+0,0005	+0,1	$4713 \cdot 10^3$	$3719 \cdot 10^3$	78,9	27,5
4	0,3756	0,3761	+0,0005	+0,1	$2726 \cdot 10^4$	$1344 \cdot 10^4$	49,3	65,9
5	0,3129	0,3129	—	—	$2514 \cdot 10^4$	$1187 \cdot 10^4$	47,2	66,1
6	0,3512	0,3512	—	—	$9897 \cdot 10^4$	$7310 \cdot 10^4$	73,9	33,4
7	0,3563	0,3561	—0,0002	—0,1	$1669 \cdot 10^5$	$1212 \cdot 10^5$	72,4	35,4

TABLE 2

The Isotopic Exchange of Sulfur Between Potassium Sulfate and SO_3 at 840°

K_2SO_4 Specimen	Na_2SO_4 added, %	Observed specific activity, imp./min.	Absolute activity, millicuries/g	No. of experiments	Degree of exchange, %
1	0,04	$6,44 \cdot 10^5$	$1,7 \cdot 10^{-2}$	5	11,7
2	0,1	$9,37 \cdot 10^5$	$2,6 \cdot 10^{-2}$	6	11,5
3	0,1	$12,5 \cdot 10^6$	$3,5 \cdot 10^{-1}$	4	26,7
4	0,4	$72,6 \cdot 10^6$	2,0	5	65,5
5	0,4	$80,4 \cdot 10^6$	2,3	5	66,9
6	2,6	$28,2 \cdot 10^7$	7,8	5	33,3
7	3,0	$58,5 \cdot 10^7$	16,2	4	36,6

where W — degree of exchange expressed as a percentage, A_0 — activity of the original salt, taken as 100%, $A_1 - A_2$ activity of the reaction product as a percentage of the activity of the original compound; $B = \frac{N_1}{N_1 + N_2}$; N_1 — atomic concentration of the element under study (sulfur) in the SO_3 being passed through; N_2 — atomic concentration of sulfur in the radioactive specimen.

It follows from the results given that the degree of isotopic exchange at a specific activity for the K_2SO_4

of the order of 0.02-0.03 microcuries/g is practically constant and amounts to approximately 12%. When the activity of the potassium sulfate rises to 0.35 microcuries/g, the degree of exchange increases to 26.7%. The maximum degree of exchange 66.9%, is observed at a specific activity of the order of 2.3 microcuries/g. Further increase in the specific activity of the potassium sulfate to 8-16 microcuries/g leads to a reduction in the degree of exchange to 33-37%. We have not yet studied the region of higher specific activities.

	Original activity of K_2SO_4 sample, impulses/minute	Activity after experiment, impulses/minute
1	$1440 \cdot 10^5$	$1439 \cdot 10^5$
2	$1186 \cdot 10^5$	$1186 \cdot 10^5$

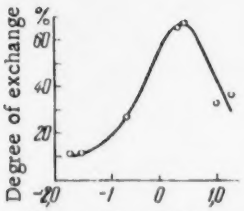

Fig. 2. The relationship between the degree of isotopic exchange and the specific activity of the K_2SO_4.

It may be assumed that when the intensity of the beta-radiation emitted by the S^{35} is sufficiently high, it causes excitation of the ions present in the K_2SO_4 crystal lattice, the SO_4^{2-} ions in particular. In this condition the SO_4^{2-} ions in the solid phase are evidently more capable of exchanging with gaseous sulfur trioxide, sulfur atoms, radicals of SO_3, SO_2, etc. This leads to an increase in the rate of exchange to a value which is several times greater than that for specimens of low activity.

The reason for the appearance of the maximum value for the exchange at a specific activity of 2 microcuries/g is not yet clear. It is possible that when the radioactivity near the surface of the solid potassium sulfate is too intense, the ionization of SO_3 molecules begins to take place to an appreciable extent. This may hinder their adsorption and consequently reduce the exchange. On the other hand, intense radiation at the surface of the potassium sulfate may produce charges there which produce the same effects.

It should be noted that the addition of sodium sulfate in itself has no influence on the rate of isotopic exchange of the sulfur in the potassium sulfate. For a specimen of K_2SO_4 with a specific activity of $1.7 \cdot 10^{-2}$ microcuries/g and Na_2SO_4 content of 0.4%, the isotopic exchange amounted to 11.9% which is practically the same as the value for the exchange at the same specific activity for a lower Na_2SO_4 content (0.04%).

In the experiments described, moreover, we do not have a simple radiation–chemical decomposition of the potassium sulfate, which would be accompanied by, for example, the removal of SO_2 and the loss of a corresponding amount of activity. When an active specimen of K_2SO_4 was ignited in a current of air under the same conditions as those of the exchange experiments using SO_3, no change in weight or in the S^{35} content was observed.

A phenomenon similar to that described above has been observed by Gordon and Hart [2]: when a solution of gaseous deuterium in ordinary water was treated with gamma-rays from Co^{60}, isotopic exchange took place between deuterium and the ordinary hydrogen, which does not take place by itself at an appreciable rate under the same conditions. The authors quoted consider that in the case which they studied the exchange takes place via products of radiolysis of the water.

In heterogeneous systems similar to that which we have studied, an important part must be played by the energy effects produced by the radiation in the adsorbed layer of gaseous or liquid products which is formed on the solid phase surface. These effects may influence the processes of isotopic and chemical exchange taking place on the surface of the solid phase, and the adsorption, catalytic and other properties of solid bodies. At the same time the possibility of radiation–chemical action produced by the influence of the radiation on the gaseous or liquid phase in contact with the radioactive solid body is not excluded. In addition, the recoil nuclei may create defects in the crystal lattice within the bulk of the solid body and on its surface, and these defects may act as further active centers for adsorption and isotopic exchange phenomena.

LITERATURE CITED

[1] Vict. I. Spitsyn and I. E. Mikhailenko, J. Inorg. Chem. 3, 1254 (1958).

[2] S. Gordon and E. J. Hart, J. Am. Chem. Soc. 77, 3981 (1955).

Institute of Physical Chemistry,
USSR Academy of Sciences
M. V. Lomonosov State University, Moscow

Received April 27, 1958

THE INFLUENCE OF CATION RADIUS ON THE PROPERTIES OF THE BOUNDARY LAYERS OF ELECTROLYTE SOLUTIONS IN THE FLAT AREAS BETWEEN QUARTZ SURFACES

G. I. Fuks and N. I. Kaverina

(Presented by Academician P. A. Rebinder, March 7, 1958)

The use of a sensitive method for measuring the kinetics of adhesion and separation of mirror-polished plane parallel discs [1, 2] has shown that the thin boundary layers of solutions of surface-active agents and electrolytes in the spaces between solid bodies show a static resistance to the forces tending to thin them out and exhibit a viscosity which is greater than that of the same solutions in the bulk [2, 3]. In connection with the part played by electrolytes in the coagulating interaction of the particles of a disperse system, a study was made of the influence of the concentration and radius of the cations on the properties of the boundary layers of solutions of the alkali and alkaline-earth metal chlorides in the spaces between negatively charged quartz discs immersed in these solutions; the properties were characterized by the method referred to above. As is well known, the radius of ions determines their position in the lyotropic series [4]. Measurements were made of: 1) thickness of the boundary layer $h_{bound.}$, equal to half the thickness of the space between approaching discs at which the hydrodynamic law governing the flow of a viscous liquid – the Stefan-Reynolds equation – breaks down; 2) the ratio between the boundary viscosity, measured by the rate of separation of the discs, and the viscosity in the bulk η_σ / η; 3) the thickness of the residual layer which cannot be pressed out from the space between the discs by a given load (up to 8 kG/cm^2) during the time of the experiment (from 3 to 9 hours); 4) the resistance of the residual layer to the thinning-out forces, given by

$$\bar{E}\,\sigma'_{app} - \sigma''_{app} = \frac{h'_{min}\,(\sigma''_{app} - \sigma'_{app})}{h'_{min} - h''_{min}},$$

where h'_{min} and h''_{min} – the thicknesses of the residual layers at specific loads of σ'_{app} and σ''_{app}; 5) the dimensionless coefficient of boundary viscosity increase $\psi = \frac{t_{sep} \cdot \sigma_{sep}}{\eta}$, where t_{sep} – time required to separate one disc from another using a normal separating force σ_{sep}; 6) the separating pressure [5, 6] corresponding to the equilibrium region of the residual layer. It has been shown [3] that the thickness of the residual layer of an electrolyte solution, when a load is alternately applied and removed, is partly reversible. It was assumed that the specific load compressing the equilibrium region of the residual layer is equal to the separating pressure.

The thickness of the boundary layer of the solutions studied does not exceed 0.35μ and decreases with increase in the load. $h_{bound.}$ for solutions of divalent ions is considerably smaller than that for monovalent ions. For cations of equal valence, the thickness of the boundary layer increases with decrease in the radius, i.e., with increase in ion hydration (see Table 1). The latter relationship is more clearly shown with monovalent cations than with divalent cations, which may be explained by the greater change in ionic radius and consequently in ion hydration in the series $Li^+ - Cs^+$ compared with the series $Mg^{2+} - Ba^{2+}$ $h_{bound.}$ decreases with increase in temperature and at 60° the difference between the ions is reduced below the limit of the sensitivity of the method (± 0.01μ). The increase in the viscosity in the boundary layer is dependent on the thickness of the latter [1,2]. The integral values of η_σ/η, measured by separating the discs after they have been brought into contact for 10-60 minutes at

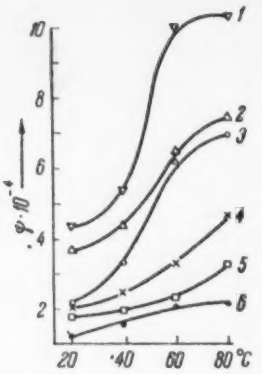

Fig. 1. The influence of temperature on the coefficient of boundary viscosity increase for electrolyte solutions in the space between quartz surfaces. t_{app} = 30 minutes, σ_{app} = 1 kg/cm^2, σ_{sep} = 0.08 kg/cm^2. 1) NaCl – 100 mg-equivs/liter; 2) $CaCl_2$ – 10 mg-equivs/liter; 3) NaCl – 10 mg-equivs/liter; 4) LiCl – 10 mg-equivs/liter; 5) NaCl – 1 mg-equiv/liter; 6) H_2O.

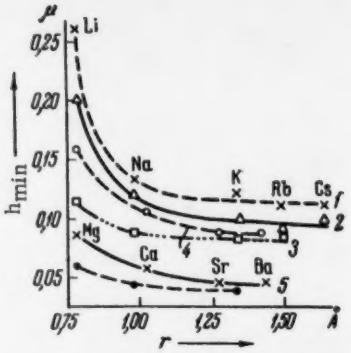

Fig. 2. The influence of cation radius and size of load on the thickness of the residual layer for 0.01 N electrolyte solutions. 1) monovalent cations, σ_{app} = 0.2 kg/cm^2; σ_{app} = 1 kg/cm^2; 3) ditto, σ_{app} = 2.0 kg/cm^2; 4) divalent cations, σ_{app} = 0.2 kg/cm^2; 5) ditto, σ_{app} = 2.0 kg/cm^2; 6) monovalent cations, σ_{app} = 1 kg/cm^2. (Curves 1-5 – at 20°, Curve 6 – at 60°).

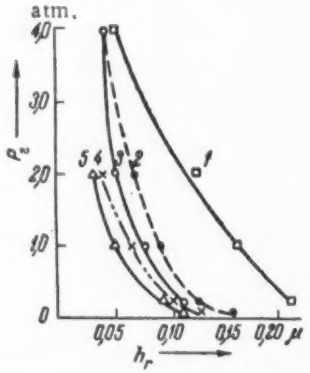

Fig. 3. The separating pressure in electrolyte solutions in the plane areas between surfaces at 20° (h_r – half the equilibrium spacing). 1) LiCl – 10 mg-equivs/liter; 2) NaCl – 10 mg-equivs/liter; 3) KCl – 10 mg-equivs/liter; 4) NaCl – 1 mg-equiv/liter; 5) $CaCl_2$ – 10 mg-equiv/liter.

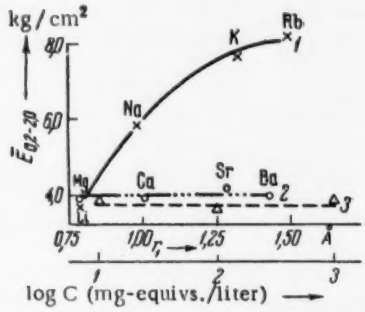

Fig. 4. The relationship between cation radius and the resistance of the residual layer in electrolyte solutions to thinning-out forces (temperature 20°). 1) relationship between the resistance and cation radius for monovalent cations (concentration 10 mg-equivs/liter); 2) the same for divalent cations; 3) the relationship between the resistance and concentration for LiCl solution.

TABLE 1

The Influence of Cation Radius, Solution Concentration and Temperature on h_{bound} (μ) With a Normal Pressure of 1 kg/cm^2

Temperature, °C	Solution conc. mg-eq./l	LiCl	NaCl	KCl	RbCl	$MgCl_2$	$CaCl_2$	$BaCl_2$
20	10	0,27	0,16	0,12	0,11	0,14	0,10	0,09
40	1	0,11	0,08	0,06	—	—	0,06	0,07
	10	0,13	0,09	0,08	0,07	0,08	0,07	0,07
	100	0,15	0,12	0,10	—	—	0,12	0,09
60	1	0,05	0,04	0,04	—	—	0,04	0,03
	10	0,08	0,07	0,06	0,06	0,06	0,05	0,06

TABLE 2

The Resistance of the Residual Layers to Thinning-Out Forces for 0.01 N Solutions of Electrolytes at 20°

Electrolyte	σ_{app} 0.2 – 2.0 kg/cm^2		σ_{app} 1.0 – 4.0 kg/cm^2		σ_{app} 2.0 – 4.0 kg/cm^2	
	h'_{min}	$\bar{E}$, kg/cm^2	h'_{min}	$\bar{E}$, kg/cm^2	h'_{min}	$\bar{E}$, kg/cm^2
LiCl	0,24	3,6	0,20	4,6	0,11	5,5
NaCl	0,13	5,8	0,12	6,0	0,09	6,7
KCl	0,12	7,7	0,10	9,0	0,08	10,6
$CaCl_2$	0,08	4,1	0,07	8,4	0,06	9,6
$BaCl_2$	0,08	4,0	0,06	9,7	0,04	17,0

contact pressures of 0.2-2.0 kg/cm^2, increases with increase in the concentration of the solution, but when the latter reaches 5-10 mg-equivs/liter, further increase in the concentration has little effect.

At the constant low solution concentration, increase in the cation radius brings about a reduction in the boundary viscosity, which corresponds qualitatively to the change in the electroviscosity effect, dependent on the electrokinetic potential. Thus at 20°, after the discs have been in contact for 30 minutes under a pressure of 1 kg/cm^2, the values of η_σ/η for 0.01 N solutions of LiCl, NaCl, KCl and RbCl are equal to 4.6, 4.2, 3.3 and 3.0.

Increase in the temperature has a varied effect on η_σ/η. In the peripheral region of the boundary layer, the increased boundary viscosity decreases more rapidly than the viscosity in the bulk, and η_σ/η decreases; for example, in the case of 0.005 N NaCl solution in a space between the discs equal to 0.23 μ, it decreases from 2.1 to 1.0 when the temperature increases from 20 to 80°. When the thickness of the space is close to 2 h_{min}, this ratio is either only slightly dependent on the temperature, or, which is more frequently the case, increases with increase in temperature (for 0.01 N LiCl solution in a space which is 0.04 μ it is greater than 2 h_{min}, the ratio increases by a factor of almost 2 when the temperature increases from 20 to 90°). The latter phenomenon, as already noted for the case of mineral oils [2] indicates a higher flow activation energy and viscosity temperature coefficient in the boundary layer than in the bulk of the liquid. The integral values of η_σ/η, measured after the discs have been in contact, also increase, by a factor of 2.9, for 0.005 N KCl solutions after 45 minutes contact, when the temperature increases from 20 to 80°, which is explained both by the particular nature of the viscosity temperature coefficient of the boundary layer and also by the decrease in the residual space between the discs (see below, and also [2, 3]).

The coefficient of boundary viscosity increase, measured after the discs have been in contact for 10 minutes and more, is very sensitive to the presence of electrolytes. As can be seen from Fig. 1, in aqueous solutions

between quartz it increases with increase in temperature, concentration, valence and radius of the cations. The value of ψ may increase as a result of the increase in viscosity of the boundary layer, as in the case of solutions of fatty acids in mineral oils, which have been studied earlier [1, 12], and also as a result of a decrease in the space between the discs. It follows from the Stefan-Reynolds equation that ψ is a function of a geometrical factor and is inversely proportional to the square of the gap distance when the radius of the discs is constant. Since the boundary viscosity decreases with increase in cation radius and at solution concentrations greater than 10 mg-equivs/liter is practically constant, their influence on ψ cannot be regarded as a consequence of the boundary viscosity increase. On the other hand it is known that these factors, like increase in valence, lead to a reduction in the ion diffusion layer [4, 10]. Finally, it seems improbable that the viscosity of the boundary layer should increase with increase in temperature, so that there is every reason to assume that the increase in ψ shown in Fig. 1 is brought about by a decrease in the space between the discs and, in the systems under study, may be taken as a measure of the latter.

The thickness of the residual layer in electrolyte solutions decreases with increase in the temperature. At low load values and a temperature of 20°, increase in the concentration at first leads to an increase in h_{min}, from a value which for high-purity water is below the limit of the sensitivity of the method, to values of 0.1-0.3 μ, after which further increase (above 7-10 mg-equivs/liter) has no influence on this value. In the case of loads which do not exceed 1-2 kg/cm^2, h_{min} decreases with increase in cation radius and especially with decrease in ion hydration (Fig. 2). At higher loads the influence of hydration becomes insignificant and the relationship between h_{min} and the cation radius r_{cat} approaches a simple relationship of the form: $h_{min} = k_1 - k_2 \cdot r_{cat}$, where k_1 – a constant which decreases with increase in the valence of the ions, the temperature and the load and with decrease in the concentration of the solution below 10 mg-equivs/liter; k_2 – a constant which is close to zero for high loads. The smaller thickness of the residual layer in solutions containing divalent cations, compared with solutions containing monovalent cations, agrees with the relationship between the thicknesses of the diffusion layers for the first and second ions.

As might have been expected, the separating pressure for the solutions under study increases with decrease in the distance between the solid bodies (Fig. 3). It also increases with decrease in cation radius and on going from divalent cations to monovalent cations. When the spaces are small, the differences between the ions are evidently smoothed out; the possibility that this phenomenon is dependent on the reduction in the sensitivity of the method is not, however, excluded.

The influence of cation radius is clearly shown on the resistance of the residual layers to thinning-out forces (Fig. 4). It is interesting to note that increase in the radius of monovalent cations brings about an increase in $\overline{E}\sigma'_{app} - \sigma''_{app}$, whereas it leads to a decrease in the separating pressure. Increase in the load and the corresponding decrease in the thickness of the residual layer leads to an increase in its resistance to thinning-out forces (Table 2).

Many of the regular relationships described may be interpreted on the basis of modern theories of the structure and thickness of diffuse layers and their interactions, but in order to explain the influence of ionic radius, particularly for ions such as Li^+ and Na^+, it is also necessary to apply ion hydration theory. The energy of the linkage between ions and water molecules lying outside the first sphere of the hydration envelope makes up a significant fraction of the total hydration energy [11]. It is therefore not surprising that at low contact pressures, the hydration of the ions in the boundary layers may have an important influence on the properties of these layers whereas at relatively high pressures the part played by the hydration is slight.

LITERATURE CITED

[1] G. I. Fuks, Zav. Labs. 21 (12) 1455 (1955).

[2] G. I. Fuks, Proc. 3rd All-Union Conference on Colloid Chemistry, Izd. AN SSSR, 1956, p. 301.

[3] G. I. Fuks, Proc. Acad. Sci. 103, 635 (1957); Colloid J. 20, 379 (1958).*

[4] A. I. Rabinerson, Problems in Colloid Chemistry, Leningrad, 1937.**

[5] B. V. Deriagin, Colloid J. 17, 207 (1955).*

*Original Russian pagination. See C. B. Translation.

**In Russian.

[6] B. V. Deriagin and E. V. Obukhov, Colloid J. 1, 385 (1935); B. V. Deriagin and M. M. Kusakov, Bull. AN SSSR, Chem. Series, No. 5, 471 (1936); No. 5, 1119 (1937); J. Phys. Chem. 10, 153 (1939); 26, 1536 (1952); M. M. Kusakov and A. S. Titievskaia, Proc. Acad. Sci. 28, 333 (1940).

[7] G. I. Fuks, V. M. Klychnikov and E. V. Tsyganova, Proc. Acad. Sci. 65, 307 (1949).

[8] A. D. Malkina and B. V. Deriagin, Colloid J. 12, 431 (1950).

[9] G. I. Fuks, Coll. Clockworks, Vol. 1, The Lubricant Properties of Instrument Oils, 1956.*

[10] E. Verwey, Chem. Rev. 16, 367 (1935).

[11] K. P. Mishchenko, J. Phys. Chem. 26, 1376 (1952); K. P. Mishchenko and A. M. Sukhotin, J. Phys. Chem. 27, 26 (1953); K. P. Mishchenko and E. I. Kviat, J. Phys. Chem. 28, 1451 (1954).

Received February 28, 1958

* In Russian.

AN INVESTIGATION OF THE STRUCTURES OF LIQUID Bi – Sn ALLOYS

N. V. Alekseev and Ia. I. Gerasimov, Corresponding Member, Acad. Sci., USSR

Basically, the properties of liquid alloys are fixed by the strength of the intermolecular bonds, and by the resulting arrangement of the molecules relative to one another. Thus there is need to experimentally establish the structures of liquid alloys and to discover at least a qualitative relationship between these structures and the alloy properties.

For a liquid consisting of atoms of several different species, the radial distribution curve can be developed from the equation [1]:

$$4\pi r^2\rho(r) = 4\pi r^2 \sum_{a=1}^{P} m_a k_a \rho_a(r) = \tag{1}$$

$$= 4\pi r^2\left(\sum_{a=1}^{P} m_a k_a^2\right)^2 V_m^{-1} + \sum_{a=1}^{P} m_a k_a^2 \frac{2r}{\pi}\int_0^\infty S\left(\frac{I_n}{\sum_{a=1}^{P} m_a f_a^2(S)} - 1\right)\sin rs\,ds.$$

The EM-4 electron diffraction apparatus which was available for the study of the Bi – Sn system had to be adapted to work at high temperatures. For this purpose a special specimen holder was constructed (Fig. 1). A strip of sheet tantalum served as the heating element, this sheet being affixed to the metal base, 3, by the special clamps, 1, and the porcelain insulators, 2. Placed on the table of the electron diffraction apparatus, the device permitted all of the necessary movements to be carried out. Current for the heater was supplied through the clamps 1, which were connected by the flexible leads 4 to the accessory socket on the EM-4 electron diffraction apparatus.

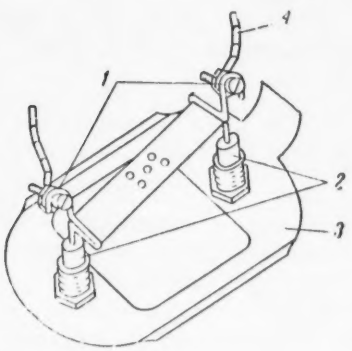

Fig. 1. Specimen holder.

The method of free metallic films which had been proposed by A. I. Bublik and B. Ia. Pines [2] did not give trustworthy results. The best results were obtained when the free metallic film was reinforced by a very thin layer of quartz.

The specimens were prepared in the following manner: a thin layer of polystyrol was deposited on an object glass, following which layers of quartz, metal, and quartz were successively deposited by vaporization in a VUP-4 apparatus. Vaporization was so carried out that the layer thickness did not exceed $1-2\cdot10^{-7}$ cm. Separation of the film was brought about by dissolving the polystyrol in a mixture of benzene and dichloroethane.

Diffraction diagrams were obtained at t = 290°. The experimental intensity curve for any given alloy was built up in the usual manner from the resulting plot [3]. The atoms of Bi and Sn are heavy enough so that the correction for incoherent scattering could be neglected. Normalization of the intensity curves was achieved by equating the areas under the $I(S)S^2$ and $\left(\sum_{a=1}^{P} f_a^2(S)m_a\right)S^2$. curves. Here $\sum_{a=1}^{P} f_a^2(S)m_a = C_1 f_1^2 + C_2 f_2^2$,

C_1 and C_2 being the concentrations of the respective components in atomic fractions.

The resulting intensity curves are shown in Fig. 2. The positions of the diffraction maxima are indicated in Table 1.

We will deal, first of all, with the pure metals. The positions of the intensity maxima in Sn are in good agreement with the data of K. Gammertsfelder [4] and A. I. Bublik [8]. It is clear that the structure of liquid Bi changes markedly with the temperature. When our data are compared with those of Khendus [6] (t = 390°), it is to be seen that the positions of the first maxima are almost indentical (2.05 S units, according to Khendus), and that in the place of our second subsidiary maximum, and the third maximum, Khendus has a weak maximum at S = 3.05, which clearly results from the effect of these two. The positions of the remaining maxima are essentially the same.

TABLE 1

Composition of alloy (wt. %)	Position of maxima ($S = 4\pi \sin\vartheta/\lambda$)				
	1	2	3	4	5
Sn_{pure}	2,22	—	2,90	4,25	6,15
80 Sn—20 Bi	2,14	—	2,57	4,07	5,10
60 Sn—40 Bi	2,12	—	—	4,05	5,85
40 Sn—60 Bi	2,10	—	3,05	3,95	6,05
20 Sn— 80Bi	2,08	—	—	3,75	5,19
Bi_{pure}	1,98	2,22	3,14	3,80	5,05

On comparing the intensity curves for the intermediate alloys, a gradual transition from the pure Sn type to the pure Bi type is noted, but additional maxima do not appear.

The experimental values of the normalized intensity were employed in developing the radial distribution functions from Equation (1).

The evaluation of the integral of Equation (1) was carried out on an electrical calculating machine, values of r being taken at intervals of 0.05 A.

In fixing the mean numbers of atoms per unit volume, use was made of the published data on the densities of the liquid Bi — Sn alloys [7]. The radial distribution curves which were built up in this way are shown in Fig. 3.

The consideration of these curves can well be divided into three steps.

1. Pure Bi and Sn (Fig. 3). The position of the first maximum on the radial distribution curve for Sn_{pure} (3.25 A) is in good agreement with published data which have been obtained at the same temperature [4]. The same is true of the number of nearest neighbors, which is 10.

The data of various authors on the radius of the first coordination sphere in Bi_{liq} shows considerable variance. Thus Khendus found this radius to be 3.32 A at 390° [6], while A. I. Bublik and A. G. Buntar' [8] reported 4.15 A at 400° and 3.85 A at 300°. The value of 3.85 A which we obtained agrees well with the results of the latter authors. The number of nearest neighbors is 7.02 (7-8, according to Khendus).

2. Alloy of eutectic composition (Fig. 3). The first maximum (from 2.95 A to 4.65 A) on the radial distribution curve results from the superposition of three maxima: a strong maximum at 3.30 A, a maximum of lower intensity at 4.15 A and another, still weaker, maximum at 3.75 A.

The position of the first of these maxima is in good agreement with the value of the shortest distance between the atoms in liquid Sn (3.25 — 3.35 A). According to the data of A. I. Bublik and A. G. Buntar', a distance corresponding to 4.15 A can exist in liquid Bi, though, to be sure, only at the very highest temperatures (400°). The value of 3.75 A is close to the arithmetical mean of r_1 and r_2 (3.72 — 3.75 A). It is thus natural to suppose that this figure represents the distance between unlike atoms (the Bi — Sb distance, and conversely). Areas corresponding to these three maxima were marked-out under the radial distribution curve, and from them the numbers of nearest neighbors were calculated.

These calculations showed that 7.8 Sn atoms were distributed around a given Sn atom at a distance of 3.35 A, 2.1 additional atoms of Bi being located at the somewhat greater distance of 3.85 A. Thus, the total coordination number, 9.9, is the same as for pure tin.

A single Bi located in the center of the coordination sphere has grouped around it 2 Sn atoms (r = 3.85 A) and 5.2 Bi atoms (r = 4.15 A). The total coordination number, 7.2, is approximately the same as the coordination number of pure bismuth [7]. This penetration of Sn atoms into the Bi coordination sphere clearly leads to an expansion of this sphere such as is characteristic of it at higher temperatures.

In this case there is a marked tendency toward microheterogeneity. The atoms of Bi and Sn strive to surround themselves with like particles. Atoms of the opposite kind are repelled from the coordination sphere and form, as it were, an additional, secondary sphere. Complete microheterogeneity, such as is met in the eutectic Bi – Pb [9] and Pb – Sn [10] alloys, is not obtained, however.

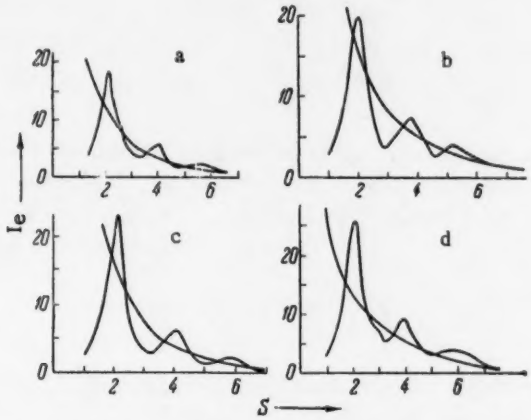

Fig. 2. Normalized intensity curves for Bi – Sn alloys. a) Alloy, Sn 80% – Bi 20%, b) Sn 60% – Bi 40%, c) Sn 20% – Bi 80%, d) eutectic (Sn 41% – Bi 59%).

3. Alloys whose compositions fall between the eutectic and the pure components. Here the maxima are no longer separated and do not coincide with the maxima for the pure components.

Such a situation could arise either because of the existence of a definite order in the distribution of the atoms, or, on the contrary, because of complete miscibility of the components, atoms of both types entering into the neighborhood of the individual particle. There is, however, no support for the first of these hypotheses, since compounds of Bi and Sn do not exist.

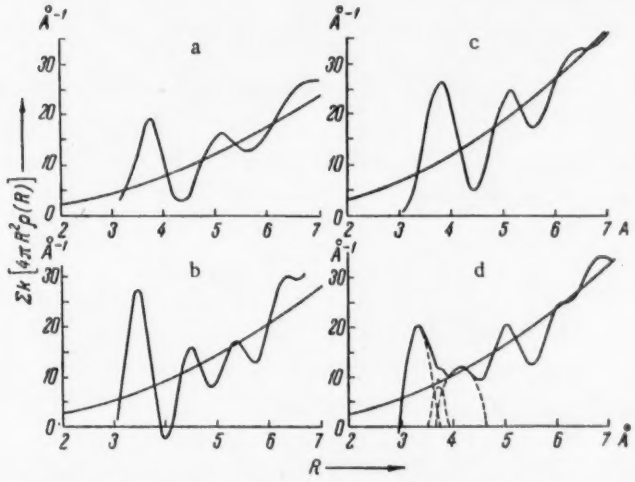

Fig. 3. Radial distribution curves for liquid Bi – Sn alloys. The letters have the same significance as in Fig. 2.

We will now consider the second case. In general, a peak on the radial distribution curve might arise as the result of the superposition of the four conceivable types of neighborhoods, i.e., neighborhoods of the types a – a, a – b, b – a and b – b. If a radial distribution function is ascribed to each type of neighborhood, separately, it is then possible to write:

$$S_{\max} = 4\pi \int_{r_1}^{r_2} \rho_{\exp}(r) r^2 dr = \\ = 4\pi \int_{r_1}^{r_2} [C_a k_a^2 \rho_{aa}(r) + C_a k_a k_b \rho_{ba}(r) + C_b k_a k_b \rho_{ba}(r) + C_b k_b^2 \rho_{bb}(r)] r^2 dr. \quad (2)$$

In an actual alloy, atoms of both sorts will enter into the neighborhood of the individual particle, the probability of such penetration being proportional to the concentrations of the respective components in the case of complete miscibility, so that $\rho_{aa} = C_a \rho^0_{aa}$, $\rho_{ab} = C_b \rho^0_{ab}$, $\rho_{ba} = C_a \rho^0_{ba}$, $\rho_{bb} = C_b \rho^0_{bb}$. Thus we can write:

$$S_{\max} = 4\pi \int_{r_1}^{r_2} \rho_{\exp}(r) r^2 dr = \\ = 4\pi \int_{r_1}^{r} [C_a^2 k_a^2 \rho^0_{aa}(r) + C_a C_b k_a k_b \rho^0_{ab}(r) + C_a C_b k_a k_b \rho^0_{ba}(r) + C_b^2 k_b^2 \rho^0_{bb}]^2 dr. \quad (3)$$

When the miscibility is complete, it can be supposed that

$$\rho^0_{aa}(r) = \rho^0_{ab}(r) = \rho^0_{ba}(r) = \rho^0_{bb}(r) = \rho^0_{av}(r). \quad (4)$$

Equation (3) can then be rearranged as:

$$S_{\max} = 4\pi \int_{r_1}^{r_2} [C_a^2 k_a^2 + 2C_a C_b k_a k_b + C_b^2 k_b^2] \rho_{av}(r) r^2 dr; \quad (5)$$

$4\pi \int_{r_1}^{r_2} \rho(r) r^2 dr = n$, because of normalization, and it follows that

$$S_{\max} = (C_a^2 k_a^2 + 2C_a C_b k_a k_b + C_b^2 k_b^2) n. \quad (6)$$

Calculated according to this equation, the following results were obtained for the coordination numbers. Alloy No. 1: $n_{tot} = 12.4$, or ~ 10 atoms of Sn and ~ 2 atoms of Bi. Alloy No. 2: $n_{tot} = 10.1$, or ~ 6 atoms of Sn and ~ 4 atoms of Bi. Alloy No. 4:* $n_{tot} = 10.2$, or, ~ 3 atoms of Sn and ~ 7 atoms of Bi.

LITERATURE CITED

[1] B. K. Vainshtein, Crystallography, 2 No. 1 (1957).**

[2] B. Ia. Pines and A. N. Bublik, J. Tech. Phys. 24, 1139 (1954).

[3] N. N. Iamzin, Trans. Ins. Crystallog. 5, 69 (1949).

[4] C. Gammertsfelder, Phys. Rev. 55, 1116 (1939).

[5] A. N. Bublik, Crystallography 2, 249 (1957).

*As in original – Publisher's note.

**Original Russian pagination. See. C. B. Translation.

[6] N. V. Radchenko, Prog. Phys. Sci. 61, 249 (1957).

[7] M. Pluss, Zs. anorg. u. allgem. Chem. 93, 1 (1915).

[8] A. N. Bublik and A. G. Buntar', Crystallography* 3, 39 (1958).

[9] A. S. Lashko, Sympos. Problems in the Physics of Metals and Metal Working (in Russian), 1957, p. 183.

[10] A. F. Skryshevskii, Sympos., Problems in the Physics of Metals and Metal Working (in Russian), 1957, p. 187.

The M. V. Lomonosov State University,
Moscow

Received April 16, 1958

*Original Russian pagination. See C. B. Translation.

THE ACTION OF THE γ-RADIATION OF Co^{60} ON $Ca(NO_3)_2 \cdot 4H_2O$

A. S. Baberkin and M. A. Proskurnin

(Presented by Academician V. A. Kargin, March 21, 1958)

Compounds of the type of $Ca(NO_3)_2 \cdot 4H_2O$ can be looked on as special instances of complex formation. Due to the neutrality of the water molecules, the complex ions which are formed in such cases have the same charge as the complex-former. Either the cations or the anions of a salt can serve as complex-forming ions.

The lack of data on the properties and internal structures of the great majority of the crystal hydrates makes it impossible to mark out any rules regarding the stabilities of these compounds. No more has been established than that an increase in the charge of the cation and a decrease in the volume usually favors an increase in the number of molecules of water of crystallization and tighter binding of these molecules.

There has been almost no study of the radiational stability of the crystal hydrates. We have only the work of Doigan and Davis [1] on the photochemical breakdown of the crystal hydrate of lanthanum nitrate and that of Hochanadel and Davis [2] on the effect of γ-radiation on this same compound. In these works it has merely been noted that the hydrated lanthanum nitrate decomposes at a higher rate than the anhydrous salt.

We have carried out several series of experiments on solid calcium nitrate, $Ca(NO_3)_2 \cdot 4H_2O$, the aim being to elucidate the peculiarities in the behavior of the inorganic crystal hydrates as compared with the anhydrous salts and concentrated solutions.

Chemically pure salt was subjected to irradiation in vacuum at 25°.

A number of experiments were performed on melts of calcium nitrate. These melts were prepared by fusing the salt in vacuum, and had the form of supercooled solutions (degree of supercooling, 30°) which could be maintained for long periods without the separation of crystals. A Co^{60} preparation with a dose strength of $6.2 \cdot 10^{19}$ ev/g·hour, was employed as the radiation source.

Qualitative and quantitative analyses of the gaseous products from the breakdown of the salt were carried out in a microburette. The precision of measurement amounted to 2-3%. Nitrites were determined colorimetrically according to the method which has been developed by Mikhal'chuk and Osherovich [3]. The error of measurement was $5 \cdot 10^{-7}$ moles of nitrite ion per gram of salt. From these experiments, it was established that hydrated calcium nitrate decomposes under the action of γ-radiation to form the nitrite and oxygen. The greater portion of the oxygen which is produced by irradiation remains in the crystal, just as in the case of the irradiation of solid anhydrous nitrates. An amount of oxygen equivalent to the product nitrite can be obtained by melting the irradiated salt.

The relation between the amount of product nitrite and the radiation dosage is shown in Fig. 1. Curves for the solid crystal hydrate, and for the anhydrous salt, are given in the left-hand portion of the figure, while in the right-hand portion the curves are for the melt, and the melt with added glucose.

Data on the yield of nitrite and oxygen per 100 ev are presented in the Table. Here the C' values use G values given in reference to the ratio of the numbers of electrons in the nitrate ion to the total number of electrons in the salt.

The radiational stability of quite a few solid hydrates has already been studied [4-6]. In the interaction of an ionizing particle and a substance, the initial step consists in the transfer of a portion of the energy to one

of the electrons of a molecule. It is supposed that approximately one half of the energy of the ionizing particle is expended in ionization, while the other half goes to the excitation of the molecule. The further course of the ionized and excited molecules depends to a considerable degree on the state of aggregation and on the physicochemical properties of the medium.

TABLE

Irradiated specimen	$G_{NO_2^-}$, moles/100 ev	Electron dose, NO_3^-	$G'_{NO_2^-}$, moles/100 ev	G_{O_2}, moles/100 ev
Solid $Ca(NO_3)_2$	0.2 ± 0.01	0.78	0.25	–
Solid $Ca(NO_3)_2 \cdot 4H_2O$	0.77 ± 0.02	0.52	1.5	0.37 ± 0.02
Molten $Ca(NO_3)_2 \cdot 4H_2O$	0.07 ± 0.01	0.52	0.13	0.02 ± 0.01
Molten $Ca(NO_3)_2 \cdot 4H_2O$ with the addition of glucose	0.26 ± 0.01	0.52	0.5	0.02

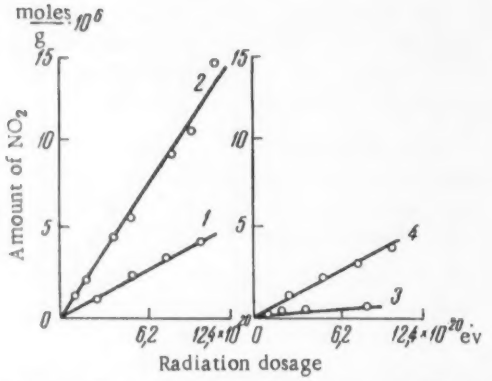

Fig. 1. The relation between the amount of product nitrite and the radiation dosage: 1) solid $Ca(NO_3)_2$, 2) solid $Ca(NO_3)_2 \cdot 4H_2O$, 3) molten $Ca(NO_3)_2 \cdot 4H_2O$, 4) molten $Ca(NO_3)_2 \cdot 4H_2O$ with added glucose.

In the anhydrous nitrates, the basic reaction processes can be considered to be:

$$NO_3^- \rightsquigarrow NO_3 + \bar{e} \qquad (1)$$

$$NO_3^- \rightsquigarrow NO_3^{-*} \rightarrow NO_2^- + O. \qquad (2)$$

It is not known to what extent each of these two processes contributes to the reaction. The oxygen which is split off in Reaction (2) clearly remains in the immediate neighborhood of the NO_2^- ion, and the reverse reaction of forming the nitrate from the nitrite and oxygen assumes an essential role. The possibility of this reverse reaction has been demonstrated by us in the case of calcium nitrate [7].

In the case of the crystal hydrates, the water molecules can be looked on as foreign substances which also capture electrons and are subject to ionization. It is obvious that the two processes which have been presented above for the reaction of the irradiated nitrate ion are ones that can also occur in the crystal hydrate. Moreover, if the water molecule is capable of capturing an electron, it follows that

$$H_2O + e^- \rightarrow H_2O^- \rightarrow H + OH^- \cdot aq, \quad 2H + NO_3^- \rightarrow NO_2^- + H_2O. \qquad (3)$$

The product hydrogen atom can here interact with a neighboring NO_3^- ion to form a nitrite ion.

It has been noted above that the reverse reaction of oxidation of the nitrite by oxygen can take place under anhydrous conditions. In the case of the crystal hydrates, the rate of the reverse reaction is markedly reduced because of the structural peculiarities of these salts, and the oxygen which is formed according to Reaction (2) can react with a neighboring NO_3^- to give NO_2^- and O_2.

It is to be seen that these two factors taken together can serve as an explanation of the increased yield of nitrite in the crystal hydrate as compared with the anhydrous salt. The structures of highly concentrated solutions of inorganic salts have been studied by a number of authors [8, 9]. The general conclusion which can be drawn from this work is that the distribution of the ions in solution tends to approach that of the crystal hydrate as the concentration is increased. In the present case, the concentration of the nitrate in the melt is approximately 26 M when calculated on the basis of the water of crystallization, and it is clear that the ion

distribution in this melt will differ but little from that of the crystal hydrate. Thus all three reaction processes: ionization, excitation and the water molecule effect, will be effective in this system. However, the contribution of each of these processes to the yield of nitrite from the breakdown of the nitrate will be different from what it is in the case of the solid crystal hydrate.

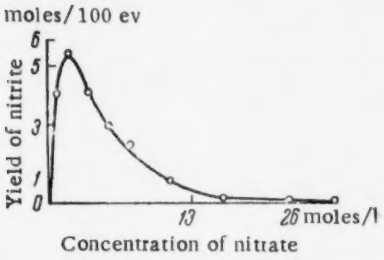

Fig. 2. The relation between the yield of nitrite and the concentration of calcium nitrate.

Most authors who have studied the concentrated nitrate solutions have observed a marked increase in the yield of nitrite (up to 4.5 moles/100 ev) in the concentration region from 0.1 to 2 M. The explanation of this effect is connected with the possibility of direct action of the radiation on the NO_3^- ions.

The sharp decrease which we have observed in the nitrite yield of the melt, as compared with the solid crystal hydrate, has prompted us to investigate the radiochemical stability of calcium nitrate over the wide concentration interval from 0.1 to 26 M.

The relation between the yield of nitrite and the concentration of calcium nitrate is shown in Fig. 2. A sharp increase in the yield of nitrite (up to 5.4 moles/100 ev) is actually observed in the region of concentrations up to 2 M. The curve falls precipitately at higher concentrations, a fact which speaks against the effectiveness of the direct action of the radiation on the nitrate ion.

In our opinion, the following reaction could be the cause of the diminished yield of nitrite in highly concentrated solutions

$$NO_3 + H_2O \rightarrow H_2O^+ + NO_3^-. \quad (4)$$

In this case, the product NO_3 radicals can prove to be stable enough to persist until the reaction $NO_3 + NO_2 \rightarrow N_2O_5$ takes place or some similar change occurs to decrease the effectiveness of the process. On solidifying the melt and ordering of the ions into a crystal lattice, the minimum distance between the product H_2O^+ ions from the radiolysis and the neighboring NO_3^- ions increases and the appearance of the NO_3 radicals is rendered more difficult. Clearly, the observed nitrite yield in the melt should be related to the direct action of the radiation on the nitrate anion. Such a hypothesis does not exclude the possibility of a partial reaction through the products from the radiolysis of water and is substantiated by the introduction into the melt of glucose, an acceptor for the OH^- radicals.

LITERATURE CITED

[1] P. Doigan and T. W. Davis, J. Phys. Chem. 56, 764 (1952).

[2] C. J. Hochanadel and T. W. Davis, J. Chem. Phys. 27, 333 (1957).

[3] B. V. Mikhal'chuk and R. E. Osherovich, Plant Lab. 9, 836 (1940).

[4] A. O. Allen and J. A. Ghormley, J. Chem. Phys. 15, 208 (1947).

[5] G. Henning, R. Lees and M. Mathesson, J. Chem. Phys. 21, 664 (1953).

[6] L. E. Lamar, Nuclear Sci. Abstracts 9, 59/13 (1955).

[7] A. S. Baberkin, M. A. Proskurnin and V. D. Orekhov, The Action of Ionizing Radiations on Organic and Inorganic Systems (in Russian), Acad. Sci. USSR, Press, 1958, p. 43.

[8] J. Beck, Phys. Zs. 40, 474 (1939).

[9] J. P. Mathieu and M. Lounsbury, Compt. rend. 229, 1315 (1949).

Received March 27, 1958

RADIOACTIVE CATALYSTS

THE DEHYDRATION OF CYCLOHEXANOL ON MAGNESIUM AND SODIUM SULFATES

A. A. Balandin, Academician; Vikt. I. Spitsyn, Academician;
N. P. Dobrosel'skaia and I. E. Mikhailenko

In recent years papers have appeared reporting the use of irradiation by gamma-rays, or neutrons, to affect the processes of heterogeneous catalysis [1-3].

In our experiments, on the other hand, it was the catalyst itself which contained various amounts of beta-radiating isotopes and served as the source of ionizing radiation for the reactions of heterogeneous catalysis of gaseous substances. It was assumed that the processes occurring at the solid – vapor interface (the adsorption of reagent molecules on the catalyst, chemical reaction between these molecules, the exchange of atoms, or, possibly, molecules, between the adsorbed layer and the gaseous boundary zone) would be energetically affected through the continuous bombardment by beta particles. The possibility that the radiation might affect the structure of the catalyst, that it might, in particular, alter the catalyst surface, or that there could be a radiochemical action of the radiation on the gaseous reagents before these latter have made contact with the catalyst, was not excluded.

For experiment, there was selected the reaction of catalytic dehydration of cyclohexanol on magnesium and sodium sulfates in which the sulfur had been replaced by various amounts of the radioactive isotope S^{35}.

These investigations were carried out in a flow-type catalytic apparatus with a detachable reactor [4], this apparatus being inserted in an automatically controlled horizontal tubular furnace; the temperature was measured with a thermocouple which was inserted in a well in the catalyst. For this cyclohexanol: b. p. = 70°/ 20mm; $n_D^{30} = 1.4625$; $d_4^{30} = 0.9445$.

Radioactive $MgSO_4$ was prepared from recrystallized inactive magnesium sulfate (CP) by addition of sodium sulfate containing radioactive sulfur and stable sodium sulfate (CP), the latter serving as a carrier. The ratio of S^{35} to ordinary sulfur was $1.8 \cdot 10^{-10}$. A weighed amount of magnesium sulfate was dissolved in water and a definite quantity of the solution of active sodium sulfate was then introduced so that ionic exchange took place. This solution was evaporated; the resulting salt was gradually heated to 400° [5] and then held this temperature for 1.5 hours. Preliminary experiments had shown that a catalyst prepared in this manner was completely anhydrous. In order to obtain comparable results, radioactive and nonradioactive catalysts were prepared to contain the same amount of sodium sulfate, this sulfate being the stable (CP) compound in the one case, and the radioactive compound in the other. In addition, the dehydration of cyclohexanol was studied on anhydrous magnesium and sodium sulfates.

The radioactivity of the catalyst was measured with an end-window counter [6]. A definite amount of solution, usually 0.1 ml, was placed on a piece of filter paper in an aluminum cup, and evaporated. The activity of the preparation was always measured under the same geometrical conditions with respect to the counter.

Kinetic experiments on the dehydration of cyclohexanol were carried out on 0.5 ml of each of the prepared catalysts (the weights of these samples were known and varied from 0.14 to 0.30 g) over the temperature interval 355 – 415° with a constant volume velocity of cyclohexanol of 0.4 min^{-1}.* Constant catalytic activity was established after 3 hours of operation, this being indicated by the fact that the degree of conversion of the

*As in original – Publisher's note.

cyclohexanol at fixed temperature was reproducible. After each experiment the catalyst was regenerated for 45 minutes in a current of dry air, flowing with a velocity of 9 l/hour. Each experiment lasted 30 minutes. No investigation was made of the catalytic products which were collected in the first 15 minutes. The degree of conversion was determined by titrating a weighed amount of the products obtained in the second 15 minutes after the beginning of the experiment, use being made of the Kaufman method of bromine numbers [7]. The applicability of this method was confirmed by titrating previously prepared mixtures of $C_6H_{11}OH$, C_6H_{10} and H_2O. The cyclohexane was separated and showed the values: b. p. = 81.5°, $n_D^{20} = 1.4472$; $d_4^{20} = 0.8117$.

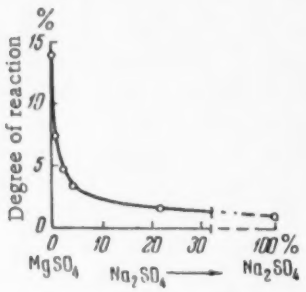

Fig. 1. The relation between the catalytic activity and the added Na_2SO_4 (380°).

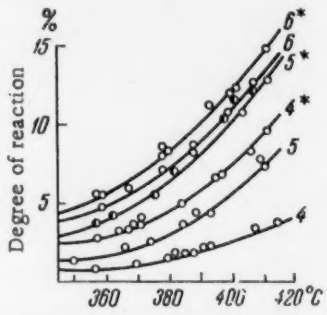

Fig. 2. The effect of the intensity of irradiation of the catalyst on the catalytic activity.

Gaseous products were not obtained in the reaction. A tagged-atom IMA-1 intensiometer which had been designed for the determination of the soft beta-radiation from S^{35} was placed in the apparatus, beyond the receiver with the catalyst. This instrument indicated the absence of any kind of radioactive contaminant.

TABLE 1

The Apparent Energy of Activation for the Dehydration of Cyclohexanol on $MgSO_4$ Containing Various Amounts of Added $NaSO_4$

Catalyst No.	Characteristics of catalyst		Number of experiments	Apparent energy of activation, kcal/mole
	Content of Na_2SO_4, wt. %	Absolute activity		
1	0	0	6	15.2
2	100	0	11	23.8
3	2.07	0	11	20.1
4	21.87	0	11	20.8
4•	21.87	105.2	9	19.2
5	4.06	0	8	21.4
5•	4.06	9.2	9	19.2
6	0.52	0	9	16.4
6•	0.52	1.26	9	15.5

The catalytic activity was characterized in terms of the degree of dehydration of the cyclohexanol, referred to 0.1 g of the catalyst. The catalytic activity proved to fall as nonradioactive sodium sulfate was added to the magnesium sulfate. From Fig. 1, it is to be seen that anhydrous sodium sulfate is also a catalyst for the dehydration of cyclohexanol, although its activity is considerably less than that of magnesium sulfate.

The experiments were set up in pairs so as to allow an interpretation of the effect on the catalytic activity of the replacement of ordinary sulfur by S^{35}. In each pair of experiments, the Na_2SO_4 : $MgSO_4$ ratio in the catalysts was the same but in one of these catalysts the sodium sulfate had been introduced in the inactive form, and in the other, in the radioactive form containing a definite amount of S^{35}. The same number has been given to each of the catalysts of such a pair, but the number for the radioactive catalyst carries a star. It is quite significant that in each of the experiments with the radioactive catalysts, enhanced catalytic activity as compared with the inactive catalyst containing the same amount of sodium sulfate was observed (Fig. 2).

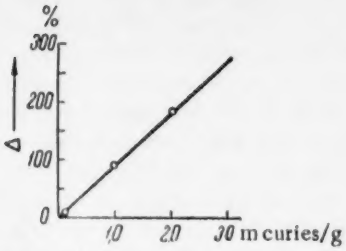

log of the specific activity

Fig. 3. The relation between the increase in the degree of reaction and the logarithm of the specific radioactivity of the catalyst (410°).

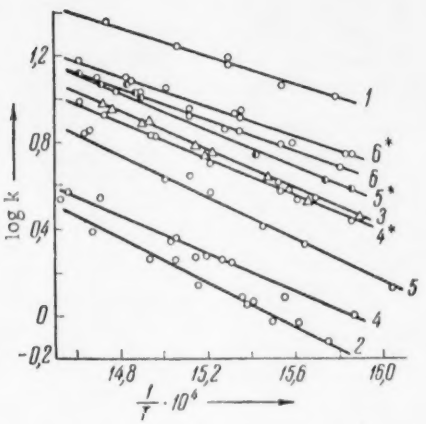

Fig. 4. The relation between the reciprocal temperature and the logarithm of the rate constant for the dehydration of cyclohexanol. 1) $MgSO_4$ (inactive), 2) Na_2SO_4 (inactive), 3) $MgSO_4$ + 2.07% Na_2SO_4 (inactive), 4) $MgSO_4$ + + 21.87% Na_2SO_4 (inactive), 4*) $MgSO_4$ + + 21.87% Na_2SO_4 (radioactive), 5) $MgSO_4$ + + 4.06% Na_2SO_4 (inactive), 5*) $MgSO_4$ + + 4.06% Na_2SO_4 (radioactive), 6) $MgSO_4$ + + 0.52% Na_2SO_4 (inactive), 6*) $MgSO_4$ + + 0.52% Na_2SO_4 (radioactive).

Under fixed conditions, the degree of conversion of cyclohexanol into cylohexene will be designated by a in the case of the inactive catalyst and by a* in the case of the radioactive catalyst. The quantity, $\Delta = 100(a^* - a)/a$, we will call the increase in the degree of conversion.

The quantity Δ proved to increase with increasing radioactivity of the catalyst, though not in the same proportion. In the kinetic experiments, the degree of conversion did not usually exceed 15%, and reached 23% only in certain individual cases. Earlier work [8] has shown that only a small error is made in setting the rate constant, k, equal to the degree of conversion; in addition, it is possible to graphically evaluate the energy of activation, ε, for the dehydration process through the Arrhenius Equation $K = k_0 e^{-\epsilon/RT}$ (Fig. 4, Table 1).

It is possible to be convinced of the validity of the Arrhenius Equation under the experimental conditions applying to the action of the radioactive catalysts by noting that all of the curves of Fig. 4 are straight lines. It was not a priori evident that this would be so for radioactive catalysts. It is to be seen from Table 1 that the apparent energy of activation rises with an increase in the added sodium sulfate and diminishes slightly, but quite definitely, on the introduction of the radioisotope S^{35}.

It has thus been established here that radioactive irradiation of the catalyst affects the catalytic activity and the energy of activation.

It is necessary to consider the possible explanation of these results. It could be supposed that the observed effect is related to collisions of the electrons (beta-particles) with the cyclohexanol molecules in the gas phase adjacent to the catalyst. This supposition is not justified since in such a case the cyclohexanol molecules would follow different decomposition paths, just as in pyrolysis. For example, not only dehydration, but also dehydrogenation, would then take place. The preservation of the selectivity of the process indicates the predominance of phenomena occurring on the catalyst surface.

It might then be supposed that the catalyst would be promoted by the elements arising from radioactive decay, or by products of secondary chemical interaction of these particles. This effect is observed, however, even when the proportion of S^{35} amounts to only $1.8 \cdot 10^{-10} \times 0.52 \cdot 142/(100 \cdot 120) = 1.1 \cdot 10^{-12}$ (catalyst No. 6*) and the proportion of the disintegration products is considerably less. On the other hand, it is known that such minute quantities of foreign substances cannot exert a promoting action on a catalyst.

It might be further thought that the surface of the solid body would be broken up under impact from the beta-particles. There is, however, very little likelihood of such an effect here since it is known that break-up becomes appreciable only in the case of bombardment by heavy particles.

In a certain sense, the action of the radioactive additive is similar to that of an elevation of the temperature. It is to be seen from Fig. 3, for example, that a 3.3% conversion is achieved with the inactive catalyst

No. 4 at 410°, and with the radioactive catalyst No. 4*, at the lower temperature of 365°. On this basis it could be supposed that the individual acts of radioactive disintegration give rise to local superheating, with the result that the reaction is accelerated by the accompanying elevation of temperature. Such a supposition is, however, not justified. In the first place, the elevation of the temperature by a mere 45° would not affect the reaction mechanism, and hence would not alter the energy of activation, which, on this basis, should remain unchanged on the addition of the radioactive component to the catalyst. On the other hand, experiment shows that the value of ϵ is not constant in such a case (at 20.8 kcal) but diminishes somewhat (to 19.2 kcal in the experiments indicated above, see Table 1). This speaks against such a supposition. In the second place, it can be shown from data obtained in the present work that the energy of radioactive decay is far from being adequate for the observed acceleration of a reaction calling for a definite energy of activation. Thus the number of places of superheating would be insufficient for the requisite elevation of temperature and this fact also forces the rejection of the supposition that local superheating plays a decisive role.

Thus we have to deal in the present work with an entirely new effect of the combined action of the electrons and the active centers of the catalyst. It should be considered that the beta-particles act here on the active centers of the catalyst which have adsorbed the cyclohexanol molecules. This action of the beta-particles would involve the lowering of the energy of activation for the chemical reaction of dehydration of the cyclohexanol. It would thus become possible to utilize the energies of particles possessing lower translation-velocities for the activation of the molecules, the numbers of such particles are large according to the Maxwell – Boltzmann law for the equilibrium distribution of energies. For a constant value of k_0 and at 410°, calculation according to the Arrhenius Equation shows that the observed diminution of ϵ by 1.6 kcal (from 20.8 to 19.2 kcal) would assure a 3.3 fold increase in the reaction rate as compared with the experimentally observed 2.8 fold increase.

It is beyond question that much interest attaches to the possibility of activating the chemical effect of a catalyst and at the same time maintaining the chosen reaction path, by the introduction of radioactive components. This investigation is being continued.

LITERATURE CITED

[1] E. H. Taylor and J. A. Wethington, Jr., J. Am. Chem. Soc. 76, 971 (1954).

[2] P. B. Weisz and E. W. Swegler, J. Chem. Phys. 23, 1567 (1955).

[3] R. W. Clarke and E. J. Gibson, Nature 180, 140 (1957).

[4] A. P. Rudenko and G. A. Slovokhotova, Zav. Lab. No. 1, 121 (1955).

[5] A. A. Balandin and M. B. Turova-Poliak, et al, Proc. Acad. Sci. USSR, 114, 773 (1958).*

[6] V. I. Spitsyn and P. N. Kodochigov, et al, Methods of Work Employing Radioactive Indicators (in Russian), Acad. Sci. USSR, Press, 1955.

[7] G. D. Gal'perin, Proc. Petroleum Inst. 4, 141 (1954).

[8] A. A. Balandin, Bull. Mos. State Univ. No. 4, 137 (1957).

The M. V. Lomonosov State University, Moscow
The Institute of Physical Chemistry of the
Academy of Sciences of the USSR

Received April 23, 1958

*Original Russian pagination. See C. B. Translation.

A SPECTROSCOPIC STUDY OF THE ADSORPTION AND CATALYTIC REACTION OF CYCLOHEXADIENE ON TRANSPARENT FILMS OF PALLADIUM

V. M. Griaznov, V. D. Iagodovskii, A. M. Bogomol'nyi and Huo Tiu-ok

(Presented by Academician A. A. Balandin, April 24, 1958)

For obtaining information about the state of molecules in the strong surface fields of adsorbents or catalysts, much interest attaches to the study of the spectra of substances in adsorption layers. Most of the investigations in this field have been carried out on reasonably transparent adsorbents, or on aluminosilicate catalysts. In recent years those experimental difficulties have been overcome which were standing in the way of obtaining the spectra of materials adsorbed on metals. Eischens, Pliskin and Francis [1] have investigated the spectra of carbon dioxide adsorbed on copper, platinum, palladium and nickel. Pliskin and Eischens [2] have obtained the infrared spectra of ethylene, propylene and acetylene adsorbed on nickel. In these works, the metals were prepared by heating a paste of nonporous silica globules and a solution of a metallic salt in a current of hydrogen. Thin layers of this paste were spread by hand on a fluorite plate. Note has been made of the difficulty [3] of preparing specimens which would transmit about 6% of the infrared radiation of 5μ wave-length and would, at the same time, have a sufficiently large surface so that it would be possible to measure the absorption bands of the chemosorbed substances. Difficulties are also known to arise from the presence of hydrogen in the reduced metallic surface.

It has seemed desirable to develop a technique for the spectroscopic investigation of adsorption and catalytic reaction on metallic films of fixed optical density; these films to be as nearly free of foreign gases and vapors as possible. We have made use of the vacuum-vaporization of metal onto the windows of an optical cell. In the ultraviolet region of the spectra a completely sealed quartz cell, 16 mm in length, was employed. The conditions required for preparing such mirror films of palladium, approximately 1000 A in thickness, and the results of an investigation of the redistribution of the hydrogen of cyclohexadiene -1,3 on them, have already been published [4]. In the present work, palladium films of a thickness of the order of 100 A were deposited on the windows of the cell at a residual pressure of $1 \cdot 10^{-6}$ mm of Hg, these films transmitting 30% of the radiation of 2600 A wavelength which was passed by the cell prior to vaporization of the metal. These films showed considerable catalytic activity, even at room temperature. Several minutes after introducing cyclohexadiene-1,3* into the cell, the absorption spectrum of this substance was replaced by the characteristic absorption bands of benzene vapors, the indicating being that the reaction $2C_6H_8 = C_6H_6 + C_6H_{10}$ had gone practically to completion.

Somewhat lower catalytic activity was shown by the palladium films of 100 A thickness which were deposited on the fluorite windows of the cell used for the work in the infrared region. These fluorite windows were attached by a special picene to the plane-ground flanges of the cylindrical glass cell, which was 25 mm in length. The absorption spectra of cyclohexadiene vapors at various pressures were obtained in the cell prior to depositing the palladium films on the windows. These spectra were recorded on a twin-beam IKS-2 spectrometer having a lithium fluoride prism. The spectral width of the slits in frequency units was as

*Cyclohexadiene-1,3 which had been synthesized according to the method of Hoffman and Damm [5] was kindly furnished by Prof. R. Ia. Levina, to whom the authors express their deep thanks. The constants of this hydrocarbon were: b. p. 78.5°/740 mm; $n_D^{20} = 1.4740$.

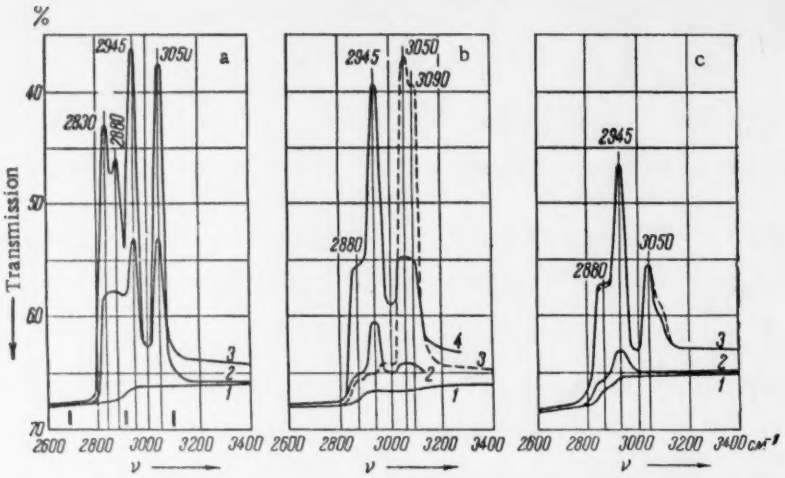

Fig. 1. The absorption spectra of cyclohexadiene as obtained in the cell with fluorite windows. a) prior to the deposition of palladium films on the windows, b and c) with palladium films transmitting 25 and 70%, respectively, of the radiation of frequency 2000 cm^{-1}.

indicated on the axis of abscissas of Fig. 1a. Curve 1 of Fig. 1a corresponds to the transmission of the cell at a residual pressure of $1 \cdot 10^{-4}$ mm of Hg, Curves 2 and 3, to the spectra of cyclohexadiene vapors at pressures of 15 and 75 mm of Hg, respectively. The cyclohexadiene absorption bands at 2945 and 3050 cm^{-1} did not change in character as the pressure fell, but with the given depth of layer, the bands at 2830 and 2880 cm^{-1} were no longer to be resolved at 15 mm of Hg. After evacuating the cell to a pressure of $1 \cdot 10^{-3}$ mm of Hg at room temperature, the transmission curve coincided with the initial Curve 1.

Palladium films were then deposited on both windows of the cell (the transmission at 2000 cm^{-1} being thereby reduced to 25% of the initial value) and, after diaphragming the comparison beam, the spectra which are shown in Fig. 1b were recorded. Curve 1 shows that the palladium films did not have absorption bands in this region of the spectrum. The spectrum of cyclohexadiene vapors which were held in the cell with the palladium films for 10 hours at 75 mm of Hg and 20° (Curve 4) differed from the spectrum which had been obtained prior to the deposition of the palladium films on the cell windows (compare Curve 3, Fig. 1a). In place of the narrow band at 3050 cm^{-1} which was well resolved even under a one to five reduction in the pressure of the cyclohexadiene vapors, there appeared a band at 3050-3090 cm^{-1}. This is exactly what would have been expected in the case of a partial conversion of the cyclohexadiene into cyclohexene and benzene on the palladium films. Among the indicated hydrocarbons, only benzene has intense absorption bands at frequencies above 3050 cm^{-1}. Brodersen and Langseth [6] have shown that the most intense absorption bands in benzene vapors are at 3047, 3083 and 3100 cm^{-1}. This data is in agreement with the spectrum of benzene vapors which is shown by the dotted Curve 3 of Fig. 1b; this spectrum was obtained in this same cell at a pressure of 75 mm of Hg after the cyclohexadiene vapors had been pumped off. At the layer depth and spectral slit-width which were employed, the bands at 3083 and 3100 cm^{-1} could not be resolved, as had been done in the work of Bailey, Hale, Ingold and Thompson [7], but formed a "shoulder" on the more intense 3047 cm^{-1} band. Thus, a widening of the 3050 cm^{-1} band in the spectrum of cyclohexadiene to 3090 cm^{-1}, or the appearance of a "shoulder" on the high frequency side of this band, gave indication of the presence of benzene vapors. It is to be seen from Curve 2 of Fig. 1b that this same situation was observed even on lowering the initial pressure of the cyclohexadiene vapors to 15 mm of Hg. At lower pressures, the absorption bands of the cyclohexadiene vapors could not be detected, a fact which indicated the absence of a firm adsorption of the compound on the palladium films of 100 A thickness, and on the fluorite windows.

Qualitatively different results were obtained with the somewhat less-dense palladium films which were deposited on these same fluorite windows after polishing. The new films transmitted 70% of that infrared radiation at 2000 cm^{-1} frequency which was passed through the fluorite windows. Curve 3 of Fig. 1c represents

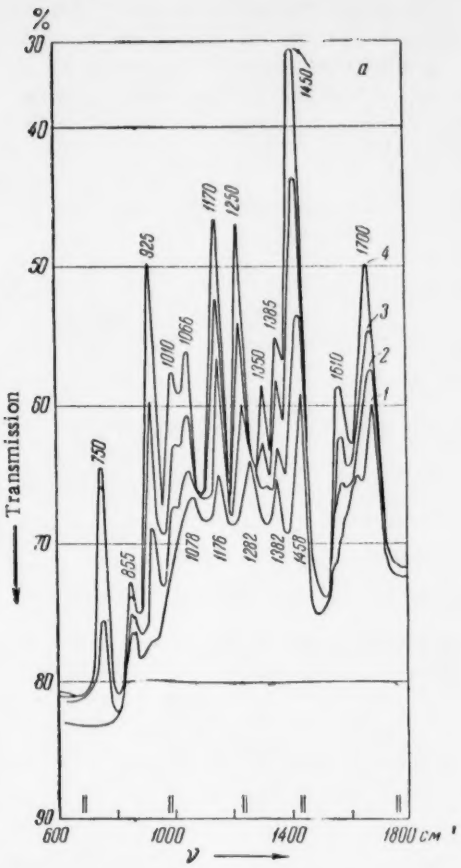

Fig. 2. Absorption spectra of cyclohexadiene as obtained in the cell with rock salt windows which were covered with palladium films. Explanation in the text.

the spectrum of cyclohexadiene vapors which, at an initial pressure of 75 mm of Hg, had been held for 2 hours and 40 minutes at room temperature in the cell with very thin palladium films on the windows. Even within a half hour, the spectrum which was obtained fully agreed with Curve 3, except for those segments which are shown in dotted form. In this case, the band at 3050 cm^{-1} had a "shoulder" on the high-frequency side. In this same section, the absorption increased with the time of contact between the cyclohexadiene vapors and the palladium films, while the intensity of the absorption band of the cyclohexadiene diminished somewhat. Thus, the extremely thin films of palladium on fluorite also possessed catalytic activity with respect to the reaction $2C_6H_8 = C_6H_6 + C_6H_{10}$.

In distinction to the experiments with the more dense palladium films, and to the experiments in which there were no films on the fluorite windows, evacuating the cell with the thin films to a 10^{-3} mm of Hg residual pressure of cyclohexadiene vapors did not lead to the disappearance of all of the absorption bands. Increasing the time of evacuation at room temperature to 30 minutes did not change the character of the spectrum, which is shown as Curve 2 of Fig. 1c.

This spectrum could not belong to the vapors of cyclohexadiene since at the given layer-thickness these vapors did not give absorption bands even at pressures a thousand times as large. The coincidence between the frequency of the 2945 cm^{-1} band and the frequency in the spectrum of cyclohexadiene vapors led to the supposition that what had been obtained was the spectrum of cyclohexadiene which had been firmly adsorbed on the very thin palladium film. This band disappeared only when the spectra were recorded in the course of an evacuation in which the cell pressure did not exceed $1 \cdot 10^{-4}$ mm of Hg (Curve 3 of Fig. 1c).

The fact is striking that the 3050 cm^{-1} band was missing in the spectrum of the firmly adsorbed cyclohexadiene. It is known (see [8], for example) that the bands of valence vibrations of the C – H bonds are to be found in the 3000-3150 cm^{-1} region when unsaturated or aromatic bonds are present at a given carbon atom. Thus in the spectrum of cyclohexadiene firmly adsorbed on palladium, the vibrations of the C – H bond of the $\overset{|}{\underset{||}{C}}$ – H group did not appear.

Similar results were obtained with very thin films of palladium on windows of rock salt, these films transmitting about 80% of the radiation at 2000 cm^{-1} which was passed by the windows before the films were deposited. In this case also, the band at 3050 cm^{-1} did not appear, the spectrum obtained at a pressure of cyclohexadiene vapors of $1 \cdot 10^{-4}$ mm of Hg being that which is represented by Curve 1 of Fig. 2. The character of this spectrum was unchanged after the cell, heated to 50°, had been evacuated for 8 hours and also after the introduction and evacuation of benzene vapors. These experiments were carried out with a glass cell, 145 mm in length, the rock salt windows being affixed to the plane flanges of the cell on vacuum grease. To show the extent of the reproducibility, 10 recordings of the spectrum were made at a residual pressure of 10^{-4} mm. In view of the fact that such spectra could not be obtained on windows which were free of palladium films, it could be assumed that they arose from cyclohexadiene which was firmly adsorbed on the palladium films.

A comparison of the spectrum of the firmly adsorbed cyclohexadiene and the spectra of the vapors at pressures of 12, 30 and 50 mm (these are represented in Fig. 2 by the Curves 2, 3, and 4) showed that a number of the bands had approximately the same frequencies. At the same time, the spectrum of the adsorbed

cyclohexadiene did not show bands at 750 and 925 cm^{-1}, although these bands are intense in the spectrum of the vapor and presumably belong to the nonplanar vibrations of the C − H bonds. The band at 1608 cm^{-1}, which is characteristic of the valence vibrations of the C = C bonds, was more weakly expressed than at comparable vapor adsorption at other frequencies. It can be supposed that these differences between the spectra of the vapors of cyclohexadiene, and of the cyclohexadiene adsorbed on palladium, were due to the formation of carbon − palladium bonds arising from the weakening and rupture of the two π - bonds of the compound during adsorption on the palladium.

The authors express their deep thanks to Prof. V. M. Tatevskii for his help in carrying out this work and for discussion of the results.

LITERATURE CITED

[1] R. P. Eischens, W. A. Pliskin and S. A. Francis, J. Chem. Phys. 22, No. 10, 1786 (1954).

[2] W. A. Pliskin and R. P. Eischens, J. Chem. Phys. 24, No. 2, 482 (1956).

[3] R. P. Eischens, S. A. Francis and W. A. Pliskin, J. Phys. Chem. 60, No. 2, 194 (1956).

[4] V. M. Griaznov and V. D. Iagodovskii, Proc. Acad. Sci. USSR, 116, No. 1, 81 (1957). *

[5] B. F. Hoffman and P. Damm, Mitteil. Schlesisch. Kohlenforsch. Inst. 2, 97 (1925).

[6] S. Brodersen and A. Langseth, Mat.-Fys. Skrifter Dat. Vid. Selsk. 1, No. 1, 1 (1956).

[7] C. R. Bailey, J. B. Hale , C. K. Ingold and J. W. Thompson, J. Chem. Soc. 1936, 931.

[8] A. V. Iogansen, The Physicochemical Properties of the Individual Hydrocarbons (in Russian) Vol. 6, Chapt. 23 (1957).

The M. V. Lomonosov State University,
Moscow

Received April 11, 1958

* Original Russian pagination. See C. B. Translation.

THE DIFFUSIONAL ELECTRICAL POTENTIAL OF A FALLING DROPLET WITH AN ADSORBED LAYER

S. S. Dukhin and B. V. Deriagin, Corresponding Member, Acad. Sci. USSR

It is known that the electrical field of a quiescent particle is localized within the electric double layer. The position is altered, however, when account is taken of the movement of a droplet relative to the surrounding medium and the mobility of its surface is considered. The development of an electric field through the movement of a liquid interface was first treated by Frumkin and Levich [1] for the case of a mercury droplet falling in an electrolytic solution. Here it was only necessary to consider the adsorption – desorption process of the mercury ions, since the inner surface of the double layer was visualized as being made up of the free electrons of the mercury. Thus it was possible to take into account only the migration of the ions in the electric field, and the diffusion was neglected. In this work consideration will be given to the qualitatively distinct process which takes place when two types of ions out of the electrolytic solution are adsorbed on the mobile droplet surface. The maintenance of approximate neutrality while the double layer is continually renewed calls for an approximate equality in the positive and negative charges which enter from the body of the solution. In the absence of an electric field, this condition can only be fulfilled when the diffusion coefficients of the ions are equal. If these coefficients are not equal, an electric field arises which equalizes the rates of delivery of positive and negative ions to the surface. This phenomenon is similar to that of a diffusion potential.

We will consider the diffusional electrical effect which arises during the fall of a droplet of an electrolytic solution in a liquid or gaseous medium (in oil, or in air, for example) which, for simplicity's sake, will be considered as free of ions.

Let Γ^+ and Γ^- represent the adsorption of positive and negative ions and v_t, the liquid velocity at the droplet surface. The movement of the droplet surface will be accompanied by a convectional transfer of adsorbed positive and negative ions, the density of the surface current of these ions being $\Gamma^+ v_t$ and $\Gamma^- v_t$, respectively. It is not difficult to show that the surface divergencies of these currents are different from zero. In addition, the local surface densities of the ions must be constant under stationary conditions. The difference between the gain and the loss of the adsorbed ions due to surface convection currents must be balanced by the corresponding normal component of the volume flow of ions, j_n, resulting from the migration of the ions in the electric field and their diffusion:

$$\operatorname{div}_s(\Gamma^+ v_l) = j_n^+ = \left(-D^+ \frac{\partial C^+}{\partial r} + \frac{F}{RT} D^+ z^+ C^+ E_{1r}\right)_a, \tag{1}$$

$$\operatorname{div}_s(\Gamma^- v_l) = j_n^- = \left(-D^- \frac{\partial C^-}{\partial r} - \frac{F}{RT} D^- z^- C^- E_{1r}\right)_a, \tag{2}$$

where E_{1r} is the radial component of the electric field at the inner side of the surface, F is the Faraday number, R is the gas constant, T is the absolute temperature and $\underline{a}$ is the radius of the droplet.

The fundamental factor which simplifies the search for the distribution of the potential in the electrolyte is the concept [2] of the electrical neutrality of the body of the electrolyte:

$$z^+ C^+ - z^- C^- = 0. \tag{3}$$

A similar condition must also be fulfilled for adsorption:

$$z^+\Gamma^+ - z^-\Gamma^- = 0. \tag{4}$$

The volume molar concentration, C, and the surface molar concentration, Γ, can be readily introduced through (3) and (4)

$$C = \frac{C^+}{z^-} = \frac{C^-}{z^+}, \qquad \Gamma = \frac{\Gamma^+}{z^-} = \frac{\Gamma^-}{z^+}.$$

Eliminating C^+ and C^- from (1) and (2) with the aid of (3), and accepting the condition (4), we obtain

$$E_{1r}(0) = \frac{RT}{F}\,\frac{D^+ - D^-}{D^+D^-}\,\frac{\operatorname{div}_s(\Gamma v_t)}{(z^+ + z^-)\,C}. \tag{5}$$

In determining the electric potential in the body of the droplet, it is necessary to consider the condition of continuity of the ionic flow in the bulk of the electrolyte; in view of the requirement of (3), this takes the form [2]:

$$\boldsymbol{v}\,\operatorname{grad} C = D_{ef}\,\Delta C \tag{6}$$

$$\frac{F}{RT}(z^+D^+ + z^-D^-)\,C\boldsymbol{E}_1 + (D^+ - D^-)\operatorname{grad} C = \frac{\boldsymbol{i}}{Fz^+z^-}, \tag{7}$$

where $D_{ef} = \dfrac{D^+D^-(z^+ + z^-)}{z^+D^+ + z^-D^-}$, $\underline{v}$ is the distribution of velocities, and $\underline{i}$ is the total electric current density.

Thus to determine the electric field, the equation for convectional diffusion (6) should first be solved, and use then made of (7); for this, knowledge of the total current distribution is called for.

Making use of (1), (2), and the condition (4), we will now show that the normal component of the current at the droplet surface is, in the first approximation, equal to zero:

$$i_n = (i_n^+ - i_n^-) = z^+ej_n^+ - z^-ej_n^- = \operatorname{div}_s[(z^+\Gamma^+ - z^-\Gamma^-)\,eV_t] = 0. \tag{8}$$

In order to prove that the total current density is everywhere equal to zero under the assumed conditions, we will rearrange (7) to the form

$$\boldsymbol{i}(r, 0) = C(r, 0)\operatorname{grad}\Psi(r, 0), \tag{9}$$

where $\Psi(r, \theta) = Fz^+z^-\left[\dfrac{F}{RT}(z^+D^+ + z^-D^-) + (D^+ - D^-)\ln C\right]$, $\varphi(r, \theta)$ is the electrical potential. We will now express the condition for the continuity of the total current, $i = 0$, and the boundary condition in terms of Ψ; this latter condition being easily obtained from (8) and (9) when account is taken of the fact that $C(a, \theta) \neq 0$:

$$\operatorname{div}[C(r, 0)\operatorname{grad}\Psi(r, 0)] = 0, \quad \frac{\partial\Psi}{\partial r}(a, 0) = 0.$$

Proceeding either analytically or by the method of thermal analogy, it can be easily shown that this problem has only the trivial solution

$$\Psi(r, \theta) = \text{const},$$

so that

$$i(r, \theta) = 0. \tag{10}$$

Taking (10) into account, we will rearrange (7) as

$$\boldsymbol{E}_1 = \frac{RT}{F}\,\frac{D^+ - D^-}{z^+D^+ + z^-D^-}\operatorname{grad}\ln C, \tag{11}$$

from which there at once follows an equation relating the potential distribution, $\varphi_1(r, \theta)$, and the concentration distribution:

$$\varphi_1(r, \theta) = \frac{RT}{F} \frac{D^+ - D^-}{z^+D^+ + z^-D^-} \ln \frac{C}{C_0} + \varphi_0, \tag{12}$$

C_0 being the concentration at the equator of the droplet.

We will consider the problem of the electric field of the droplet for the special case in which the ion concentration differences are small

$$C(r,\theta) - C_0 \ll C_0. \tag{13}$$

According to (13), the volume concentration at the surface is everywhere almost identical with C_0, and from this it follows that the difference between $\Gamma(\theta)$ and Γ_0 must be insignificant:*

$$\Gamma(\theta) - \Gamma_0 \ll \Gamma_0. \tag{14}$$

For Re <<1, the distribution of velocities along the surface of the droplet has the form [3]

$$v_t = v_0 \sin \theta. \tag{15}$$

Setting (15) into (5), and taking (14) and (13) into account, we rearrange (5) to the form

$$E_{1r}(\theta) = \frac{2RT}{F(z^+ + z^-)} \frac{D^+ - D^-}{D^+D^-} \frac{v_0}{a} \frac{\Gamma_0}{C_0} \cos \theta. \tag{16}$$

Making use of (3), (4) and (15) we will eliminate E_{1r} from (1) and (2) so that when (14) is taken into account a simple boundary condition for the determination of $C(r,\theta)$ results:

$$\frac{\partial C}{\partial r}(a, \theta) = 2 \frac{v_0 \Gamma_0}{D_{ef} a} \cos \theta. \tag{17}$$

We will now build up the following criterion to characterize the condition for diffusion within the droplet and give the value of the ratio between the convectional and the diffusional currents:

$$\mathrm{Pe} = \frac{a v_0}{D_{ef}} \frac{C_0}{\delta C},$$

the concentration drop within the droplet being set equal to the drop along the surface (between the equator and the pole)

$$\delta C = C_0 - C(a, 0), \quad v_0 = \frac{3}{2} U_0 \frac{\eta_2 + \eta_1 + \gamma}{2\eta_2 + 3\gamma}, \qquad U_0 = \frac{2}{9} \frac{a^2 g (\rho_1 - \rho_2)}{\eta_2},$$

here U_0 is the rate of fall of the droplet in the given medium, η_2 and ρ_2, are the viscosity and the density of the medium, η_1 and ρ_1, are the viscosity and the density of the material composing the droplet and γ is a retardation coefficient which we will neglect. When

$$\mathrm{Pe} \ll 1 \tag{18}$$

the convectional ionic transfer can be neglected in comparison with the diffusional, so that (6) can, in this

*It is supposed that the departure from adsorptional equilibrium is small at each point on the surface.

instance, be replaced by the Laplace Equation

$$\Delta C = 0. \tag{19}$$

There is no difficulty in solving this equation with the boundary condition $C\left(a, \frac{\pi}{2}\right) = C_0$ and (17):

$$C(r, \vartheta) = C_0\left(1 + \frac{\delta C}{C_0}\frac{r}{a}\cos\vartheta\right), \tag{20}$$

where, as is to be seen from (17),

$$\frac{\delta C}{C_0} = 2\frac{v_0}{D_{ef}}\frac{\Gamma_0}{C_0}, \tag{21}$$

so that the condition (13) is replaced by $2\ \frac{v_0\Gamma_0}{D_{ef}C_0} \ll 1$, or

$$\Gamma_0/C_0 \ll \tfrac{1}{2}D_{ef}/v_0. \tag{13'}$$

Setting (21) into the dimensionless criterion Pe, we will now write condition (18) in the following form

$$Pe \sim \frac{aC_0}{\Gamma_0} \ll 1. \tag{18'}$$

Conditions (13') and (18') are conveniently combined as:

$$a \ll \frac{\Gamma_0}{C_0} \ll \frac{1}{2}\frac{D_{ef}}{v_0}. \tag{22}$$

In the case of a droplet of an aqueous aerosol, numerical calculations show that this condition is well fulfilled • when $a \leq 1\mu$. When $a \approx 3\mu$, the results which have been outlined above can only be used to evaluate the strength of the electric field when the value of Γ_0/C_0 lies within the narrow limits defined by (22).

Setting (20) into (12) and neglecting terms in $\delta C/C_0$ which are of higher orders of infinitesimals than the first, we obtain

$$\varphi_1(r, \vartheta) = \frac{2RT}{F}\frac{D^+ - D^-}{z^+D^+ + z^-D^-}\frac{v_0}{D_{ef}}\frac{\Gamma_0}{C_0}\frac{r}{a}\cos\vartheta + \varphi_0. \tag{23}$$

In determining the external electric field of the droplet, we will not take the ionization of the air into account, so that the potential distribution in the air, $\varphi_2(r, \theta)$, will satisfy the Laplace Equation

$$\Delta\varphi_2 = 0. \tag{24}$$

The potential drop at the droplet surface will be supposed to be independent of the angle θ, this corresponding to the assumption that the adsorption is so small so as to bring about no change in the potential drop ••

• The theory which has been outlined can, without difficulty, be generalized to the case in which Pe >> 1, and the electric field in the droplet then proves to be localized at a point in the boundary layer. This problem will be dealt with in a separate article.

•• The theory which has been outlined can readily be generalized to the case of high concentrations of a surface-active substance, in which account must be taken of the change of the potential drop along the surface, and of the retardation of the movement of the drop by the adsorbed material. This case will not be considered here since it is of minor interest in view of the fact that the electric field diminishes when the surface is retarded.

$$\varphi_2(a, \theta) - \varphi_1(a, \theta) = \delta V. \tag{25}$$

The potential distribution which satisfied (24) and (25) has the form

$$\varphi_2(r, \theta) = \frac{2RT}{F} \frac{D^+ - D^-}{z^+ D^+ + z^- D^-} \frac{v_0}{D_{cf}} \frac{\Gamma_0}{C_0} \frac{a^2}{r^2} \cos\theta, \tag{26}$$

if it is supposed that $\varphi_0 = -\delta V$ so as to assure a zero value of the potential at infinity.

If it is assumed that $a \sim 3\mu$, $\delta C/C_0 \sim 0.3$, the strength of the electric field at the droplet surface, $E_2(a, \pi) = \text{grad}\ \varphi_2(a, \pi)$, amounts to 100 v/cm.

Because of electrocapillary retardation which we have not taken into account, such a large value of the strength of the electric field is not realized in these concrete cases. When $E \sim 100$ v/cm, calculation shows that the electric field so far retards the movement of the droplet that such an electric field cannot be attained. On the other hand, the tangential electric forces retarding the movement of the surface are one order less than the viscous forces, even at 10 v/cm, so that the electrocapillary effect can be neglected in this case.

LITERATURE CITED

[1] A. N. Frumkin and V. G. Levich, Acta Physikochim, URSS 2, 193 (1946); A. N. Frumkin, Bull. Acad. Sci. USSR, chem. ser., 1945, 223; V. G. Levich, J. Phys. Chem. 21, 689 (1947); I. N. Bagotskaia and A. N. Frumkin, J. Phys. Chem. 21, 1033 (1947).

[2] V. G. Levich, Physicochemical Hydrodynamics (in Russian), § 39, Acad. Sci. USSR, Press, 1952.

[3] V. G. Levich, Physicochemical Hydrodynamics (in Russian), § § 53-61, Acad. Sci. USSR, Press, 1952.

The Institute of Physical Chemistry of the Academy of Sciences of the USSR

Received April 5, 1958

TWO TYPES OF MANGANESE LUMINESCENCE CENTERS IN THE CADMIUM – LITHIUM ORTHOSILICATE PHASE

V. V. Osiko

(Presented by Academician A. N. Terenin, March 3, 1958)

In a brief communication, McKeag and Steward have described various luminophors, including zinc – lithium and cadmium – lithium silicates, which were activated by manganese [1]. These luminophors showed green or red luminescence, depending on their composition and method of preparation. Earlier, we carried out a detailed investigation of the zinc – lithium luminophors and showed the possibility of explaining the appearance of luminesence of the one color or the other [5]; the present communication is devoted to the cadmium – lithium luminophors.

On the basis of x-ray data, McKeag and Steward drew the conclusion that the green and the red luminesence should be ascribed to different crystal phases; namely, the green to a cadmium – lithium orthosilicate, activated by manganese and having the composition $CdO \cdot Li_2O \cdot SiO_2 \cdot Mn$, and the red to a cadmium – lithium metasilicate activated by manganese and having the composition $CdO \cdot Li_2O \cdot 2SiO_2 \cdot Mn$. We have prepared a series of specimens of manganese-activated cadmium – lithium orthosilicates having the general formula $(6 - x)CdO \cdot xLi_2O \cdot 3SiO_2 \cdot 0.015$ Mn, in which $\underline{x}$ was equal to 0; 0.5; 1; 1.5; 2.0; 2.5; 3.0; 3.5; 4.0; 4.5; 6.0. These specimens were prepared by two different procedures: by the calcining of powders, and by a method based on the use of the ethyl orthosilicate and solutions of the nitrates of cadmium, lithium, and manganese. The starting materials were: specially prepared, high purity carbonates of cadmium and lithium; silicon dioxide of the "for luminophors" grade; manganese nitrate of analytical grade, and a triply-distilled ethyl orthosilicate. In our second method, the mix for the luminophor was obtained by dissolving the cadmium and lithium carbonates in distilled nitric acid (the original acid was chemically pure), the manganese nitrate being then introduced in the form of an aqueous solution.

These mixes were carried through a high temperature sintering; the temperature and time of sintering being experimentally so chosen for each specimen that the intensity of luminescence would be at maximum. The temperature of sintering was varied in the interval 800-1000°, and the time from 2 to 3 hours, depending on the composition. The use of different syntheses and the repetition of single syntheses permitted an evaluation of the reproducibility of the luminescence properties of the cadmium – lithium silicates with manganese; in this way it was shown that there was no difference in the color, or the intensity of the illumination from luminophors which had the same composition and which had been obtained by the various indicated syntheses, or by resynthesis. The ability to luminesce was shown by specimens varying in composition from $5.5CdO \cdot 0.5Li_2O \cdot 3SiO_2 \cdot 0.015$ Mn to $2CdO \cdot 4Li_2O \cdot 3SiO_2 \cdot 0.015$ Mn. Specimens with a still higher content of lithium oxide possessed an intense color. Cadmium orthosilicate with manganese did not luminesce, although it was without color. The luminescence of cadmium – lithium orthosilicates with manganese was readily excited by short ultraviolet rays and by cathode rays.

In Figs. 1 and 2, respectively, there are presented the spectra of photo-luminescence, and of cathode-luminescence of manganese-activated cadmium – lithium orthosilicates. Excitation was carried out, either through the 254 mμ mercury resonance line, or through an electron beam of 6 kv potential at a current density of $3 \cdot 10^{-7}$ amp/cm^2. These spectra were measured with a UM-2 monochromator, a FEU-32 photomultiplier serving as the radiation receiver.

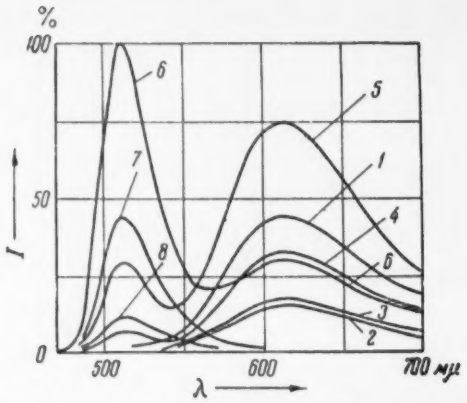

Fig. 1. The luminescence spectra of manganese-activated cadmium – lithium orthosilicates of various compositions. Excitation by the 254 mμ resonance line of mercury. 1) 5.5 CdO · 0.5Li_2O · · 3SiO_2 · 0.015Mn; 2) 5CdO · 1Li_2O · 3SiO_2 · 0.015 Mn; 3) 4.5CdO · 1.5Li_2O · 3SiO_2 · 0.015Mn; 4) 4CdO · 2Li_2O · 3SiO_2 · 0.015Mn; 5) 3.5CdO · 2.5 Li_2O · 3SiO_2 · 0.015Mn; 6) 3CdO · 3Li_2O · 3SiO_2 · · 0.015Mn; 7) 2.5CdO · 3.5Li_2O · 3SiO_2 · 0.015 Mn; 8) 2CdO · 4Li_2O · 3SiO_2 · 0.015Mn.

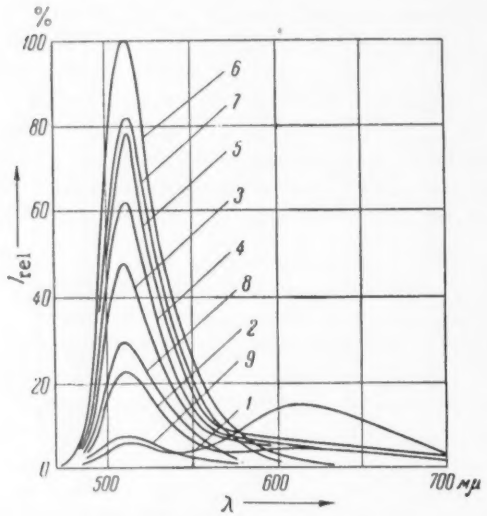

Fig. 2. Cathodo-luminescence spectra of manganese-activated cadmium – lithium orthosilicates of various compositions. Excitation by an electron beam at a potential of 6 kv and a current density of $3 \cdot 10^{-7}$ amp/cm^2. 9) 1.5CdO · 4.5 Li_2O · 3SiO_2 · 0.015Mn. The remaining curve indices are the same as in Fig. 1.

From Figs. 1 and 2, it is to be seen that these spectra showed a green or an orange-red band, or a combination of such bands. The positions of the maxima on the green and the red bands (514 and 615 mμ) were independent of the method of excitation and of the composition of the luminophor. The ratio of the intensities of the green and red bands varied, depending on the CdO/ Li_2O ratio in the orthosilicate, but the variation was not the same for photo- and for cathodo- excitation. The relation between the intensities of these bands and the composition is a more complex one, and it was therefore difficult to draw any sort of conclusions on the basis of a mere comparison of the luminescence spectra of Figs. 1 and 2. In order to analyze these results, the luminescence spectra were broken down into their two component bands and the integral intensities of the green and red bands determined by measuring the areas under the respective spectral curves. Figure 3 shows the relation between the compositions of the luminophors and the intensities of the two bands for photo- and for cathodo- excitation. From these data it followed that with either photo- or with cathodo- excitation, the maximum integral intensity in the green band, and in the two bands taken together, was to be observed in specimens of composition approaching 3CdO · 3Li_2O · · 3SiO_2 · 0.015Mn.

The maxima on the integral intensity curves for the green band were the same for both types of excitation, but with cathodo- excitation, the green luminescence was observed over a much wider range of compositions than was the case with photo-excitation. On the other hand, the integral intensity curves for the red band were fundamentally different for the various modes of excitation; specifically, as a part of the lithium of a luminophor of composition 3CdO · 3Li_2O · 3SiO_2 · 0.015Mn was replaced by cadmium, the integral intensity curve for the red band under photo-excitation rose sharply and passed through a maximum at the composition of 3.5CdO · 2.5Li_2O · 3SiO_2 · · 0.015Mn, whereas the red band was almost completely missing from the luminescence spectrum obtained with cathodo-excitation of a specimen of this composition.

It was natural that the attempt be made to interpret the appearance of the two bands in the luminescence spectra of the manganese-activated cadmium – lithium orthosilicates as indication of the existence of two phases in the luminophors, a change in the band intensities corresponding to an alteration in the relative amounts of these phases in the system. For a solution of this problem, additional data were required. x-Ray diagrams were developed for several of the prepared luminophors (Table 1).

Powder diagrams were obtained in a camera of 86 cm diameter, using a tube with a copper anticathode and separating the K_α line with a nickel filter. Three systems of lines could be distinguished on these diagrams: line systems for the cadmium and the lithium orthosilicates (6 : 0 and 0 : 6), and a distinct system of lines

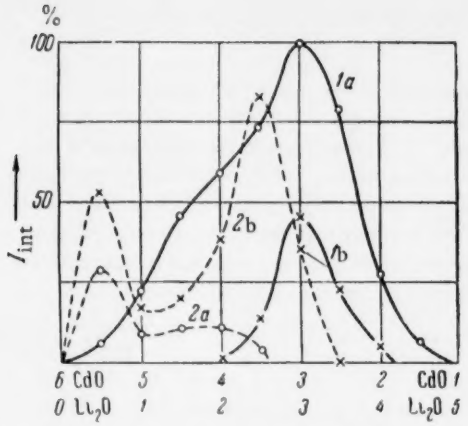

Fig. 3. The relation between CdO/Li_2O ratio in manganese-activated cadmium – lithium orthosilicates, and the integral intensity of the green and the red bands in the photo- and cathodo-luminescence spectra. 1) green band, 2) red band: a) cathodo – excitation, b) photo–excitation.

which appeared in the diagrams for specimens of intermediate composition. This system undoubtedly belonged to the mixed cadmium – lithium orthosilicate phase. As the cadmium in cadmium orthosilicate was replaced by lithium, the system of cadmium orthosilicate lines gradually gave way to the cadmium – lithium orthosilicate line system. Only these latter lines were present in the x-ray diagrams for specimens ranging in composition from $3.5CdO \cdot 2.5Li_2O \cdot 3SiO_2 \cdot 0.015Mn$ to $1.5CdO \cdot 4.5Li_2O \cdot 3SiO_2 \cdot 0.015Mn$, the lines for cadmium and for lithium orthosilicate being entirely lacking.

It is to be seen from Fig. 3 that neither cadmium orthosilicate with manganese, nor lithium orthosilicate with manganese, luminesced under either photo- or cathodo- excitation and it therefore follows that both the green and the red luminescence in specimens of compositions approaching that of $3CdO \cdot 3Li_2O \cdot 3SiO_2 \cdot 0.015Mn$ should be ascribed to the single phase of cadmium – lithium orthosilicate with manganese.

Against this conclusion, it might be argued that luminophors of these compositions were two-phase systems, and that under both photo- and cathodo- excitation the phase which was responsible for green luminescence quantitatively predominated over the phase causing the red luminescence; in such a case, it was possible that the lines of this second phase did not appear on the x-ray diagrams because of the limited sensitivity of the x-ray method when applied to systems of low symmetry. But under photo-excitation, the ratio of the integral intensities of the red and green bands changed by more than 5 fold in passing from the composition $3CdO \cdot 3Li_2O \cdot 3SiO_2 \cdot 0.015Mn$ to the composition $3.5CdO \cdot 2.5Li_2O \cdot 3SiO_2 \cdot 0.015Mn$, and if the concentration of the "red" phase had increased at the expense of the "green" phase to the same extent, this fact could not help but be reflected in the x-ray diagrams. It is known, moreover, that the intensity of cathodo-luminescence sharply diminishes when nonluminescing additives are introduced into a luminophor, and in our case, the introduction into the system of a "red" phase, i.e., of a phase which failed to luminesce under cathodo-excitation, should have led to a sharp decrease in the integral intensity of the cathodo-luminescing "green" phase, an effect which was not in actuality observed.

TABLE 1

The Interplanar Distances for the Cadmium – Lithium Orthosilicates

CdO/Li_2O Ratio							CdO/Li_2O Ratio						
6 : 0	5 : 1	3,5 : 2,5	3 : 3	2,5:3,5	1,5:4,5	0:6	6:0	5:1	3,5:2,5	3 : 3	2,5 : 3,5	1,5:4,5	0 : 6
—	—	—	—	—	—	5,26	—	—	—	—	—	—	1,52
—	—	—	—	—	—	3,96	1,44	1,44	—	—	—	—	—
—	3,62	3,62	3,62	3,62	3,62	—	—	—	1,37	1,37	1,37	1,37	—
—	—	3,18	3,18	3,18	3,18	—	1,32	1,32	1,32	1,32	1,33	1,32	—
—	—	—	—	—	—	3,15	—	—	—	—	—	—	1,31
2,73	2,73	—	—	—	—	—	—	—	1,20	1,19	1,19	1,19	—
—	—	—	—	—	—	2,62	—	—	1,10	1,10	1,10	1,10	1,10
2,58	2,58	—	—	—	—	—	—	—	—	—	—	—	1,07
2,27	2,28	—	—	—	—	—	—	—	1,03	1,03	1,03	1,03	—
—	—	2,13	2,14	2,14	2,14	—	—	—	—	—	—	—	0,93
—	—	1,95	1,95	1,95	1,95	—	0,85	0,85	—	—	—	—	—
—	—	—	—	—	—	1,83	—	—	0,82	0,82	0,82	0,82	—
1,73	1,73	—	—	—	—	—	0,81	0,81	—	—	—	—	—
1,66	1,66	—	—	—	—	—	—	—	—	—	—	—	0,79
—	—	1,55	1,55	1,55	1,55	—							

Thus by combining the data obtained on the luminescence spectra with data from the x-ray analysis, we were led to the conclusion that the one phase of manganese-activated cadmium – lithium orthosilicate was responsible for both the green and the red luminescence. In this phase, the molar ratio of cadmium oxide to lithium oxide could be somewhat altered without disrupting the phase homogeneity.*

There is at the present time a widespread belief that the luminescence colors of manganese-activated oxygen-containing crystal phosphors are determined by the manganese neighborhoods; specifically, that the green luminescence arises when the manganese is surrounded by four, and the red when the manganese is surrounded by six, oxygen atoms [2-4]. Extending this point of view to the luminescence spectra of the manganese-activated cadmium – lithium orthosilicates, we consider that the green and orange-red bands arise from these two indicated types of luminescence centers. The change in the intensity ratio for the green and the red bands which is observed on altering the CdO/Li_2O ratio in the cadmium – lithium orthosilicate phase, we ascribe to the related probabilities of finding the manganese in regions containing four or six oxygen atoms.

In an earlier investigation of manganese-activated zinc-lithium silicate luminophors we have met a similar case of "green" and "red" luminescence centers which were produced by manganese in a single phase.

I wish to express my deep thanks to Prof. M. A. Konstantinova-Shlezinger for continued interest in this work and for valuable advice.

LITERATURE CITED

[1] A. H. McKeag and E. G. Steward, J. Appl. Phys. Suppl. No. 4, 29 (1955).

[2] H. W. Lewerenz, An Introduction to Luminescence of Solids, 1950.

[3] S. H. Linwood and W. A. Weyl, J. Opt. Soc. Am. 32, 443 (1942).

[4] J. H. Shulman, J. Appl. Phys. 17, 902 (1946).

[5] M. A. Konstantinova-Shlezinger, V. V. Osiko and L. S. Ulanovskaia, J. Inorg. Chem. 3, vol. 6 (1958).

The P. N. Lebedev Institute of Physics of the Academy of Sciences of the USSR

Received February 17, 1958

*The exact determination of the limits of phase homogeneity of cadmium – lithium orthosilicate with manganese lies beyond the scope of the present paper.

FORMAL KINETIC LAWS FOR THE THERMAL DECOMPOSITION OF EXPLOSIVES IN THE LIQUID PHASE

F. I. Dubovitskii, G. B. Manelis and A. G. Merzhanov

(Presented by Academician V. N. Kondrat'ev, April 4, 1958)

With most explosive substances, isothermal decomposition is an autoaccelerating process. In the technical literature on explosives, and in textbooks, the classical equation for autocatalysis:

$$\frac{d\eta}{dt} = k_1(1-\eta) + k_2\eta(1-\eta), \tag{1}$$

is used for describing the kinetics of these reactions: here η is the extent of reaction and k_1 and k_2 are the kinetic constants. In many instances, however, the kinetic curves do not follow this equation. Between the experimental and the theoretical curves fundamental differences exist, not only as to general form, but also in regard to the position of the maximum reaction rate. The existence of these differences leads to a certain amount of confusion in the question of the reaction mechanism. For example, cases are met in the literature [1] in which the autoaccelerated thermal decomposition of explosives is explained in terms of branching, or consecutive, chain reactions, without the presentation of experimental material to confirm the existence of these processes. At the same time, most of the experimental work indicates that the thermal decomposition of condensed explosives is a reaction which is autocatalyzed by the final products [2].

A detailed consideration of the thermal decomposition of explosives leads to the conclusion that the reaction conditions are here quite different from those applying to the simple reactions for which the classical equation of autocatalysis was developed (reactions in the gaseous phase and in solution). This difference is to be found in the fact that gases make up the greater portion of the products from the decomposition of condensed explosives. The removal of these gaseous products from the reaction zone results in a decrease in the reaction volume during the decomposition process and this, in turn, affects the kinetics of the reaction.

In this work we will consider those formal kinetic laws for the thermal decomposition of liquid phase explosives which apply when this volume change is taken into account. In view of the fact that there is, for the most part, practically no volume change when two or more components are mixed together, it can, to a first approximation, be considered that the volume of the condensed phase at a given instant is composed additively of the volumes of the unreacted substance and the condensed product which has been formed up to this point. The volume of the liquid phase can thus be looked on as a linear function of the degree of reaction:

$$v = v_0(1-\mu\eta),$$

$\mu = \frac{v_0 - v_{prd}}{v_0}$ being the relative volume change for complete decomposition, v_0 the initial volume and v_{prd} the volume of the condensed product.

The derived kinetic equation for a reaction of the n-th order which involves a variation in the volume, has the form

$$\frac{d\eta}{dt} = k\frac{(1-\eta)^n}{(1-\mu\eta)^{n-1}} \tag{2}$$

Equation (2) goes over into the equation for a simpler monomolecular reaction when the volume change in decomposition is sufficiently great ($\mu \approx 1$). This indicates that a reaction of the first order, such as is frequently observed in the decomposition of explosives, can in actuality proceed according to either a monomolecular or a bimolecular law.

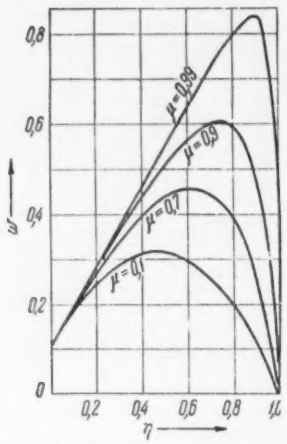

Fig. 1. The relation between the reaction rate, $w = \frac{d\eta}{d\tau}$, and the extent of reaction, according to Equation (3). $\eta_0 = 0.1$.

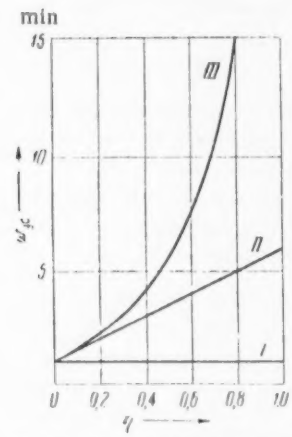

Fig. 2. The relation between the specific rate, $w_{sp} = \frac{1}{1-\eta} \cdot \frac{d\eta}{dt}$, and the extent of reaction. I) first order reaction, II) autocatalysis of the first order (Equation (1), III) curve according to Equation (3).

On taking into account the volume change which accompanies a reaction autocatalyzed by the final products, kinetic curves of altered form are obtained. In this case, the kinetic equation has the form:

$$\frac{d\eta}{dt} = k_1(1-\eta) + k_2\alpha(1-\mu)\frac{\eta(1-\eta)}{1-\mu\eta}, \qquad (3)$$

where α is the fraction of the catalyst in the condensed product.

When $\mu = 0$ (the limiting case of zero volume change in the course of the reaction), Equation (3) goes over into (1), the classical equation for autocatalysis. Integration of (3) gives

$$[1 + (1-\mu)\eta_0]\, k_2\alpha(1-\mu)\, t =$$

$$= \frac{1}{1-\mu\eta_0}\ln\left(1 + \frac{1-\mu\eta_0}{\eta_0}\eta\right) - (1-\mu)\ln(1-\eta),$$

where $\eta_0 = \frac{k_1}{k_2\alpha(1-\mu)}$.

In Fig. 1 there is shown the theoretical relationship between the reaction rate and the extent of reaction for fixed η_0 and for various values of μ. It is to be seen from this figure that the maximum rate, and the extent of reaction η_{max}, corresponding to it, strongly depend on the value of μ. For high values of μ, η_{max} is close to unity, i.e., the maximum rate is met at the end of the decomposition. The value of η_{max} can be determined from the equation:

$$\eta_{max} = \frac{(1-\mu\eta_0) - \sqrt{(1-\mu)(1-\mu\eta_0)}}{\mu(1-\mu\eta_0)}.$$

The difference between Equations (1) and (3) appears in a particularly striking form in the curves showing the relation between the specific rate, $\frac{1}{1+\eta} \cdot \frac{dn}{dt}$, and the extent of reaction (Fig. 2).

When the thermal decomposition of explosives is carried out in the presence of relatively large amounts of strong catalysts, the reaction is of simple catalytic type. In this case a kinetic equation allowing for the alteration in volume has the form

$$\frac{d\eta}{dt} = k_1\beta\frac{1-\eta}{1-\mu\eta},$$

where β is the fraction of the added catalyst in the mixture.

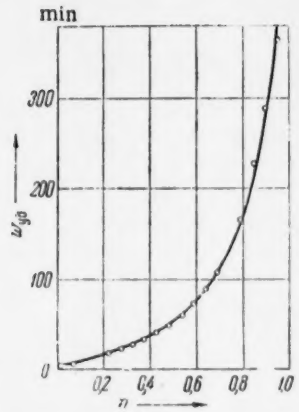

Fig. 3. The relation between the specific rate and the extent of reaction in the decomposition of ethylenediaminedinitrate. The points represent the experimental data of Robertson [3]. The curve was calculated from Equation (3). $k_1 = 4 \cdot 10^{-3}$ min^{-1}; $k_2\ \alpha\ (1-\mu) = 58.1 \cdot 10^{-3}$ min^{-1}; $\mu = 0.90$; t = 238°C.

The volume change in the reacting substance plays no role in cases of autocatalysis by gaseous products, since the concentration of the dissolved gases is then determined by the pressure and temperature alone and does not depend on the volume of the liquid phase. For this reason, the decomposition of explosives must be subject to the classical equation of autocatalysis when the reaction is carried out in a closed system in which the pressure of the gaseous products is proportional to the extent of reaction.

Thus, by taking into account the volume alteration which accompanies decomposition, it is possible to obtain an expression describing the kinetics of decomposition in a reaction autocatalyzed by the final products. The experimental data on the decomposition of a number of substances in the liquid phase are in good agreement with this proposed equation. This point can be illustrated by the following example. In Fig. 3 there is shown the relation between the specific rate and the extent of reaction in the thermal decomposition of ethylenediaminedinitrate (according to the data of Robertson [3]) at T = 238°C. The concordance between the theoretical curve and the experimental points shows the validity of Equation (3).

LITERATURE CITED

[1] K. K. Andreev, The Combustion and Thermal Decomposition of Explosives (in Russian), Moscow, 1957.

[2] C. N. Hinschelwood, J. Chem. Soc. 1920, 721; S. Z. Roginskii and A. M. Magid, J. Phys. Chem. 2, 263 (1931).

[3] A. J. B. Robertson, J. Am. Chem. Soc. 67, 221 (1948).

Received March 8, 1958

THE USE OF WATER AS A SENSITIZER FOR THE RADIATION INITIATION OF THE OXIDATION OF BENZENE

M. A. Proskurnin, E. V. Barelko and L. I. Kartasheva

(Presented by Academician V. N. Kondrat'ev, March 15, 1958)

The preparation of phenol by the direct oxidation of benzene is an important process, to which a number of works have been devoted [1-3]. The authors of the present communication have previously made a study of the radiolytic oxidation of benzene to phenol in aqueous solution during which it was discovered that iron ions have a catalytic influence on this radiation - chemical reaction at room temperature [4]. When the temperature of the experiment was raised, spontaneous acceleration of the reaction was observed, indicating the development of a chain mechanism for the oxidation reaction [5]. The radiation initiation of branched chain processes has also been used, as is well known, for the oxidation of saturated hydrocarbons [6, 7].

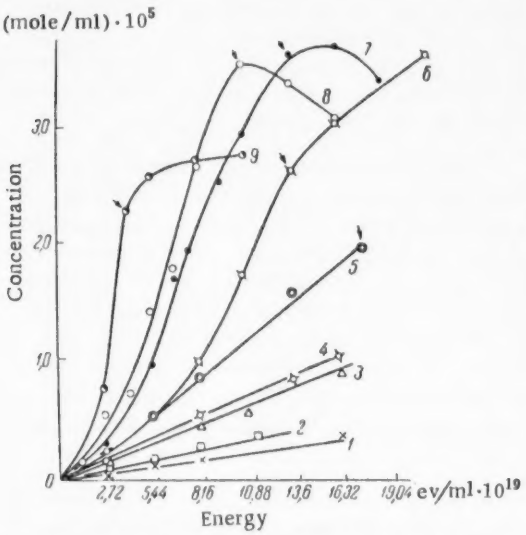

Fig. 1. The relationship between the yield of phenol and the radiation dose at various temperatures (dose strength 140 r/second). 1) oxidation of pure benzene at t = 165°; 2-9) oxidation of benzene in aqueous solution: 2) at t = 20°, 3) at 100°, 4) at 115°, 5) at 135°, 6) at 165°, 7) at 190°, 8) at 200°, 9) at 220°.

The present communication is devoted to the oxidation of benzene in an aqueous phase by a branched-chain mechanism, discovered by the authors, and in particular to the study of the role of water as a sensitizer for the process of radiation initiation.

The radiation source used was Co^{60}, with an activity of approximately 1400 g-equivs. of radium. The experiments were carried out in an autoclave made of Mark 1X18N9T stainless steel and fitted with a special heating furnace and manometer for measuring pressure.

The average strength of the radiation dose, determined in a glass vessel of the same geometrical form as the ampoule used for the radiation, amounted to 140 r/second. The calibration of the source was carried out by the ferrous sulfate method, the yield of the oxidation of divalent iron ions being taken as equal to 15.6 molecules per 100 ev. The ratio of the volumes of water and benzene in the autoclave was equal to 32:1. Pure benzene and twice-distilled water were used for the experiments. All the experiments were carried out at an initial oxygen pressure of 10 atmospheres in the temperature range 20-220°. The analysis for the phenol was carried out by extracting the reaction mixture with benzene, which was then treated with sodium carbonate solution (1 N). The phenol was determined in the sodium carbonate solution from the ultraviolet absorption at $\lambda = 286$ mμ. The concentration of resinous products was determined by distilling the water–benzene mixture in vacuo and weighing the polymerized product which did not distil from the vessel.

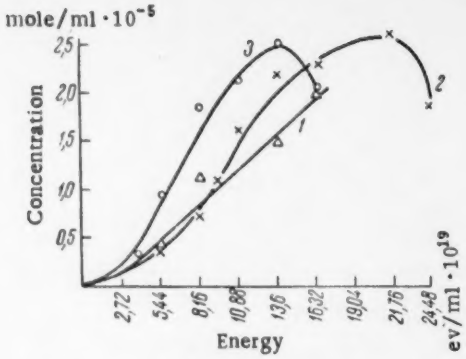

Fig. 2. The relationship between the yield of resinous reaction products and the radiation dose. 1) at t = 135°; 2) at 165°; 3) at 200°.

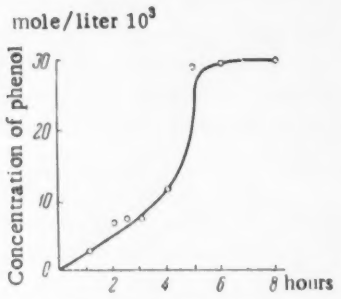

Fig. 3. The radiation aftereffect.

Figure 1 gives curves showing the relationship between the concentration of phenol and the radiation dose at various temperatures. An analogous curve for the oxidation of benzene in the absence of water is given for comparison (Curve 1). It can be seen that in aqueous solution, even at a temperature as low as 165°, the reaction has a clearly defined autocatalytic character. Observations were made of resin formation in parallel with the observations on the formation of the phenol in the liquid phase (Fig. 2). The kinetics of the formation of resinous oxidation products is identical in character with the kinetics of phenol formation, and, in particular, the concentration maxima on the concentration–radiation dose curves are obtained at the same time in both cases (Fig. 1; 5, 7, Fig. 2; 2, 3). Phenolic derivatives and polyphenols were found in these products.

A further proof that the reaction under study is a branched chain process, in which radiation may be used as an initiating agent, is provided by the kinetic curve for phenol formation in the case where the radiation was removed 2 hours after the start of the experiment and the reaction continued with spontaneous acceleration (Fig. 3).* To the 8 molecules of phenol per 100 ev of energy during the radiation period, 26 molecules are added during the period of the aftereffect, and the total yield of phenol at a temperature of 190° is 15-20 times greater than the yield of phenol in the radiation oxidation of benzene in aqueous solution at room temperature [8].

At the same time, at temperatures up to 220° and under analogous radiation conditions, no change to a spontaneously accelerating reaction can be observed in the absence of water. The problem of the reason for this influence shown by water on the radiation initiation seems to us to be fundamental for the understanding of the oxidation processes. In our opinion, the reason lies for the most part in the differing radiation stability of benzene and water. The yield of free radicals from benzene at room temperature, according to the data of Shapiro [9] and Weber [10], is equal to 0.5–0.7 per 100 ev. Under the same conditions the yield from the decomposition of water is 3.66 molecules per 100 ev [11], which is equivalent to the formation of 7–8 H and OH radicals. Thus it may be taken that the quantity of free radicals and atoms formed under the influence of radiation and responsible in the last analysis, for the initiation of the chain process, is greater by one order of magnitude in the case of water.

We consider that the use of substances such as water, which are inert chemically but which are unstable to radiation, as sensitizers for the radiation initiation of branched chain processes, may be of extremely wide importance. It should be noted, however, that in the present case the role of the water may not be limited to its influence on the initiation process. The presence of water may also have an influence on subsequent stages of the chain process. Thus, for example, the thermal decomposition of hydrogen peroxide formed by radiation of the water may be one of the elementary stages of the degenerate branching. We have been able to bring about the oxidation of benzene by adding hydrogen peroxide to the aqueous solution and heating the mixture.

*A similar kinetic curve for the aftereffect was obtained for the process of resin formation.

LITERATURE CITED

[1] I. I. Ioffe and Ia. S. Levin, et al., J. Phys. Chem. 28, 1386 (1954).

[2] H. Frank, Über die katalytische Oxidation von Benzol zu Phenol, Dissertation for the Doctorate, Zurich, 1955.

[3] N. M. Emanuel' and E. M. Denisov, Proc. Acad. Sci. 117, No. 3, 458 (1957).*

[4] M. A. Proskurnin and E. V. Barelko, Coll. of Works on Radiation Chemistry, 1955, p. 99.

[5] E. V. Barelko, L. I. Kartasheva, P. D. Novikov and M. A. Proskurnin, Coll. of Reports from the 1st All-Union Conference on Radiation Chemistry, 1957 (in the press).

[6] M. A. Proskurnin and Iu. L. Khmel'nitskii, et al., Proc. Acad. Sci. 112, No. 5, 886 (1957).*

[7] N. M. Emanuel', Proc. Acad. Sci. 111, 6, 1286 (1956).

[8] G. Stein and J. Weiss, J. Chem. Soc. 1949, 3245.

[9] L. Bouby and A. Shapiro, J. Chem. Phys. 52, 645 (1955).

[10] E. Weber, P. Forsyth and R. Schuler, Rad. Res. 3, 68 (1955).

[11] C. Hochanadel and G. Ghormley, J. Chem. Soc. 21, 880 (1953).

L. Ia. Karpov Physicochemical Scientific Research Institute

Received March 12, 1958

*Original Russian pagination. See C. B. Translation.

THE CATALYTIC SYNTHESIS OF UNSATURATED HYDROCARBONS OF THE C_4 SERIES LABELED WITH RADIOACTIVE CARBON C^{14}, USING VAPOR-PHASE DISTRIBUTION RADIOCHROMATOGRAPHY

Corresponding Member AN SSSR S. Z. Roginskii and M. I. Ianovskii

G. M. Zhabrova, I. M. Vinogradova, B. M. Kadenatsi and Z. A. Markova

The fact that work on methods of synthesizing compounds of unusual isotopic composition has been insufficiently developed is hindering the extension of the use of labeled substances in various branches of science and technology. Very often the preparation of these substances places fundamental difficulties in the way of carrying out an experimental study.

It has been shown by one of us [1] that it is incorrect to assume, as is widely done, that all the problems associated with the synthesis of compounds of unusual isotopic composition can be resolved by direct repetition of the techniques and methods of ordinary synthetic chemistry. Allowance often has to be made for the phenomenon of intermolecular isotopic exchange, which brings about a reduction in the concentration of tracer isotope in the product aimed at. A factor which is likewise of significance is the relatively high cost of most isotopes and the desirability of arranging for the minimum loss and greatest possible use of the tracer substance. All these factors make it necessary to avoid the use of the more lengthy techniques of ordinary synthetic chemistry and make it natural to seek out standard simplified techniques by making wider use of the extensive possibilities presented by the methods of heterogeneous catalysis, which make it possible to control precisely the direction and extent of a desired reaction.

The present work gives the results of studies on the preparation of labeled unsaturated hydrocarbons from ethyl alcohol labeled with radioactive carbon C^{14}. The distinctive feature of the method described is the fact that all the labeled molecules are obtained simultaneously as the result of one catalytic process taking place on the catalyst used for the synthesis of divinyl according to S. V. Lebedev's method, thus avoiding the lengthy and complex stages which are involved in the preparation of these substances in ordinary synthetic chemistry.

This work is a particular example of the application of a general principle to the synthesis of labeled molecules [1], in which a group synthesis is carried out, leading to the production of a mixture of a number of substances of unusual isotopic composition, after which physicochemical methods of separation are applied to isolate the individual labeled substances.

Particular interest has been attached to the separation of labeled hydrocarbons of the C_4 series with various degrees of unsaturation and in various structurally isomeric forms, characterized by boiling points which are extremely close to one another. These hydrocarbons are: butadiene (divinyl) with b. p. 4.5°; α-butylene with b. p. 6.3°; β-butylene (cis-form) with b. p. +3.64°; β-butylene (trans-form) with b. p. +0.86°.

The Catalytic Synthesis Process

The catalytic synthesis was carried out using the S. V. Lebedev catalyst [2], at a temperature of 390°, in an ordinary dynamic system, which has been described earlier [5]. The alcohol used was labeled ethyl alcohol $C^{14}H_3C^{14}H_2OH$ with a certified specific activity of 0.724 curies/ml. Since the aim of the present study was not the separation of products with a maximum specific activity, the labeled radioactive alcohol was diluted for convenience in working, by from 5 to 40 times in separate experiments.

The Chromatographic Separation of the Gaseous Labeled Products

The chemical and radiochemical analysis and the separation of the gaseous radioactive products was

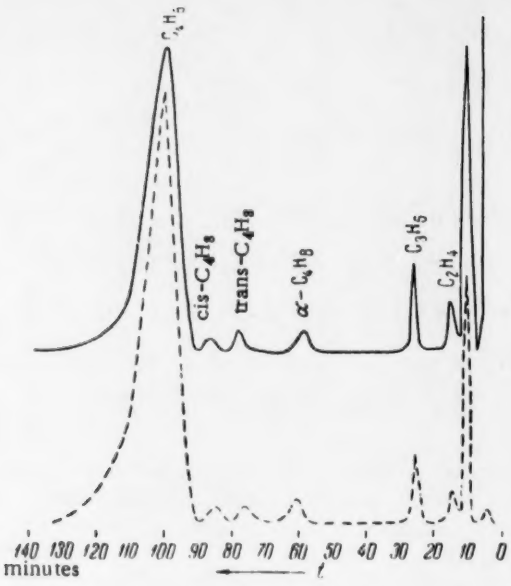

Fig. 1. Chromatogram for a mixture of the gaseous radioactive products obtained on the usual catalyst.

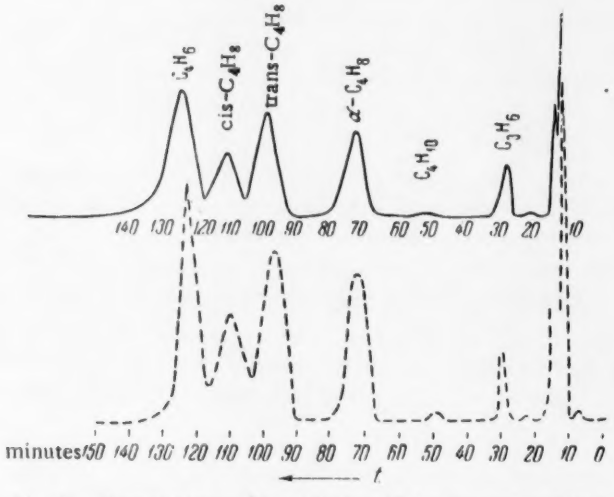

Fig. 2. Chromatogram for a mixture of the gaseous products obtained when the catalytic synthesis is carried out on a carbonized catalyst.

carried out using a gas radiochromatography apparatus, which has been described, together with the principles of its operation, in an earlier paper [3]. The apparatus consists of an ordinary gas-liquid or vapor-phase chromatography assembly combined with a device for recording simultaneously and continuously the radioactivity and the concentration of the vapors (or gases) leaving the chromatographic column. The vapor concentrations in the gas carrier stream (nitrogen or hydrogen) were recorded by means of the usual thermal conductivity gas analyzer. The radioactivity was recorded using a flow-through radiometric tube with two thin-walled end-window counters [4] (window density 0.8-1 mg/cm^2), mounted inside and connected to a system for measuring

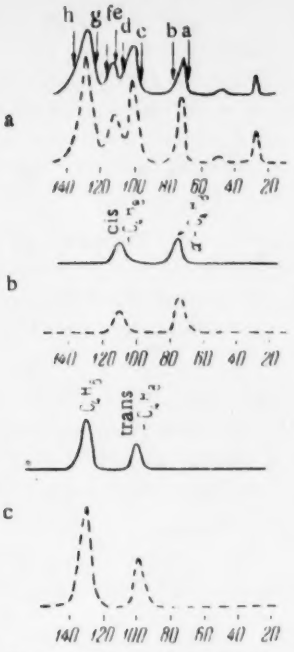

Fig. 3. Chromatograms of a mixture of hydrocarbons with successive separation of the compounds. a) original chromatogram; b) chromatogram of the α- and β-cis-C_4H_8 fractions separated; c) chromatogram of the β-trans-C_4H_8 and divinyl fractions separated.

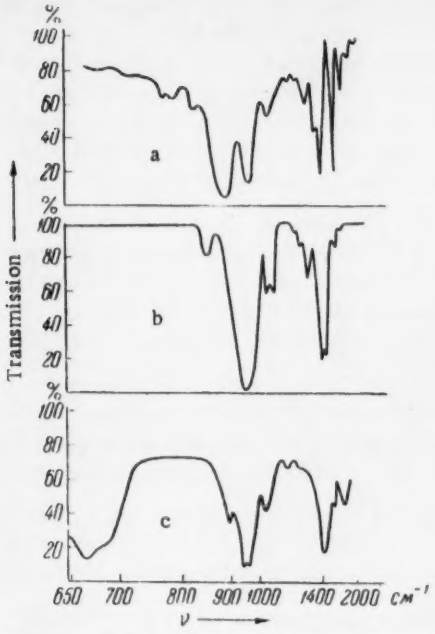

Fig. 4. Absorption spectra for the butylenes. a) Fraction I; b) Fraction II; c) Fraction III. Cell thickness 20 cm.

the count rate over six ranges of 200, 600, 2000, 6000, 20,000 and 60,000 impulses/minute. The readings from the gas analyzer and from the count rate detector were recorded simultaneously on the ribbon of a multiposition electronic potentiometer EPP-09 with 5 mv and 10 mv ranges.

Figure 1 gives a typical chromatogram for a mixture of gaseous radioactive products from the synthesis of divinyl using S. V. Lebedev's method from labeled alcohol ($C_2^{14}H_5^{14}OH$), from one catalyst specimen. The chromatogram consists of two curves. The lower curve represents the recorded activity, while the upper curve represents the recorded concentration of the substances in the effluent from the column. It can readily be shown [4] that the specific activity of any component, on a definitely chosen scale, is given by the ratio of the areas under the peaks corresponding to the substance on the left- and right-hand curves of the chromatogram.

The radiochromatogram shows that under the conditions of the experiment the chief gaseous product is divinyl (81.3%). The concentration of butylenes is less than 4.7%.

It is possible to alter the ratio of the products obtained by appropriate thermal treatment of the catalyst and by the addition of other materials, as can be seen from a chromatogram (Fig. 2) recorded after the synthesis had been carried out on a catalyst treated with carbon. It can be seen from Fig. 2 that in this case the main bulk of the gaseous product consists of butylenes (51%) while the concentration of divinyl is not more than 25%. The increase in the concentration of butylenes is related to the hydrogenation of the divinyl on the carbonized catalyst [5]. Saturated hydrocarbons (butane) also appear in the gas.

It is characteristic that the specific activities of the hydrocarbons (in impulses/minute · cm^3) represented on the chromatograms of Figs. 1 and 2 are approximately the same. The gas mixture obtained on the carbonized catalyst was separated chromatographically. At the moment indicated by the point A on the chromatogram (Fig. 3a), the gas stream leaving the column was directed into a trap containing liquid air. The α-C_4H_8 continued to be frozen out until the point B, after which the gas was directed into the extraction system. At the moment corresponding to the point C, the gas was directed into a second trap, in which the β-trans-C_4H_8

was frozen out until the moment corresponding to the point D. The β-cis-C_4H_8 and the C_4H_6 fractions were frozen out in exactly similar fashion (Points E, F, G, H). In order to check the chemical and radiochemical purity of the substances separated, the α-C_4H_8 and β-cis-C_4H_8 were unfrozen and passed again through the chromatographic column to give a second radiochromatogram. The radiochromatogram obtained is shown in Fig. 3c. A comparison of Figs. 3a and 3b shows that the C_4H_8 and β-cis-C_4H_8 from the chromatogram 3a were transferred to the chromatogram 3b in a pure state with no trace of adjoining fractions. The β-trans-C_4H_8 and C_4H_6 fractions were transferred similarly (Fig. 3c).

The separate fractions were identified from their infrared absorption spectra. The absorption spectra were obtained using an IKS-1 spectrograph in the range 2-15 μ, covering the frequencies of deformational vibrations of the C−H bonds and the valence vibrations of the C=C and C−C bonds. The position of the absorption bands, corresponding to given frequencies, is related to the definite atomic groupings in the butylene molecule and may serve to indicate the presence of a particular isomer.

The absorption spectra of the separate fractions are shown in Fig. 4. In accordance with the literature data [7], the first fraction must be related to α-butylene, the second to β-trans-butylene and the third to β-cis-butylene. The immobile phase employed in our work consisted of different natural forms of silica (diatomite, infusorial earth, etc.), impregnated with nitrobenzene (40 g of nitrobenzene per 100 g of sorbent).

Considerable promise is shown by methods employing a combination of chromatography with fractional distillation, extraction and counter-current distribution. These methods have a much greater productivity and may be used for a preliminary group separation of mixtures for subsequent resolution into separate components.

The results presented from the synthesis of labeled divinyl and butylenes seem to us to illustrate the simplicity and convenience of the method. The catalytic experiment requires approximately 1 hour while the chromatographic separation requires 2-2.5 hours. In 3-4 hours, therefore, it is possible to prepare four radiochemically pure products, whose synthesis and separation by the ordinary method would require several days.

Extensive possibilities are revealed for the preparation of various compounds labeled with C^{14} by the hydrogenation of CO by the Orlov-Fischer-Tropsch process, the syntol process [1] and hydrolytic condensation by the Eidus [8] and Zelinskii [9] methods.

LITERATURE CITED

[1] S. Z. Roginskii, Coll. Isotopes in Catalysis, Izd. AN SSSR, 1957, p. 411.

[2] S. V. Lebedev, J. Gen. Chem. 3, 698 (1933).

[3] M. I. Ianovskii, Instruments and Assemblies, P-57-99/8 (1957).

[4] M. I. Ianovskii, D. S. Kapustin and V. A. Nogotkov-Riutin, Coll. Isotopes in Catalysis, Izd. AN SSSR, 1957, p. 391.

[5] G. M. Zhabrova and B. M. Kadenatsi, Coll. Isotopes in Catalysis, Izd. AN SSSR, 1957, p. 187.

[6] C. Phillips, Gas. Chromatography, 1956.

[7] R. S. Rasmussen and R. Brattain, J. Chem. Phys. 15, 120, 131 (1947).

[8] Ia. T. Eidus and K. V. Puzitskii, Proc. Acad. Sci. 54, 35 (1946).

[9] N. D. Zelinskii, Proc. Acad. Sci. 60, 235 (1948).

Institute of Physical Chemistry,
USSR Academy of Sciences

Received April 16, 1958

THE EQUATION FOR ISOTHERMAL DIFFUSION IN THE CRITICAL REGION

L. A. Rott

(Presented by Academician S. I. Vol'fkovich, April 10, 1958)

It was first shown in [1-3] that the rate of diffusion falls to practically zero in the critical region of a binary system even when there is a considerable concentration gradient of one of the components. This extremely important fact points up the inapplicability of the ordinary Fick Equation for the description of diffusion in this region. The deduction of an acceptable equation for isothermal diffusion must start from the fact that the rate of change in the concentration of a component is fixed by the gradient of its chemical potential:

$$dm_2 = -\frac{D_0}{RT} c_2 \operatorname{grad}_n \mu_2 ds\, dt, \tag{1}$$

here dm_2 is the amount of the one component diffusing in the time dt across the area ds along the direction of the unit vector $\underline{n}$ normal to the area; c_2 and μ_2 are, respectively, the concentration and the chemical potential of the second component; T is the temperature; R is the gas constant; and D_0 is a constant of proportionality which will be considered as constant in what follows.

From (1), by a familiar rearrangement, it is possible to obtain the equation

$$\frac{\partial c_2}{\partial t} = -\frac{D_0}{RT} \operatorname{div}(c_2 \operatorname{grad} \mu_2). \tag{2}$$

The conditions

$$\left(\frac{\partial \mu_2}{\partial N_2}\right)_{P,T} = 0, \quad \left(\frac{\partial^2 \mu_2}{\partial N_2^2}\right)_{P,T} = 0, \tag{3}$$

must be fulfilled at the critical point in a binary system, N_2 being the mole fraction of the second component.

From this it follows that terms of the first or second, power will not enter into a development giving the the chemical potential, μ_2, as a series in $N_2 - N_{2,k}$ ($N_{2,k}$ designates the mole fraction at the critical point). Limiting ourselves to the first two members of this expression, it is possible to write

$$\mu_2 = \text{const} + \beta (N_2 - N_{2,k})^3. \tag{4}$$

We will consider the diffusion equation for a system in which the partial specific volumes and the partial molar volumes in the region of the critical concentration depend very weakly on the solution composition. The system which was investigated in [3] was of this type. Considering that

$$V = \bar{v}_0 N_1 + \bar{v}_2 N_2, \quad c_2 = \frac{N_2}{V} \tag{5}$$

(here V is the volume of the solution, and $\bar{v}_1$ and $\bar{v}_2$ are the partial molar volumes of the components), and taking the condition(3) into account, we will for the case of unidimensional diffusion write Equation (2) as

$$\frac{\partial N_2}{\partial t} = -\frac{3\beta D_0}{RT}(N_2 - N_{2,k})\left\{\left(\frac{\partial N_2}{\partial x}\right)^2\left[N_2 - N_{2,k} + \frac{2N_2}{1-\frac{N_2}{V}(\bar{v}_2-\bar{v}_1)}\right] + \right.$$
$$\left. + \frac{N_2(N_2-N_{2,k})}{1-\frac{N_2}{V}(\bar{v}_2-\bar{v}_1)}\frac{\partial^2 N_2}{\partial x^2}\right\}. \tag{6}$$

The condition

$$\frac{N_2}{V}(\bar{v}_2-\bar{v}_1) \ll 1, \tag{7}$$

is valid for a number of systems and when it is applied here, Equation (6) can be simplified to

$$\frac{\partial N_2}{\partial t} = 2aN_2(N_2-N_{2,k})\left(\frac{\partial N_2}{\partial x}\right)^2 + a(N_2-N_{2,k})^2\left[\left(\frac{\partial N_2}{\partial x}\right)^2 + N_2\frac{\partial^2 N_2}{\partial x^2}\right], \tag{8}$$
$$a = -\frac{3\beta D_0}{RT}.$$

Since the solution which is being considered is to be valid in the neighborhood of the critical point ($N_2 \to N_{2,k}$), the transformation

$$N_2 = N_{2,k}e^{\varphi} \tag{9}$$

plus the fact that $|\varphi| \ll 1$, leads to an approximation for the unidimensional isothermal diffusion equation in the critical region:

$$\frac{\partial \varphi}{\partial t} = A\varphi\left(\frac{\partial \varphi}{\partial x}\right)^2, \tag{10}$$

where $A = 2aN_{2,k}^3$.

The solution of (10) is

$$N_2 = N_{2,k}\exp\left\{\frac{\sqrt{\frac{c_1}{A}}x + c_2}{\sqrt{2(-c_1 t+1)}}\right\}, \tag{11}$$

where c_1 and c_2 are constants determined by the initial and the boundary conditions.

According to the Onsager hypothesis from the thermodynamics of irreversible processes [4], the mean rate of damping of the concentration fluctuations should depend linearly on the diffusional current. From this it follows that concentration equilibrium is slowly established in the critical region. In this connection it is of interest to consider the variation in the mole fraction (concentration) of the second component over a relatively small volume, whose linear dimensions are comparable to the wavelength of light, this study being essential for the validation of the above hypothesis.

If $N_2 = \alpha_2 N_{2,k}$ when $t = 0$ and $x = 0$, and $N_2 = \alpha_2 N_{2,k}$ ($\alpha_2 < \alpha_1 < 1$) when $x = l$, then

$$c_1 = \frac{2A}{l^2}\left[\ln\frac{\alpha^2}{\alpha_1}\right]^2, \qquad c_2 = \sqrt{2}\ln^*\alpha_1. \tag{12}$$

For a number of liquids, the coefficient β of (4) is of the order of 10^2 cal·(mole fraction)$^{-3}$·mole^{-1}; if $D_0 \sim 10^{-6} - 10^{-7}$ cm^2·sec^{-1} and $N_{2,k} \sim 0.2 - 0.3$, it follows that $A \sim -(10^{-9} - 10^{-10})$ cm^2·sec^{-1} at room temperature. Then for a length l equal to the wavelength of visible light, say 6000 A, and with $\ln\frac{\alpha_2}{\alpha_1} \sim 10^{-1}$ ($\alpha_1, \alpha_2 \to 1$)

$$c_1 \sim -10^{-3}\ \text{sec}^{-1}.$$

According to the solution (11), the alteration in the mole fraction of the one component becomes appreciable when $-c_1 t$ is comparable with unity, i.e., when the elapsed time is $t \sim 10^3$ sec. (Fig. 1, for $\alpha_1 = 0.95$ and $\alpha_2 = 0.9$).

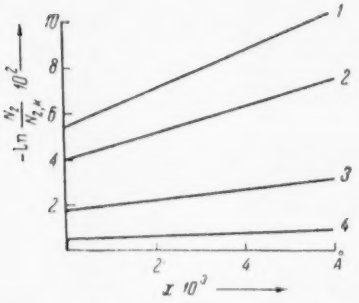

Fig. 1. 1) $t = 0$; 2) 10^3 sec; 3) 10^4 sec; 4) 10^5 sec.

The fact that the relaxation times are large makes it possible to utilize optical methods in investigating diffusional processes in the critical region. For pure substances, it has been shown in [5] that a vertical equilibrium distribution of concentrations is slowly established following intermixing in the critical region. This the authors explain by supposing consolidated associations (clusters) of molecules to form at the top of the column and subsequently slowly settle downward under the action of the force of gravity. The calculations which have been presented above show that the existence of large relaxation times is by no means bound up with this model. Moreover, such consolidated molecular groupings do not of necessity move downward, since they can break up in the upper part of the column and form in the lower part of it.

The diffusion equation (10) can be brought into the form of the ordinary Fick Equation

$$\frac{\partial c_2}{\partial t} = \frac{\partial}{\partial x}\left(D\frac{\partial c_2}{\partial x}\right). \tag{13}$$

For this purpose it is necessary to define a function $D(N_2)$ which we will interpret as the diffusion coefficient in the critical region.

Supposing V = const., we obtain a defining equation for the desired function D

$$\frac{\partial D}{\partial x} + f(t)D = F(x, t), \tag{14}$$

where

$$f(t) = \frac{\partial}{\partial x}\frac{N_2}{N_{2,k}}, \qquad F(x, t) = \frac{c_1(x + c_2)}{2(-c_1 t + 1)}. \tag{15}$$

When $c_2 = 0$ (this corresponds to the condition that $N_2 = N_{2,k}$, when $t = 0$ and $x = 0$)

$$F(x, t) = A|f(t)|^2 x. \tag{16}$$

Making use of (15) and (16) and supposing $D(N_{2,k}) = 0$, the solution of Equation (14) can be written in the form

$$D(N_2) = A\left(\frac{N_{2,k}}{N_2} + \ln\frac{N_2}{N_{2,k}} - 1\right). \tag{17}$$

The author wishes to express his thanks to Prof. I. R. Krichevskii for his interest in this work and for his valuable advice.

LITERATURE CITED

[1] I. R. Krichevskii, N. E. Khazanova and L. R. Linshits, Proc. Acad. Sci. 99, 113 (1954).

[2] I. R. Krichevskii and Iu. V. Tsekhanskaia, J. Phys. Chem. 30, 2315 (1956).

[3] Iu. V. Tsekhanskaia, Dissertation, State Inst. for the Petroleum Ind., Moscow, 1955.

[4] S. R. de Groot, The Thermodynamics of Irreversible Processes (in Russian) 1956.

[5] F. E. Murray and S. G. Mason, Canad. J. Chem. 30, 550 (1952); 33, 1408 (1955).

Received April 10, 1958

THE COEFFICIENTS FOR THE EQUILIBRIUM DISTRIBUTION OF DEUTERIUM IN THE ISOTOPIC EXCHANGE BETWEEN WATER AND CERTAIN THIOLS

K. I. Sakodynskii, S. I. Babkov, and N. M. Zhavoronkov,
Corresponding Member, Acad. Sci. USSR

Most of the work on the exchange reactions of the hydrogen isotopes has involved a study of the exchange between water and the O–H, N–H, and C–H groups. In this field, relatively little study has been given to the exchange between water and the S–H group [1-4].

It is customary to characterize the equilibrium in the isotopic exchange reaction

$$RSD + H_2O \rightleftharpoons RSH + HDO$$

by α, the coefficient for the equilibrium deuterium distribution. This coefficient is defined as the ratio of the ratios of the equilibrium concentrations of deuterium and protonium in water and in the thiol

$$\alpha = \left\{[D] / [H]\right\}_{water} / \left\{[D] / [H]\right\}_{thiol}. \quad (1)$$

Small [1] has determined the value of α for the exchange between water and hydrogen sulfide (2.28 at 15°). Benedict [2] has presented the data of German investigators on the temperature dependence of the coefficient for the equilibrium distribution of deuterium in this same exchange reaction (2.34 at 25° and 1.92 at 100°). Hobden, et al. [3] have obtained α values for the exchange reaction between water and ethylthiol (2.32 at 25°). Hutchison and Gillies [4] have given data on the temperature dependence of the coefficient for the equilibrium distribution in the exchange between water and isopropylthiol (2.02 at 27° and 1.77 at 95°).

Values of α can be calculated from spectral data, provided this data is sufficiently detailed. Hobden et al. [3] have calculated α values for the exchange between water and ethylthiol, and have obtained satisfactory agreement with the experimental results. In view of the fact that detailed spectral data is lacking for the thiols of higher molecular weights, α values can here be only approximated (to within ± 15%) from the β-factors for the exchanging hydrides by the method proposed by Varshavskii and Vaisberg [5]. It has seemed of interest to experimentally determine the values of the coefficients for the equilibrium distribution of deuterium in the exchange reactions between water and certain thiols.

The present work has studied the equilibria in the deuterium exchange between water and normal butylthiol, n-C_4H_9SH; secondary butylthiol, sec-C_4H_9SH; isoamylthiol, i-$C_5H_{11}SH$; normal hexylthiol, n-$C_6H_{13}SH$; and thiophenol, C_6H_5SH. The first four of these thiols were synthesized from the corresponding alcohols by the method of Frank and Smith [6]; the thiophenol was obtained from the acid chloride of benzenesulfonic acid [7]. The resulting thiols were carefully purified by distillation in a fractionating column which was packed with glass spirals and had an effectiveness of 10-12 plates. The purity of the thiols resulting from this distillation was checked by comparing their boiling-temperatures and refractive indices with the values taken from the literature.

The coefficients, α, for the equilibrium distribution of deuterium in the exchange reactions between water and the thiols were determined in the following manner. Into the vessel which was to be used for the study of the equilibrium there was introduced 0.5 – 1 cm^3 of water having a deuterium concentration of

~ 3 mole % and 8 – 15 cm^3 of thiol with the naturally occuring deuterium concentration (0.016 mole %). This vessel was in the form of a glass cylinder, 27 mm in diameter and 40 cm^3 in volume, with a 7 mm side arm which was constricted in the middle. The amounts of water and thiol which had been introduced were determined by subsequent weighing on an analytical balance. The side arm was then sealed off at the constriction and the vessel placed in a thermostat where the temperature was held constant to ±0.1°. The contents of this vessel were agitated on a shaking device having a frequency of 136 vibrations per minute.

Preliminary experiments had shown isotopic equilibrium to be attained in the exchange between water and the thiols within 8-10 hours at a temperature of 20° (in 2 hours in the case of the exchange with thiophenol), and within 2-4 hours at 80°. Thus, agitation was continued in each of the equilibrium experiments for 12-15 hours (5-7 hours for the exchange with thiophenol) at 20° and for 6-8 hours at 80°. After the agitation had been completed, the apparatus was taken out of the thermostat and rapidly and carefully wiped with a piece of filter paper; the end of the side-arm was then broken and the contents transferred to a separatory funnel through the jacket of which water from the thermostat was circulated. Thus, the temperature in the funnel was close to that under which the experiment had been carried out. Since the experiment and the separation of the components were carried out at the same temperature, it was possible to avoid a displacement in the equilibrium during the latter operation. The water layer parted from the thiol on standing and was then subjected to purification prior to isotopic analysis. This purification consisted in passing the water in vapor formed over heated copper oxide, followed by a two-fold microdistillation under vacuum [8]. The isotopic composition of the water was determined by the drop method. The concentration of the deuterium in the thiol was not measured directly but was calculated from a material balance on the deuterium in the system.

In addition to direct exchange between deuterium-enriched water and thiols with the naturally occurring deuterium concentration, an experiment on the inverse exchange was carried out on each thiol at 20°. The technique of these experiments was the same as that which has already been described. The water which was employed in these experiments contained the natural concentration of deuterium, and the thiols were those which had been enriched to ~1 % in preceding experiments on direct exchange. The experiments on inverse exchange confirmed the fact that true thermodynamic equilibrium had been achieved.

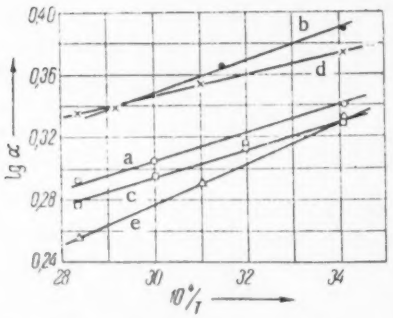

Fig. 1. The relation between the logarithm of the coefficient, α, for the equilibrium deuterium distribution and the reciprocal temperature. a) exchange between water and n-butylthiol; b) exchange between water and secondary butylthiol; c) exchange between water and i-amylthiol; d) exchange between water and n-hexylthiol; e) exchange between water and thiophenol.

The coefficient, α, for the equilibrium deuterium distribution was calculated in the following manner. Let X_0 be the initial concentration of deuterium in the water; X_p, the deuterium concentration in the water after equilibrium has been attained; y_0, the initial deuterium concentration in thiol (all concentrations being in mole %); n_T, the number of moles of thiol, and n_B, the number of moles of water; then on the basis of the definition of (1) and the material balance of deuterium in the system, α is to be determined from the expression

$$\alpha = \frac{X_p}{100 - X_p} \cdot \frac{100 - \left[y_0 + 2\frac{n_T}{n_B}(X_0 - X_p) \right]}{y_0 + 2\frac{n_T}{n_B}(X_0 - X_p)}. \qquad (2)$$

The determinations of α were carried out over the temperature interval 20-80°. For the exchange between water and secondary butylthiol, the experiments were in the interval 20-70°. 9-13 experiments were performed on each system with 2-5 determinations of α at each temperature. The resulting values for the coefficient, α, of the equilibrium distribution at various temperatures are shown in Table 1. In this table there are also given mean values of the arithmetic error in the determinations of α.

An analysis of Equation (2) shows that errors in the determination of X_0 and X_p are those of greatest significance in fixing the accuracy of the measurement of α. The drop method of isotopic analysis is accurate to

TABLE 1

Values of the Coefficients for the Equilibrium Distribution of Deuterium at Various Temperatures (the number of experiments is given in parenthesis)

System	20°	40°	50°	60°	80°
Water – n-butylthiol	2.20 ± 0.01 (4)	2.07 ± 0.07 (2)	– –	2.02 ± 0.02 (2)	1.96 ± 0.02 (4)
Water – secondary butylthiol	2.46 ± 0.03 (5)	– –	2.32 ± 0.00* (2)	– –	2.18 ± 0.02** (3)
Water – i-amylthiol	2.14 ± 0.03 (5)	2.07 ± 0.02 (2)	– –	1.97 ± 0.01 (2)	1.89 ± 0.01 (4)
Water – n-hexylthiol	2.37 ± 0.02 (4)	–	2.26 ± 0.03 (2)	–	2.16 ± 0.03 (4)
Water – thiophenol	2.15 ± 0.02 (4)	–	1.95 ± 0.02 (2)	–	1.80 ± 0.05 (3)

*At 45°

**At 70°

±1% of the measured quantity and by applying it at the working deuterium concentrations it is possible to obtain α values of an accuracy not less than ±5-6%. From the values of the mean arithmetical error which are given in Table 1, it is to be seen that the error in the α determinations amounts to ±1% in most cases and is as high as ± 3% in only one instance.

Under the described conditions, it is only the hydrogen isotope of the S–H group which participates in the exchange reaction. The hydrogen isotopes from the C–H units of the radical can be considered as failing to enter into exchange with water [9].

The temperature dependence of the coefficients for the equilibrium distribution of deuterium between water and the investigated thiols is given in Fig. 1 in the coordinates $\log \alpha$ vs. $1/T$. Over the temperature interval 20-80°, these relationships can be analytically expressed by the equations:

for the exchange between water and normal butylthiol

$$\log \alpha = 92.07/T + 0.0282 \quad (3)$$

for the exchange between water and secondary butylthiol

$$\log \alpha = 105.62/T + 0.0313 \quad (4)$$

for the exchange between water and isoamylthiol

$$\log \alpha = 88.52/T + 0.0283 \quad (5)$$

for the exchange between water and normal hexylthiol

$$\log \alpha = 69.48/T + 0.1376 \quad (6)$$

for the exchange between water and thiophenol

$$\log \alpha = 132.93/T - 0.213 \quad (7)$$

Making use of the relation proposed by Brodskii [10] for relating the coefficient α, for the equilibrium deuterium distribution and the equilibrium constant K, for the exchange reaction, the heat of reaction ΔH, for the isotopic exchange between water and the thiols can be calculated from the Clausius-Clapeyron Equation. Thus evaluated $-\Delta H$ proves to be equal to 600-1200 cal/mole.

Neither from our data, nor from the data of others, is it possible to establish a direct relation between the values of α and the composition and structure of the molecular radical. The one fact that is clear is that these factors have only a small effect on α.

LITERATURE CITED

[1] P. A. Small, Trans. Farad. Soc. 33, 820 (1937).

[2] M. Benedict, Progr. Nucl. Energy, N. Y., Ser. IV, 3, 3 (1956).

[3] F. W. Hobden, E. F. Johnston, L. H. Weldon and C. L. Wilson, J. Chem. Soc. 1939, 61.

[4] G. Hutchison and D. Gillies, Nucl. Sci. Abstr. 10, No. 11 Suppl. 3462 (1956); G. Murphy, Production of Heavy Water, N. Y., 1955; H. Urey, US Pat. 2741543, 10 IV, 1956.

[5] Ia. M. Varshavskii and S. E. Vaisberg, Proc. Acad. Sci. USSR 100, No. 1, 97 (1955).

[6] R. L. Frank and P. V. Smith, J. Am. Chem. Soc. 68, 2103 (1946).

[7] The Synthesis of Organic Compounds, Monog. 1, (Russian Trans.), Foreign Lit. Press, 1949, p. 381.

[8] A. I. Shatenshtein, et al., The Isotopic Analysis of Water (in Russian) Acad. Sci. USSR Press, 1957.

[9] V. N. Setkina, D. N. Kursanov, O. D. Sterligov and A. L. Liberman, Proc. Acad. Sci. USSR 85, 1045 (1952).

[10] A. I. Brodskii, The Chemistry of Isotopes (in Russian) Acad. Sci. USSR Press, 1957, p. 348.

The L. Ia. Karpov Physicochemical Institute
of the Academy of Sciences of the USSR

Received May 13, 1958

EQUILIBRIUM POTENTIALS OF TITANIUM IN CHLORIDE MELTS

M. V. Smirnov, L. E. Ivanovskii and N. A. Loginov

(Presented by Academician A. N. Frumkin, April 11, 1958)

The literature contains no data on the equilibrium potentials of titanium in salt melts. Since these potentials are a most important characteristic of the processes of cathodic deposition and anodic dissolution which form the basis of the electrolytic production and purification of the metal, we have undertaken the measurement of these potentials in electrolytes of varying compositions. In the present communication the results of studies using chloride melts are reported.

It is well known [1, 2] that in chloride melts in equilibrium with metallic titanium, the greater part of the titanium is present in the form of divalent ions, which are powerful reducing agents. For this reason the measurement of the equilibrium potentials was carried out in an atmosphere of pure argon in a hermetically sealed cell (Fig. 1). This consisted of a wide quartz tube containing at the foot a molten eutectic mixture of lithium and potassium chlorides, which was first of all treated by passing through a stream of dry hydrogen chloride and then maintained under reduced pressure of the order of 0.1 mm mercury until the evolution of dissolved gases had ceased.

An electrode of titanium prepared by the iodide method was fastened to a molybdenum conductor and immersed in a salt melt of the same composition contained in an alundum crucible, the walls of which acted as a diaphragm preventing transfer of electrolyte, but allowing the passage of a current of up to 2 amperes. In order to make the arrangement stable, the crucible was fixed in a narrow tube with an opening in the foot, and immersed in the melt in the wide tube in such a way that the level of the electrolyte in the crucible was slightly higher than that of the electrolyte in the remainder of the cell. Titanium was introduced into the electrolyte in the alundum crucible by anodic dissolution of the metal electrode, brought about by the passage of a definite quantity of electricity, measured by means of a copper coulometer. The electrolysis was carried out using an auxiliary cathode consisting of a molybdenum wire placed in a separate tube, the wall of which had an opening closed with an asbestos diaphragm. Lead chloride was added to the tube to prevent the liberation of alkali metal, which would attack the walls of the tube.

When the required concentration of titanium in the electrolyte had been reached (the concentration was checked at the end of the experiment by chemical analysis of the contents of the alundum crucible), the required temperature was established and the potential of the titanium electrode measured relative to the lead reference electrode. The latter consisted of a tube, containing at the foot a layer of pure molten lead covered with a molten eutectic mixture of lithium and potassium chlorides containing 8.05% by weight of $PbCl_2$. The wall of the tube had an opening closed with an asbestos diaphragm. Contact with the lead electrode was made by means of a molybdenum conductor.

Special experiments were carried out to measure the potential of the auxiliary lead electrode relative to the chlorine electrode whose construction has been described in previous works. The measurement of the e.m.f. of the cell: Pb/8.05% $PbCl_2$, LiCl, KCl (molten) ‖ LiCl, KCl (molten)/Cl_2, C was carried out in a cell of analogous construction except that the titanium electrode was replaced by the chlorine electrode [3]. The results of these experiments are presented graphically in Fig. 2. The experimental points recorded in the temperature range 450-700°C, lie on the straight line described by the empirical equation:

$$E = (1.616 - 3.21 \cdot 10^{-4} T) \pm 0.003 \text{ volts.}$$

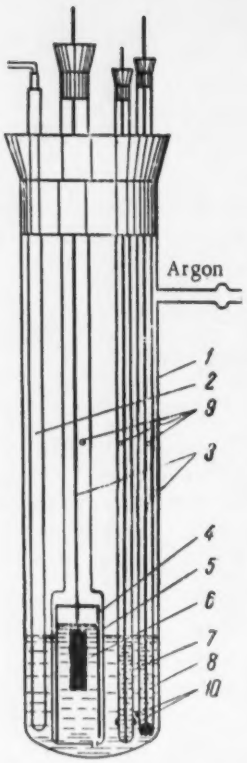

Fig. 1. The cell. 1) quartz tube; 2) thermocouple; 3) molybdenum conductors to the titanium and lead electrodes; 4) alundum crucible; 5) narrow tube; 6) titanium electrode; 7) auxiliary cathode; 8) lead reference electrode; 9) openings in the tubes to provide a passage between the gas spaces; 10) asbestos diaphragm.

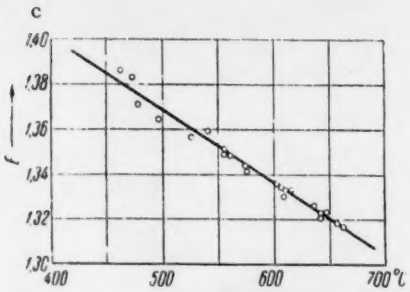

Fig. 2. The relationship between the temperature and the e.m.f. between the lead and chlorine electrodes.

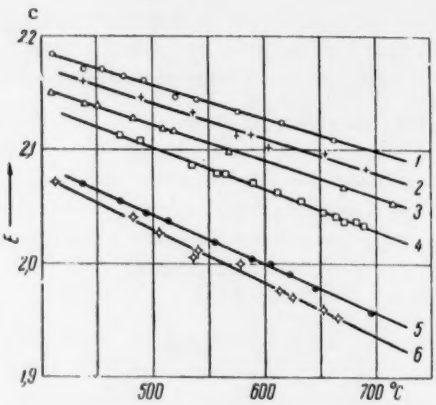

Fig. 3. The relationship between temperature and the e.m.f. between the titanium and chlorine electrodes for various concentrations of titanium in the electrolyte.

During the measurements the cell was kept in a solid metal block heated in an electrical resistance furnace with automatic control of the temperature (measured by means of a thermocouple placed in the electrolyte), which could be maintained constant at a given value to within ±1°. The potential values taken as being reliable were those which remained constant to within ± 1 mv at a given temperature for a considerable length of time (1-2 hours).

The e.m.f. of the cell Ti/X $TiCl_2$, LiCl, KCl (molten) || LiCl, KCl (molten) || 8.05% $PbCl_2$, LiCl, KCl (molten)/Pb was measured within the temperature range from 410 to 710° for the following concentrations of titanium in the electrolyte: 0.2; 0.32; 0.49; 0.94; 5.3 and 5.7% by weight of Ti, which corresponds to the following concentrations as mole fractions: $4.66 \cdot 10^{-4}$; $7.45 \cdot 10^{-4}$; $1.14 \cdot 10^{-3}$; $2.19 \cdot 10^{-3}$; $1.25 \cdot 10^{-2}$ and $1.35 \cdot 10^{-2}$.

The results of the measurements, recalculated relative to the chlorine electrode, are given in Fig. 3 in the form of a graph showing the relationship between the temperature and the e.m.f. for the given concentrations of titanium in the electrolyte. It can be seen that the experimental points lie fairly accurately on straight lines (Fig. 3) given by the following empirical equations:

$$E_{0.2\%Ti} = (2.374 - 2.82 \cdot 10^{-4}T) \pm 0.002 \text{ volts (Curve 1);}$$

$$E_{0.32\%Ti} = (2.380 - 3.11 \cdot 10^{-4}T) \pm 0.004 \text{ volts (Curve 2)};$$

$$E_{0.49\%Ti} = (2.367 - 3.17 \cdot 10^{-4}T) \pm 0.002 \text{ volts (Curve 3)};$$

$$E_{0.94\%Ti} = (2.385 - 3.67 \cdot 10^{-4}T) \pm 0.002 \text{ volts (Curve 4)};$$

$$E_{5.3\%Ti} = (2.374 - 4.30 \cdot 10^{-4}T) \pm 0.001 \text{ volts (Curve 5)};$$

$$E_{5.7\%Ti} = (2.389 - 4.66 \cdot 10^{-4}T) \pm 0.003 \text{ volts (Curve 6)}.$$

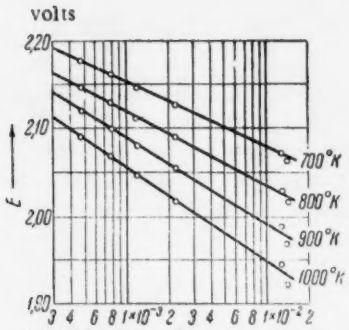

Fig. 4. Isotherms for the e.m.f. between titanium and chlorine electrodes.

To show how the e.m.f. changes with change in the concentration of titanium in the melt, the temperature remaining constant, Fig. 4 gives isotherms calculated from these empirical equations for 700, 800, 900 and 1000°K. The e.m.f. values are plotted against the logarithms of the mole fraction concentrations of titanium in the electrolyte. The recalculated experimental points lie on straight lines with slopes very close to the values 2.3 RT/2F for the corresponding temperatures.

Thus the equilibrium potential of a metallic titanium electrode in chloride melts containing up to 6% by weight of Ti varies with the mole fraction concentration of titanium in the melt in accordance with the thermodynamic equation:

$$E = E^0_{Ti/Ti^{2+}} + \frac{2.3RT}{2F} \log [Ti^{2+}].$$

This provides evidence that these melts contain predominantly ions divalent titanium and behave as ideal solutions.

The quantity $E^0_{Ti/Ti^{2+}}$ in this equation may be found from the experimental data obtained by eliminating the thermal e.m.f. between the molybdenum and carbon conductors attached to the titanium and chlorine electrodes; this e.m.f. is opposite in sign to the measured electrochemical potential difference [4]. It is found to be equal to:

$$E^0_{Ti/Ti^{2+}} = (-2.371 + 6.09 \cdot 10^{-4}T) \text{ volts}$$

relative to the chlorine reference electrode.

It is interesting to compare this value with that previously obtained by us for thorium, E^0Th/Th^{2+}. As was to be expected from the general features observed in the periodic system of the elements, titanium proves to be considerably more positive than thorium. In chloride melts containing the dichlorides of these metals in equilibrium with the corresponding metals, the difference

$$E^0_{Ti/Ti^{2+}} - E^0_{Th/Th^{2+}} = (0.82 - 4.34 \cdot 10^{-4}T) \text{ volts}$$

amounts to 0.4 volt at 700° and 0.3 volt at 900°.

It can readily be shown that the decomposition potential of pure molten titanium dichloride is equal to:

$$E_{decomp.} = 0.225 \cdot 10^{-4}T - E^0_{Ti/Ti^{2+}} - \frac{RT}{2F} \ln f_{Ti^{2+}} \cdot f^2_{Cl^-}.$$

where $f_{Ti^{2+}}$ and f_{Cl^-} are the activity coefficients of the titanium and chlorine ions in the pure salt melt, taking as standard state ($f_{Ti^{2+}} \cdot f^2_{Cl^-} = 1$) dilute solutions of the salt in a molten mixture of alkali metal chlorides. If it is assumed that these melts behave as ideal solutions up to the state where pure molten titanium dichloride is obtained, then its decomposition potential is given by the expression:

$$E_{decomp.} = (2.371 - 5.86 \cdot 10^{-4} T) \text{ volts.}$$

From this it is possible to calculate the change in the isobaric potential for the formation of liquid titanium dichloride from its elements: $Ti_{(s)} + Cl_{2(g)} = TiCl_{2(l)}$

$$\Delta Z = (-109\,360 + 27.03\,T) \text{ cal/mole } TiCl_2.$$

Consequently, $\Delta H_{rev.} = -109360$ cal/mole $TiCl_2$. From the entropy of reaction, $\Delta S = -27.03$ cal/degree, it is easy to calculate the standard value for the entropy of liquid titanium dichloride, if it is assumed that $S^0_{Ti(s)} = 7.24$ and $S^0_{Cl_2(g)} = 53.29$ cal/degree · mole [5]. It is found to be equal to $S^0_{TiCl_2(l)} = 33.5$ cal/degree · mole.

Data can be found in the literature [6-11] for the heat of formation and entropy of solid titanium dichloride. If the average values are taken for these quantities [11]: $\Delta H^0_{TiCl_2(s)} = 120.6$ kcal/mole and $S^0_{TiCl_2(s)} = 24.7$ cal/degree · mole, then we obtain the following values for the heat and entropy of fusion of titanium dichloride: $\Delta H_{fus.} = 11.2$ kcal/mole and $\Delta S_{fus.} = 8.8$ cal/mole. According to these values the salt should melt at approximately 1000°. It is reported in the literature [12] that the melting point of this salt lies in the region of 900°.

LITERATURE CITED

[1] W. C. Kreye and H. H. Kellogg, J. Electrochem. Soc. 104, 504 (1957).

[2] M. B. Alpert, F. J. Schultz and W. F. Sullivan, J. Electrochem. Soc. 104, 555 (1957).

[3] M. V. Smirnov, S. F. Pal'guev and L. E. Ivanovskii, J. Phys. Chem. 29, 774 (1955).

[4] M. V. Smirnov and L. E. Ivanovskii, J. Phys. Chem. 31, 802 (1957).

[5] W. Latimer, Oxidation States of the Elements and Their Potentials in Aqueous Solution, IL, 1954.*

[6] M. Farber and A. J. Darnell, J. Phys. Chem. 59, 156 (1955).

[7] M. Farber and A. J. Darnell, J. Chem. Phys. 25, 526 (1956).

[8] W. F. Krieve, S. P. Vango and D. M. Mason, J. Chem. Phys. 25, 519 (1956).

[9] G. B. Skinner and R. A. Ruehrwein, J. Phys. Chem. 59, 113 (1955).

[10] D. G. Clifton and G. E. MacWood, J. Phys. Chem. 60, 309 (1956).

[11] D. Altman, M. Farber and D. M. Mason, J. Chem. Phys. 25, 531.

[12] N. Van Orden and M. Cannon, Proc. Utah Acad. Sci. Arts and Letters, 32, 214 (1955).

Electrochemistry Laboratory, Ural Section,
USSR Academy of Sciences

Received March 25, 1958

*Russian translation.

THE KINETIC ISOTOPIC EFFECT IN THE REACTION OF HYDROGEN AND TRITIUM WITH THE OXIDES OF CERTAIN METALS*

V. A. Shushunov and B. Ia. Andreev

(Presented by Academician V. N. Kondrat'ev, April 2, 1958)

There are only a few works in the literature [1-6] which mention the difference in the rates of topochemical reactions in which hydrogen and deuterium take part. As far as we are aware, no one has up to the present carried out any analogous work using tritium in place of deuterium.

The study of the difference in the rates of topochemical reactions in which hydrogen and tritium take part, together with the examination of the influence of a number of factors on the kinetic isotopic effect in such reactions, may, in our opinion, give many interesting results. The present work contains the results of a study of the influence of isotopy on the rate of reduction of the oxides of a number of metals by hydrogen and tritium.

The experiments were carried out under dynamic conditions in an apparatus which differed little in essentials from that described earlier [7]. We followed the course of the reaction by measuring the fall in the pressure of the gas, while the isotopic composition of the gas was followed by determining the intensity of its radiation using a Geiger-Muller counter with internal loading. In order to ensure the reversibility of the reactions taking place during the reduction of the oxides under study, the water vapor was removed rapidly from the reaction vessel and frozen in a trap cooled with liquid nitrogen.

The mixture of hydrogen and tritium was obtained by chemical decomposition of water. Since the concentration of tritium in the water and in the gas amounted to not more than $2 \cdot 10^{-4}$ %, it may be assumed that the mixture of gases consisted of H_2 and HT molecules only. The isotopic effect in the reactions under study therefore relate to the reactions of these molecules only, and not to those of H_2 and T_2 molecules.

The oxides of the metals were prepared by various methods described in widely known textbooks [8, 9] and fractionated by screening through sieves. As a rule, powder of a definite degree of dispersion was used in the experiments.

Assuming that the reduction of the oxides takes place by means of a first order reaction in the case of both H_2 and HT, and making certain reasonable further assumptions, we obtained the following equation expressing the relationship between the specific activity (A) of the gas and its pressure (p), which is applicable to the reaction carried out at constant temperature and constant volume of the system:

$$\log A = \left(\frac{1}{\alpha} - 1\right) \log p + B. \qquad (1)$$

The isotopic kinetic effect α is equal to the ratio of the rate constant (k_1) for the reaction between H_2 and the metal oxides to the rate constant (k_2) for the reaction between HT and the metal oxides; B is a constant characterizing the initial state of the gas.

A strict linear relationship was observed between log A and log p in all the reactions involving the reduction of the oxides studied, which confirms the accuracy of the assumptions which we made in the derivation of equation (1). The nature of this relationship does not change with change in the initial pressure of the gas, the weight of oxide taken for reduction, or the temperature. This can be seen from Figs. 1 and 2, which show several graphs constructed using experimental data for the reaction of cupric oxide with hydrogen.

*G. M. Vlasov, Iu. A. Ivanov and A. L. Buchachenko took part in the experimental work.

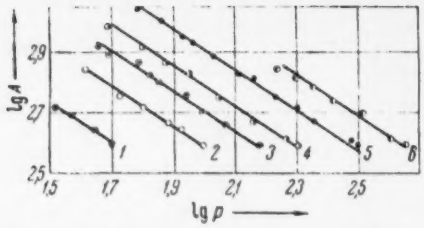

Fig. 1. The reduction of cupric oxide at different initial pressures of gas. Weight of oxide 1 g, t = 150°. Initial pressure of gas: 1) 50; 2) 100; 3) 150; 4) 200; 5) 314; 6) 453 mm mercury.

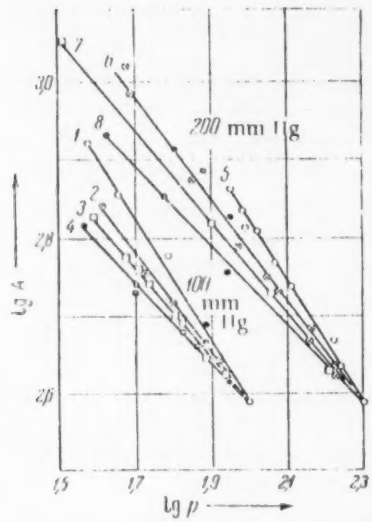

Fig. 2. The reduction of cupric oxide at different temperatures. Weight of oxide 1 g. 1 and 5) 125; 2 and 6) 150; 3 and 7) 175; 4 and 8) 200°.

Equation (1) is of course not applicable in those cases where simultaneous reduction of two or three oxides of the same metal is taking place, for example during the reduction of MnO_2 and the Mn_2O_3 formed in the process. In this case a linear relationship between log A and log p will be observed only at the very beginning of the reaction, when the second oxide has not had time to accumulate in sufficient amount.

By making use of Equation (1), we have constructed graphs with coordinates log A – log p and have used the slope of the straight line expressing this relationship to calculate the value of the kinetic isotopic effect (α) for each experiment. The results of these calculations are given in Table 1.

It should be noted that the value of α is independent of the initial pressure of the gas, the weight of oxide sample taken for reduction, and also of the method used for its preparation and its degree of dispersion. On the other hand, as can be seen from Table 1, the magnitude of this effect is dependent to a great extent on the temperature and on the nature of the oxides taken for reduction.

All the oxides whose reduction we have studied may be divided into two groups. The first group contains those oxides which react with hydrogen more rapidly than with tritium. In this case the value of the kinetic isotopic effect (α), i.e., the ratio k_1/k_2, is greater than unity. For these reactions we have arbitrarily taken α as positive. It can be seen from Table 1 that the reduction of Ag_2O, Cu_2O, CuO, HgO, PbO_2, MnO_2 and, at high temperatures, Fe_2O_3, is characterized by positive values for the kinetic isotopic effect.

The second group consists of those oxides which react with hydrogen less rapidly than with tritium. In this case the value of the kinetic isotopic effect (α) is less than unity and we have taken it arbitrarily as negative. The oxides Mn_3O_4, Mn_2O_3, NiO, CoO, Fe_3O_4 and Fe_2O_3 belong to this group. The reduction of ferric oxide takes place with a negative kinetic isotopic effect only at temperatures of up to 320°, and at higher temperatures α becomes positive.

In the study of the kinetic isotopic effect for the reaction involved in the reduction of metal oxides by hydrogen and tritium it is necessary to take into account the possibility of isotopic exchange under these conditions:

$$HT + H_2O \rightleftharpoons HTO + H_2. \qquad (I)$$

This reaction may be catalyzed both by the oxides and also by the metals formed by their reduction. Special experiments which we have carried out showed that the oxides of the first group and the corresponding metals catalyze reaction (1) only to a very slight extent. The rate of isotopic exchange under the conditions of our experiments is extremely low compared with the rate of reduction of the oxides of the first group by hydrogen and tritium. For the second group of oxides, on the other hand, the ability to catalyze reaction (1) is a very characteristic property both of the oxides themselves and of the pure metals. Our results in this case must therefore be regarded with some care.

The methods adopted in our experiments, however, ensured rapid removal of the water vapor formed in

TABLE 1

Ag_2O		Cu_2O		CuO		HgO		PbO_2		MnO_2	
t, °C	α	t, °C	α	t, °C	α	t, °C	α	t, °C	α	t, °C	α
20	1,38	80	4,76	80	8,00	120	2,54	140	1,55	100	2,18
40	1,56	100	3,85	100	6,60	200	2,11	160	1,48	120	1,92
60	1,72	120	3,03	125	4,17	300	1,74	180	1,42	140	1,75
70	1,67	160	2,50	140	3,33	380	1,53	200	1,38	160	1,56
80	1,58	180	2,08	150	2,94					180	1,46
90	1,51			175	2,33					200	1,30
				200	2,00					220	1,23

Mn_3O_4		Mn_2O_3		NiO		CoO		Fe_3O_4		Fe_2O_3	
t, °C	α	t, °C	α	t, °C	α	t, °C	α	t, °C	α	t, °C	α
300	0,50	220	0,68	150	0,30	160	0,30	280	0,47	240	0,54
360	0,56			175	0,33	180	0,32	320	0,51	260	0,58
400	0,59			200	0,40	200	0,33	340	0,53	280	0,73
460	9,64			225	0,42	220	0,37	360	0,55	300	0,85
500	0,68			250	0,45	240	0,40	380	0,57	320	1,00
						260	0,41			340	1,10
						280	0,43			380	1,21
										400	1,25

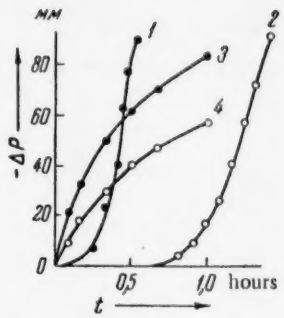

Fig. 3. The reduction of CuO at 180° by hydrogen (1) and deuterium (2), and of MnO_2 at 200° by hydrogen (3) and deuterium (4). Initial pressure of gas 200 mm mercury.

the reduction of the metal oxides from the sphere of reaction, which reduced considerably the rate of reaction. It may therefore be assumed that reaction (1) did not play a decisive part in our experiments.

This assumption was very convincingly confirmed by experiments which we carried out on the reduction of the metal oxides by hydrogen and deuterium.* It turned out that the reduction of the oxides of the first group by hydrogen takes place much more rapidly (1.4-1.8 times) than the reduction by deuterium. On the other hand, the reduction of the oxides of the second group by hydrogen takes place much more slowly (1.4-1.6 times) than reduction by deuterium. Figures 3 and 4 show several kinetic graphs which illustrate clearly these effects.

These experiments prove convincingly that the kinetic isotopic effect in the reactions of hydrogen isotopes with metal oxides acquires a sign dependent on their nature and on the conditions under which the process is carried out.

It was later found that the relationship between α and temperature obeys Arrhenius' law. We have used the temperature coefficient of α to calculate the difference in the values of the energies of activation for the reduction of the metal oxides by hydrogen (E_1) and by tritium (E_2) (Table 2).

TABLE 2

Oxide	Cu_2O	CuO	HgO	PbO_2	MnO_2
$(E_2 - E_1)$, kcal.	2.6	3.9	1.0	0.9	1.8
Oxide	NiO	CoO	Mn_3O_4	Fe_3O_4	
$(E_1 - E_2)$, kcal.	1.4	1.5	1.4	1.4	

*The deuterium contained 2-4% hydrogen.

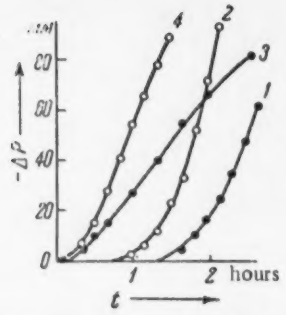

Fig. 4. The reduction of NiO at 180° by hydrogen (1) and deuterium (2), and of Fe_3O_4 at 280° by hydrogen (3) and deuterium (4). Initial pressure of gas for NiO 200 mm mercury; for Fe_3O_4, 150 mm mercury.

It can be seen from Table 2 that the nature of the oxides of the first group has a fairly strong influence on E_1-E_2, whereas this influence is quite insignificant for the second group of oxides. For the oxides of the first group, $E_1 < E_2$ and the value of α decreases with increase in temperature, while for the oxides of the second group $E_1 > E_2$ and the value of α increases with increase in temperature.

In the case of the reduction of silver oxide and ferric oxide, we observed an unusual relationship between α and the temperature. In the reduction of silver oxide the value of α at first increases with increase in temperature, which is unusual for oxides of the first group, and then decreases. At relatively low temperatures the reduction of ferric oxide takes place with a negative value of α, but at temperatures above 320° it takes place with a positive value of α. These two anomalous cases probably result from a change in the mechanism of the reduction of the oxides with increase in the temperature.

LITERATURE CITED

[1] J. Higuchi and J. Kawana, J. Chem. Soc. Japan, Pure Chem. Sect. 71, 624 (1950); Chem. Abstr. 45, 7461 (1951).

[2] H. Svec and F. Duke, Study of Kinetics of the Reactions between Uranium, H_2, HD and D_2. Oak Ridge, Tenn., 1955.

[3] H. W. Melville and E. K. Rideal, Proc. Roy. Soc. A. 153, 77 (1936).

[4] J. Higuchi, Bull. Inst. Phys. Chem. Res. (Tokyo) 21, 843 (1942); Chem. Abstr. 42, 5318 (1948).

[5] F. Ishikawa and K. Mikai, Bull. Inst. Phys. Chem. Res. (Tokyo) 22, 665 (1943); Chem. Abstr. 41, 5778 (1947).

[6] H. A. Smith and J. C. Posey, J. Am. Chem. Soc. 79, 1310 (1957).

[7] V. A. Shushunov and B. G. Zateev, J. Phys. Chem. 30, 321 (1956).

[8] Iu. V. Kariakin, Pure Chemical Reagents, 1947.*

[9] G. Brauer, Textbook of Preparative Inorganic Chemistry, IL, 1956.**

Chemical Research Institute,
N. I. Lobachevskii State University
Gorkii

Received March 27, 1958

*In Russian.

**Russian translation.

THE ELECTROCHEMICAL PROPERTIES AND CORROSION BEHAVIOR OF TITANIUM IN SULFURIC ACID SOLUTIONS

V. V. Andreeva and V. I. Kazarin

(Presented by Academician A. N. Frumkin, April 10, 1958)

The relationship between the rate of dissolution of titanium in sulfuric acid solutions and the concentration is very complex [1].

Figure 1 gives a graph showing the relationship between the rate of corrosion of titanium and the concentration of the sulfuric acid solutions (the Curves K)* at 40°. As shown in Fig. 1, two maxima are observed for the rate of dissolution of titanium. The first maximum corresponds to 40% acid, the second to 75% acid.

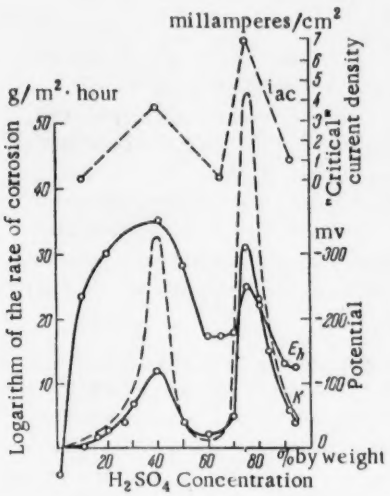

Fig. 1. The change in the rate of corrosion, dissolution potential and critical anodic current density for titanium in various sulfuric acid solutions at 40°. (The dissolution potentials and the critical anodic current densities relate to technical titanium (99% purity), the rate of corrosion of which is given by the broken line).

During the dissolution of titanium in solutions corresponding to the region of the first maximum (40% H_2SO_4), gaseous hydrogen is evolved. In this concentration region the sulfuric acid has maximum electrical conductivity and maximum hydrogen ion concentration. The process of hydrogen evolution is facilitated by the ready adsorption of hydrogen by the titanium. In the region of the second maximum (75% H_2SO_4), the titanium dissolves with reduction of the sulfuric acid to H_2S and free sulfur, while at sulfuric acid concentrations of 80-90% dissolution takes place with the liberation of SO_2 and free sulfur. The oxidation–reduction processes take place very vigorously in the region of the second maximum, since concentrated sulfuric is a powerful oxidizing agent while the trivalent titanium ion is a powerful reducing agent.

The low rate of dissolution of titanium in dilute sulfuric acid solutions (the first minimum) indicates the protective character of the natural oxide film which is formed on titanium in the atmosphere (titanium dioxide). The rate of corrosion of titanium in the region of the second minimum (50-70% H_2SO_4) is of particular interest. In this concentration region the rate of corrosion of titanium remains unchanged with increase in the temperature from 30 to 50° and it is only at 100° that the magnitude of the loss in weight of titanium becomes slightly higher. A study of the system $TiO_2 \cdot SO_3 \cdot H_2O$ shows that the formation of two compounds of TiO_2 and H_2SO_4 is possible, while the solubility of these compounds at 100° is exceptionally low in the region of acid concentrations 50-70%. These compounds have the following composition: $TiOSO_4 \cdot H_2O$ and $Ti_2O(SO_4)_3 \cdot 5H_2O$ with ratios $TiO_2 : SO_3 : H_2O = 1 : 1 : 1$ for the first compound and 2 : 3 : 5 for the second.

*The two Curves K are: for titanium of 99% purity – the broken line, and for titanium of 99.5% purity – the continuous line.

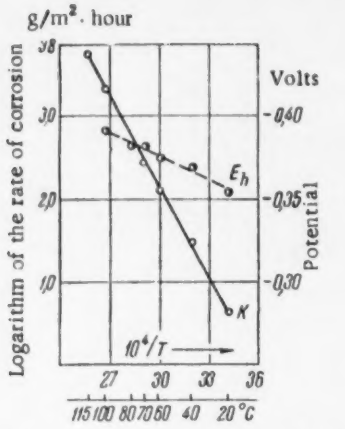

Fig. 2. The relationship between the logarithm of the rate of corrosion of titanium and T^{-1} in 40% H_2SO_4 solution.

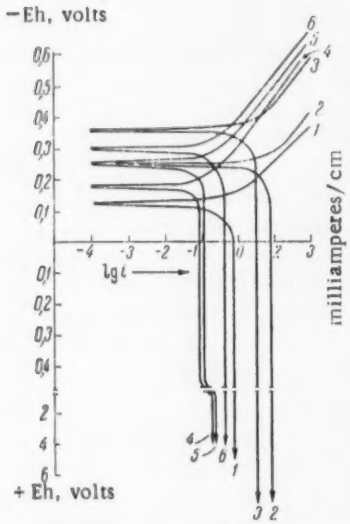

Fig. 3. Cathodic and anodic polarization curves for titanium in sulfuric acid solutions at 40°. 1) 94%; 2) 75%; 3) 40%; 4) 60%; 5) 10%; 6) 20%.

The fact that in this region of acid concentrations new compounds are formed on the titanium surface in the form of protective films, differing in composition from hydrated titanium dioxide, has been established by an experiment in which measurements were made of the change in potential with time in 60% H_2SO_4 solution. In this experiment, a shift of the positive potential into the region of negative values took place initially, indicating the process of dissolution of the natural film, after which the potential began to become gradually more noble, reaching constant values of +0.2 volt, and indicating the formation of a new phase compound.

Figure 1 also gives the relationship between the values of the titanium electrode potentials and the acid concentration (Curve Eh). The electrode potential values are different in those acid solutions corresponding to the maxima and minima of the rate of dissolution of the titanium, which indicates a difference in the nature of the reactions taking place at the electrode surface.

At the boiling point of the H_2SO_4 solutions the rate of corrosion of titanium increases with increase in the concentration of the acid up to 75%. The sharp decrease in the rate of corrosion of titanium observed in acid concentrations of 80% and above (from 5180 g/m²·hour in 75% H_2SO_4 to 70 g/m²·hour in 80% H_2SO_4) may be explained by the formation of titanium corrosion products in the form of titanium sulphate compounds $Ti_2(SO_4)_3$, sparingly soluble in concentrated acid.

The relationship between the rate of corrosion of titanium and temperature has been studied in 40% H_2SO_4 solution. It can be seen from Fig. 2, in which the results obtained are presented, that the points giving the relationship between the logarithm of the rate of corrosion of titanium and T^{-1} lie accurately on a straight line (the straight line K). Calculations have shown that the activation energy of the process of metal ionization amounts to 16.7 kcal/mole, which is very close to the values obtained by Berg [4] for the activation energy of the dissolution of titanium in phosphoric acid, 15.67 kcal/mole.

Such high values for the acitvation energy indicate that under these conditions the diffusion processes do not have a controlling influence (their activation energy amounts to between 3 and 6 kcal/mole). The displacement of the potential into the region of more negative values with increase in the temperature (the straight line Eh) provides evidence of the reduced anodic polarizability of the titanium. The polarization curves for titanium were recorded in 10, 20, 40, 65, 75 and 90% H_2SO_4 solutions at 40° after stationary potential values had been established. These concentrations correspond to the most characteristic points on the corrosion—concentration curve, namely, the maxima and minima of the rate of dissolution.

These data are given in Fig. 3. It can be seen from this figure that both the cathodic and the anodic curves have horizontal sections corresponding to regions where the anodic process is facilitated and the process of metal dissolution takes place with great intensity, i.e., the spontaneous dissolution current is considerably greater than the external current which can be applied. The magnitude of the current density at which the formation of oxide films begins and dissolution of titanium ceases depends on the acid concentration. Anodic polarization begins sharply at a definite "critical" current density for a given solution. For an initial displacement of the potential from −0.2 volt to between + 0.5 and + 0.6 volt, no changes are observed on the outer

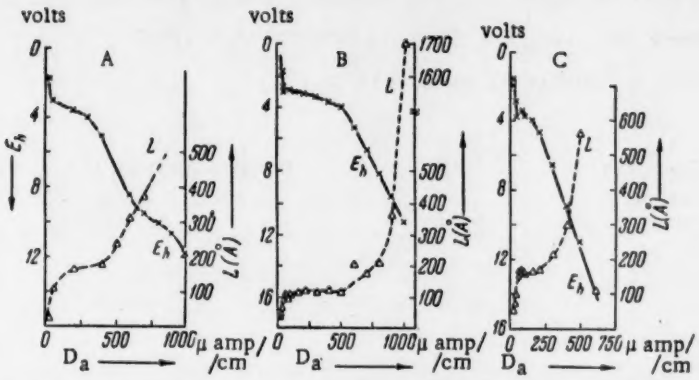

Fig. 4. The change in the potential and in the thickness of the surface film on titanium in sulfuric acid solutions at 20° with change in current density: A) 10%, B) 40%, C) 60%. (Polarization began from a potential of the order of + 0.1 volt from the passive state).

surface of the specimen. Measurements carried out simultaneously on the thickness of the films formed on the titanium during this time, using an optical polarization method [2, 3], showed that in this region of potential values the film is very thin – its thickness does not exceed 200 A (Fig. 4). With further displacement of the potential, a colored film begins to be formed, but without any visible evolution of oxygen. The thickness of the film reaches various values within the range 600-2000 A.

The evolution of oxygen on titanium begins at a fairly high overvoltage, equal to ~ + 2 volts. The oxide film has high electric resistance (its growth is accompanied by a fall in the current strength in the circuit).

The values of the "critical" current density, i.e., of the minimum current capable of bringing about the sharp displacement of the potential into the positive region, are given in the upper part of Fig. 1 by the broken dotted line i_{ac}. As was to be expected, the same dependence on acid concentration is observed in this case as in the case of the corrosion of titanium; the minimum values of the current densities correspond to the corrosion minima and vice versa.

The anodic and cathodic polarization curves for titanium were recorded in sulfuric acid solutions at various temperatures. It was shown, for example, that in 40% H_2SO_4 solution the overvoltage of hydrogen liberation on titanium decreases with increase in temperature while the critical anodic current density increases. Thus at 20, 40 and 60° the cathodic process may be described by a Tafel equation of the form:

$$\eta H_2 = 0.41b - 0.16 \log i \text{ (milliamperes/cm}^2\text{) (20°)}$$

$$\eta H_2 = 0.29b - 0.16 \log i \text{ (milliamperes/cm}^2\text{) (40°)}$$

$$\eta H_2 = 0.18b - 0.16 \log i \text{ (milliamperes/cm}^2\text{) (60°)}$$

The critical anodic current densities correspond to the values: 0.4 milliamperes/cm^2 at 20°, 2 milliamperes/cm^2 at 40° and 12.5 milliamperes/cm^2 at 60°.

It should be noted that the region over which the Tafel equation is applicable to the cathodic process of hydrogen liberation on titanium was displaced, with increase in temperature, to higher current density values, in accordance with the increase in the spontaneous dissolution current.

LITERATURE CITED

[1] V. V. Andreeva and V. I. Kazarin, The Corrosion Resistance of Titanium in Agressive Solutions, Inst. Tech. and Econ. Inform. AN SSSR, subject 23, I-56-159 (1956).*

*In Russian.

[2] V. V. Andreeva, The Use of an Optical Polarization Method for the Study of Corrosion and Passivity in Metals, Inst. Tech. and Econ. Inform. AN SSSR, subject 9, PS-55-503 (1955).*

[3] V. V. Andreeva, Proc. Inst. Phys. Chem. AN SSSR, No. 6, 79 (1957).

[4] T.G.Owe Berg, Chim. Phys. 52, No. 5, 363 (1955).

Institute of Physical Chemistry,
USSR Academy of Sciences

Received April 10, 1958

*In Russian.

THE ELECTRON THEORY OF THE ADHESION OF METALS WHICH ARE JOINED BY A SEMICONDUCTING FILM

B. V. Deriagin, Corresponding Member, Acad. Sci. USSR and V. P. Smilga

For an extensive class of phenomena it has been shown in [1] that electrostatic forces play a decisive role in adhesion. In [2] the electrostatic component of the force of adhesion which arises from the presence of a double layer at a metal-semiconductor interface has been considered in light of modern theories of contact. But although this double layer and the force of adhesion of a thin semiconducting film included between two unlike metals are of great interest from the practical point of view, their study has been essentially qualitative.

We have obtained an exact solution of this problem by making use of its mathematical similarity with the problem of the electrostatic interaction of two oppositely charged surfaces separated by a layer of electrolyte, which has been treated in the theory of heterocoagulation and of colloids.

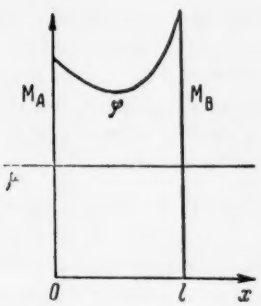

Fig. 1

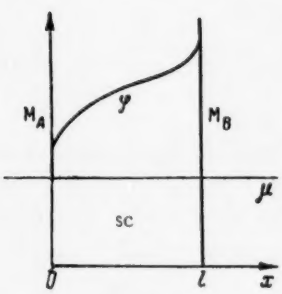

Fig. 2

As in [2], we will limit ourselves in what follows to a consideration of the case in which the semiconductor contains a single type of carrier and only a small fraction of the additive centers are ionized. It is known that the equilibrium charge distribution is here determined by the Poisson-Boltzmann Equation

$$\frac{d^2\tilde{V}}{dx^2} = \varkappa^2 \operatorname{sh} \tilde{V}, \qquad (1)$$

in which $\tilde{V}$ is the dimensionless potential energy of the electron in the conducting zone, $\tilde{V} = eV/kT$, $\varkappa = \sqrt{8\pi n_{\infty} e^2/\epsilon kT}$ is the reciprocal screening distance, ϵ is the dielectric constant and n_{∞} is the concentration of conducting electrons in the free semiconductor. The force of adhesion of the film to one of the metals is equal to $F = \epsilon^2 E_{bd}^2/8\pi$, where E_{bd} is the field strength within the semiconductor at the boundary with the metal in question. Thus, the problem comes down to that of determining E at the right and the left film boundaries.

It is at the outset clear that E(0) and E(l) are functions of the film thickness l when this thickness is of the order of $1/\varkappa$ and there is overlapping of the electric double layers which arise on the metal interfaces.

By φ_{ma}, φ_{sc}, and φ_{mb}, we will designate the work function of the metal A, of the semiconductor, and of the metal B, respectively (Fig. 1, in which φ is the potential energy and μ the Fermi level). The boundary conditions for Equation (1) then have the form:

$$\tilde{V}(0) = e(\varphi_{ma} - \varphi_{sc})/kT, \quad \tilde{V}(l) = e(\varphi_{mb} - \varphi_{sc})/kT. \qquad (2)$$

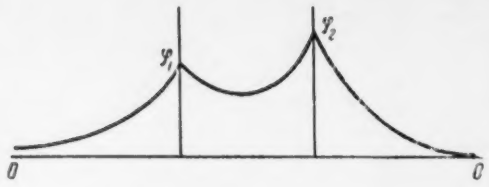

Fig. 3

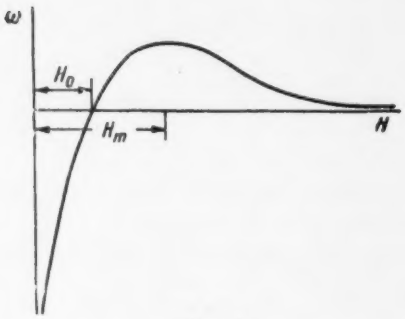

Fig. 4

Although Fig. 1 represents the case in which the work function of each metal exceeds the work function of the semiconductor, this limitation is not necessary to mathematical solution. It should be noted, however, that the case of Fig. 1 is the one which is of most interest for analysis, since when $\varphi_{ma} < \varphi_{sc} < \varphi_{mb}$ (Fig. 2) the field strengths at the right and the left ends of the film clearly increase as the film thickness diminishes, the potential differences between these boundaries being a constant quantity. Equation (1) with the boundary conditions of (2) is identical with the formulation which was given to the problem of the interaction through a symmetric binary electrolyte in the theory of the heterocoagulation of colloids. The physical reasons for this analogy are quite clear and we will not enlarge upon them.

The following point of difference is to be noted. The force of interaction through an electrolyte of the plane surfaces, charged to the potentials φ_1 and φ_2 and separated by the distance l, is given by the expression:

$$F(l) = \frac{\varepsilon}{8\pi}[E_2^2(0) - E_1^2(0)] = \frac{\varepsilon}{8\pi}[E_2^2(l) - E_1^2(l)], \qquad (3)$$

in which E_2 and E_1 are the field strengths at the outer and the inner surfaces of the film, respectively.

In our case, the metal surfaces play the role of charged films, although subject to the definition of the force of adhesion as being equal to $F_{ad}(l) = \epsilon E_{bd}^2/8\pi$. Translated into the language of the theory of heterocoagulation, F_{ad} becomes the force acting on the inner film surface. It is thus natural that $F_{ad}(0) \neq F_{ad}(l)$. We will now explain the physical meaning of E_2 in our problem (in the theory of heterocoagulation, this is the force acting on the external side of the charged film). E_2 is readily determined as the first integral of (l), the potential being equal to zero at infinity, and to a fixed value at the film surface (Fig. 3).

Thus, in our problem, $E_2(0)$ and $E_2(l)$ determine the force of adhesion of an infinite semiconductor to the metal A and to the metal B, respectively, since with the conditions $\tilde{V}(0) = e[\varphi_m - \varphi_{sc}]/kT$, $\tilde{V}(\infty) = 0$, the solution of Equation (1) corresponds to this case exactly. In the light of this analogy of the forces of interaction of the two films, the force of adhesion of the film to the metal A, or B, will in our problem differ from the adhesion of an infinite layer of semiconductor to the same metal.

From this, it can at once be concluded that the forces of adhesion of the two metals will alter in the same direction on changing the film thickness. In actuality,

$$F(0) = \varepsilon/8\pi[E_2^2(0) - E_1^2(0)] = F(l) = \frac{\varepsilon}{8\pi}[E_2^2(l) - E_1^2(l)], \qquad (4)$$

appears in the theory of heterocoagulation as a simple affirmation of Newton's Third law which follows naturally from the solution of Equation (1) with the conditions of (2) (see [3,4]). Since our problem, as has been pointed out, is mathematically identical with the latter, Equation (4) is still in order although its physical content is now somewhat different. In what follows, we will investigate the quantity

$$\Delta F_{ad} = \frac{\varepsilon^2}{8\pi}[E_{ma\infty}^2 - E^2(0)] = \frac{\varepsilon^2}{8\pi}[E_{mb\infty}^2 - E^2(l)], \qquad (5)$$

in which $E_{ma\infty}$ and $E_{mb\infty}$ are the field strengths at the boundary of an infinite layer of semiconductor with the metal a, or b, respectively. This will be done for two reasons: first, because it has been shown in the theory of heterocoagulation that it is very convenient to determine (5) in solving Equation (1) with the conditions of (2) and, second, because the analogy can thereby be maintained and the possibility preserved of making use of the results obtained earlier.

From what has been said it is clear that the further mathematical analysis is but a repetition of the work on the theory of heterocoagulation [3]. It is convenient to bring Equation (1) into a dimensionless form by introducing the variable $\nu = \kappa x$. The result is

$$d^2V / d\nu^2 = \operatorname{sh} \widetilde{V}, \tag{6}$$

from which it follows that

$$(d\widetilde{V} / d\nu)^2 = \operatorname{ch} \widetilde{V} - C. \tag{7}$$

The integration constant C is so determined that the value of ν_2, which corresponds to the potential $\widetilde{V}_2 = e[\varphi_{mb} - \varphi_{sc}] / kT$ under the condition that $\nu = 0$, $\widetilde{V}_1 = e[\varphi_{ma} - \varphi_{sc}] / kT$ when $\nu = 0$, will be consistent with $\kappa l = H$.

It was shown in the theory of heterocoagulation, that the repulsion between the films per unit area, and in our case, the alteration in the force of adhesion, is equal to

$$\Delta F_{ad} = 2kTn(\infty)\omega = C - 2. \tag{8}$$

For various values of the parameters $\widetilde{V}_1$ and $\widetilde{V}_2$, the relation between H and ω has been established in the theory of heterocoagulation (see [3]). Here, we will only present the fundamental results, referring to [3] for their derivation. We first note that a positive value of the dimensionless force ω corresponds in the theory of heterocoagulation to a repulsion of the films and indicates, in our case, a diminution of adhesion, whereas a negative value of ω (corresponding to attraction) indicates an increase in the adhesion of the semiconducting film.

1. When $\widetilde{V}_1$ and $\widetilde{V}_2$ are of different sign (the work function of one of the metals is greater and that of the other metal is less than the work function of the semiconductor), ω is negative for all values of H and monotonically increases in absolute value as the latter diminishes.

As $H \to 0$, ω tends toward negative infinity according to the asymptotic law

$$\omega \approx -(\widetilde{V}_2 - \widetilde{V}_1)^2 / H^2. \tag{9}$$

The relation between H and ω is given by the elliptic integral

$$H = \int_{\widetilde{V}_1}^{\widetilde{V}_2} \frac{d\widetilde{V}}{\sqrt{4\operatorname{sh}^2 \widetilde{V} - \omega}}, \quad \omega < 0. \tag{10}$$

Thus the film adhesion steadily increases with decreasing H.

2. When $\widetilde{V}_1$ and $\widetilde{V}_2$ are of opposite sign, the dependence of ω and H is schematically represented by the graph of Fig. 4. Here, the force of adhesion at first diminishes with diminishing H. At a certain value H_m the decrease in the force of adhesion reaches an absolute maximum, after which the adhesion begins to increase,

reaching the value for the adhesion of an infinite layer of semiconductor at $H = H_0$ and continuing to steadily increase with further decrease in H. The region $\omega < 0$ is that which is described by the equations (9) and (10) which were presented above. The maximum decrease in the force of adhesion ω_m is determined by the expression

$$\omega_m = 4\mathrm{sh}^2(\tilde{V}_{\min}/2), \tag{11}$$

in which $\tilde{V}_{\min}$ designates the smaller, in absolute magnitude, of the two numbers $\tilde{V}_1$ and $\tilde{V}_2$. Thus the maximum decrease in the force of adhesion is fixed by that one of the metals whose work function least differs from the work function of the semiconductor and is totally independent of the other metal.

The value H_0 at which ω changes sign is given by

$$H_0 = \int_{\tilde{V}_1}^{\tilde{V}_2} \frac{d\tilde{V}}{2\mathrm{sh}(\tilde{V}/2)} = \frac{1}{2}\ln\left\{\frac{(e^{\tilde{V}_2/2}-1)(e^{\tilde{V}_1/2}+1)}{(e^{\tilde{V}_2/2}+1)(e^{\tilde{V}_1/2}-1)}\right\}, \quad \tilde{V}_1 < \tilde{V}_2 \tag{12}$$

The thickness H_m corresponding to the minimum force of adhesion is equal to

$$H_m = \frac{1}{\sqrt{2}}\int_{\tilde{V}_1}^{\tilde{V}_2} \frac{d\tilde{V}}{\sqrt{\mathrm{ch}\,\tilde{V} - \mathrm{ch}\,\tilde{V}_1}}, \quad \tilde{V}_1 < \tilde{V}_2. \tag{13}$$

The elliptical integral of (13) can be brought into the form

$$H^m = k\int_{u_0}^{1} \frac{du}{\sqrt{(1-u^2)(1-k^2u^2)}}, \tag{14}$$

where

$$k = \frac{1}{\mathrm{ch}(\tilde{V}_1/2)}, \quad u_0 = \frac{\mathrm{ch}(\tilde{V}_1/2)}{\mathrm{ch}(\tilde{V}_2/2)}, \quad \tilde{V}_1 < \tilde{V}_2. \tag{15}$$

It is to be seen from Fig. 4 that each value of ω which is greater than 0 (except ω_m, of course) is associated with two different values of H. The analytic expression for the relation between H and ω has been given in [3]. The relation between H and ω is fixed by elliptic integrals, so that the numerical determination of ω as a function of H and the parameters $\tilde{V}_1$ and $\tilde{V}_2$ necessitates tabulation.

A number of graphs expressing the dependence of ω on H are presented in [3].

To us, one of the most interesting conclusions is that by sufficiently diminishing the thickness of a film between two unlike metallic surfaces, it is always possible to increase the density of the double layer and thereby increase the force of adhesion. It is possible that an explanation for the increased adhesion resulting from a decrease in the thickness of thin adhesive layers is to be found in this fact. It should be noted that these calculations have always supposed small depletion of the additive centers, even though this depletion becomes progressively more significant as the film thickness is diminished. The result is that the force of adhesion will not increase indefinitely but will rise only to a definite value. Another important factor determining the force

of adhesion is the existence of surface states. It is proposed to subsequently carry out calculations on these details.

LITERATURE CITED

[1] B. V. Deriagin and N. A. Krotova, Adhesion (in Russian) Acad. Sci. USSR Press, 1949; B. V. Deriagin and N. A. Krotova, Proc. Acad. Sci. USSR 61, No. 5 (1948).

[2] V. B. Sandomirskii and V. P. Smilga, J. Tech. Phys. (in the press).

[3] B. V. Deriagin, Colloid J. 16, vol. 6 (1954);* B. V. Deriagin and V. G. Levich, Proc. Acad. Sci. USSR 98, No. 6 (1954).

[4] B. V. Deriagin, Bull. Acad. Sci. USSR, Div. Expt. Med., chem. ser. 5, 1153 (1937); Acta Physicochim. USSR 10, 333 (1939); Trans. Farad. Soc. 36, 1, 203 (1940); 36, 2, 730 (1940); Colloid J. 6, 291 (1940); 7, 285 (1941); B. V. Deriagin and L. D. Landau, J. Exp. Theo. Phys. 2, 802 (1941); J. Exp. Theo. Phys. 15, 662 (1945).

The Institute of Physical Chemistry of the Academy of Sciences of the USSR

Received April 8, 1958

*See C. B. Translation.

CONCERNING CALCULATIONS ON ELECTROCHEMICAL REACTIONS WITH AN INTERMEDIATE REAGENT

M. A. Loshkarev and I. P. Chernobaev

(Presented by Academician A. N. Frumkin, April 11, 1958)

Among the many electrochemical processes, there is an extensive group of reactions which can be expeditiously followed either through the current density or through the time variation of the concentration of the reacting substances. The electroextraction of metals, the anodic oxidations and the cathodic reductions of variable ionic valences, the reactions of electroorganic syntheses, etc., are included here. Processes of this type can be treated theoretically by combining the kinetics of the electrode reaction with the differential equations of the chemical kinetics.

For investigation, we have selected both a special instance of a direct electrode process and a more general case in which the oxidation or reduction of the selected compound (the depolarizer) proceeds in the presence of an intermediate reagent in the electrolyte. In this latter instance (for example, in anodic oxidation) the two parallel reaction paths for the process can be represented by the scheme:

1) $K - e \rightarrow K^+$ (on the electrode)

2) $B - e \rightarrow B^+$ (on the electrode) and $B^+ + K \rightarrow K^+ + B$ (in the diffusion layer and in the body of the electrolyte.

Here, K is the principal depolarizer and B, is the intermediate reagent.

These systems are of great significance to technical electrochemistry and are also of interest in connection with the possibility of accelerating a number of slow electrochemical reactions.

The action of intermediate reagents or carriers had been considered in [1-5], and especially in [6-9], and in other papers on the kinetics of electrode processes which are combined with chemical reactions in solution. In distinction to most of these works, we, starting from the scheme shown above, have set ourselves the problem of obtaining theoretical equations for the process rate and testing these equations under stationary conditions in various systems involving solid electrodes.

We will suppose that the selected depolarizer is present in a solution which contains no intermediate reagent. If, in this case, the volume of the diffusion layer is considerably less than the total volume of the electrolyte, v, the decrease in the concentration of the depolarizer with time must be governed by the equation:

$$-v\,dC = \frac{SD}{nF}\,dt, \tag{1}$$

in which S is the surface of the electrode, n is the valence change accompanying electrolysis, D is the current density, C is the concentration and t is the time in seconds.

In the general case in which the rate of the electrode process is determined by both the discharge step and the diffusion of the depolarizer to the electrode, the dependence of the current density on the potential under stationary conditions is given, according to A. N. Frumkin, by the equation:

$$D = k_1 \exp \frac{\pm \alpha (\varphi - \psi_1) nF - \psi_1 ZF}{RT} C \left(1 - \frac{D}{D_{max}}\right), \quad (2)$$

in which k_1 is the discharge rate constant, C and Z are the concentration and the valence of the depolarizer and $D_{max} = k_d C$, is the maximum diffusion current. The signs + and − which stand before the first member of the exponential designate the anode and the cathode processes, respectively.

Setting the quantity D as defined from (2) into (1), and integrating with constant φ and T, we finally obtain

$$\ln \frac{C_0}{C} = \frac{S}{vnF} \left\{ \frac{k_d \cdot k_1 \exp \frac{\pm \alpha(\varphi - \psi_1) nF - z\psi_1 F}{RT}}{k_d + k_1 \exp \frac{\pm \alpha(\varphi - \psi_1) nF - z\psi_1 F}{RT}} \right\} t \quad (3)$$

or

$$\ln \frac{C_0}{C} = mt, \quad (3a)$$

where C_0 is the initial concentration of the depolarizer. For pure diffusion kinetics $m = Sk_d/vnF$.

When the discharge is the slowest step, $m = \frac{S}{vnF} \Phi(\varphi)$ in Equation (3a). In conformity with Equation (3), the concrete value of the function $\Phi(\varphi)$ is determined by the exchange current and the values of the φ and ψ_1 potentials. Equation (3) is readily brought into the form:

$$\ln \frac{i_0}{i} = \frac{i_0}{vnFC_0} t, \quad (4)$$

a result which has been obtained by Gilbert and Rideal [10], and later, by Stromberg [11], in work on polarographic coulometry. Here, i_0 is the initial value of the current. It is to be seen from (3) that it is impossible to achieve full oxidation or reduction here since the current decreases with falling concentration. Even making use of such a reservoir as an increase in the potential, leads in the final analysis only to the appearance of limitations of diffusional character.

This defect can be easily eliminated by the introduction of an intermediate reagent. In this case, the general kinetic equation has the form:

$$-dC = \frac{S}{vnF} (D_K + D_B)\, dt, \quad (5)$$

where D_K and D_B are the respective densities of the currents which are expended on the direct electrode reaction with the depolarizer and on the reaction with the intermediate reagent.

Taking into account the fact that D = kC for constant φ and T, and integrating with the boundary conditions t = 0, $C = C_0 = b$, we obtain

$$\ln \frac{b + a}{C + a} = \frac{i_0}{vnFC_0} t, \quad (6)$$

where $a = D_B/k$. The fraction $a/c = D_B/D_K$ characterizes the relative increase in the rate which results from the carrier. a is a function of the concentration of the intermediate reagent, the potential, the temperature

and the hydrodynamic regime. Just as before, the quantity $m = i_0/vnFC_0$ in (6) depends on the ratio of the discharge current for the depolarizer (i_0) and the latter's concentration (C_0). (6) is an equation of variable fractional order. It is characteristic that the larger a is in comparison with C_0, the smaller is the actual reaction order and the higher the reaction rate. In the general case in which the rates of the two parallel processes are determined by the potential, the values of φ and ψ_1 enter into both the logarithmic function and the value of m.

Since the value of the current is given by $I = Sk(c + a)$, when the solution contains both the basic depolarizer and the carriers, it follows by analogy with (4) that

$$\ln \frac{I_0}{I} = \frac{i_0}{vnFC_0} t. \tag{7}$$

It is interesting to note the similiarity of the C, t relations of Equations (3a) and (6). The introduction of the intermediate oxidizer is here equivalent to an increase in the total concentration, displacing the reaction into the initial, more favorable region. From (6) it follows that the concentration C will fall to zero at the instant

$$\tau = \frac{vnFC_0}{i_0} \ln\left(1 + \frac{b}{a}\right) \tag{8}$$

We will designate the time for completion of the electrolysis,* as τ.

From the dependence of τ on the experimental conditions it is also possible to draw a number of conclusions concerning the behavior of the intermediate reagent. At the same time the value of τ is an important practical characteristic of the process.

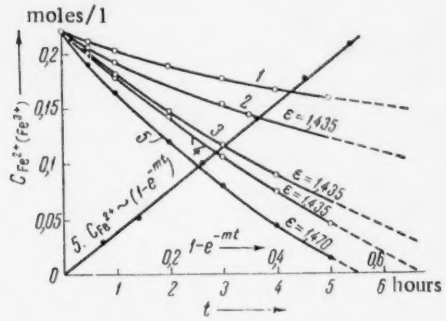

Fig. 1. The effect of NaCl on the rate of anodic oxidation of Fe^{2+} on platinum. Electrolyte composition: 0.22 M $FeSO_4$, 1 N H_2SO_4. Temperature 25°. 1) without NaCl; 2) 0.5 N NaCl; 3) 1 N NaCl; 4) 2 N NaCl; 5) 0.5 N NaCl.

The equations proposed above have been tested on a number of oxidation-reduction reactions. In Fig. 1, data is given on the oxidation of $FeSO_4$, in pure H_2SO_4, and in solutions of H_2SO_4 containing NaCl. These experiments were carried out at 25°. The values of the anode potential were varied from 1.40 to 1.47 v.

Curve 1 which characterizes the dependence of the Fe^{2+} concentration on the time when the reaction is carried out in the absence of an intermediate reagent, is quite flat. In this case more than 70 hours are needed for 99% oxidation of the iron. In this same figure there have been plotted C(t) curves for solutions containing sodium chloride. All of these are much steeper than Curve 1 and none of them approach the time axis asymptotically. Thus only 55 hours are required for 100% oxidation of the iron in the electrolysis of a solution containing 0.5 N NaCl at $\varphi = 1.47$ v, i.e., the time is only 1/12th of that needed in the absence of NaCl. In this same graph (Curve 5) there is given a recalculation of the experimental data using the equation

$$C_{Fe^{3+}} = b - c = (a + b)(1 - e^{-mt}), \tag{9}$$

*Because of the nature of the rate, the reaction between the transmitter and the depolarizer is actually completed somewhat later. This is naturally not reflected in the amount of electricity which is required: $Q = \int_0^\tau I dt$.

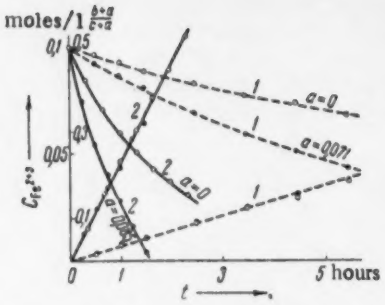

Fig. 2. The effect of Ti^{4+} ions on the cathodic reduction of $Fe_2(SO_4)_3$ on lead. Electrolyte composition: 0.1 M $Fe_2(SO_4)_3$, 1 N H_2SO_4, temperature 20°. 1) without agitation; 2) with agitation.

which was obtained from Equation (6). Here, the value $m = 1.73 \cdot 10^{-5}$ was taken from the experiments on the anodic oxidation in an electrolyte which was free of NaCl. The corresponding value of m, calculated from the limiting current ($m = i_0/vnFC_0$) under these same conditions was $1.86 \cdot 10^{-5}$.

It is to be seen that in the coordinates C_{Fe}^{3+} vs. $(1-e^{-mt})$ there is obtained a straight line of slope equal to 0.85. The value of the sum (a + b) as calculated from the current ratio was 0.80. In Table 1 there are shown the results of recalculation of the experimental data on the oxidation of iron under various conditions. The results were obtained from the values of the currents. The constancy of the coefficient m shows the agreement with Equation (6) to be good in every case.

In Fig. 2 there are given curves for the reduction of Fe^{3+} in pure H_2SO_4, and in H_2SO_4 solutions containing the sulfate of tetravalent titanium as an intermediate compound. These experiments were carried out at $\varphi = -0.6$ v, so that the limiting diffusion currents were reached for both the Fe^{3+} and the Ti^{4+} ions. Values of a were determined from the current. In the coordinates $\log [(b + a) / (c + a)]$ vs t straight lines with the slopes $2.25 \cdot 10^{-5}$ (without agitation) and $14.2 \cdot 10^{-5}$ (with agitation) were obtained, these results being in good agreement with the calculated values of m.

TABLE 1

The Anodic Oxidation of Fe^{2+}. Volume of Electrolyte, 100 cm^3. Anode, Smooth Platinum (S = 10 cm^2); Temperature 25°. Electrolysis with a Diaphragm, Without Agitation. Values of the Constant in the Equation $\ln \frac{b+a}{c+a} = mt$

Expt. No.	Composition of electrolyte, moles/l			φ, v	Constants		
	Fe^{2+}	NaCl	$\frac{1}{2} H_2SO_4$		a	b + a	$m \cdot 10^{-5}$
1	0,22	0,0	1,0	1,435	0,0	0,22	1,80
2	0,1	0,0	1,0	1,435	0,0	0,1	1,81
3	0,05	0,0	1,0	1,435	0,0	0,05	1,86
4	0,22	0,5	2,0	1,435	0,198	0,418	1,83
5	0,22	0,5	1,0	1,435	0,156	0,376	1,75
6	0,22	2,0	1,0	1,435	0,427	0,647	1,83
7	0,1	0,5	1,0	1,435	0,198	0,298	1,83
8	0,05	0,5	1,0	1,435	0,220	0,270	1,83
9	0,22	0,5	1,0	1,400	0,088	0,308	1,83
10	0,22	0,5	1,0	1,470	0,574	0,794	1,73

Study was made of the effect of the intermediate reagents on the various reactions in the electrosynthesis of organic compounds, on the precipitation of metallic hydroxides and on the overvoltage of titanium ions. In each case the agreement with the adduced equations was good. The application of intermediate reagents in organic electrosyntheses deserves special attention, since it thereby becomes possible not only to accelerate the reaction, but to apply homogeneous catalysts and to regulate the "severity" of the oxidation or reduction by the choice of the corresponding carrier. The use of intermediate reagents makes it possible to avoid the spatial difficulties which are characteristic of heterogeneous processes. Finally, the carrier can serve as a catalyst when there are exceptional kinetic difficulties in the direct electrode reaction of the depolarizer.

LITERATURE CITED

[1] F. Foerster, Elektrochemie der wässerigen Lösungen, Leipzig, 1922.

[2] A. N. Frumkin, V. S. Bagotskii, Z. A. Iofa and B. N. Kabanov, The Kinetics of Electrode Processes (in Russian) Moscow, 1952; A. N. Frumkin, Mono., Problems of Chemical Kinetics, Catalysis and Reactivity (in Russian) Moscow, 1955, p. 402.

[3] P. Ia. Florenskii and K. T. Metelkin, J. Aniline Dye Inds., 1, 8, 9 (1931); 1, 9, 7 (1931).

[4] K. Ia. Grachev, J. Appl. Chem. 12, 2, 196 (1939); 12, 5, 642 (1939); 13, 4, 5, 16 (1940).

[5] R. K. Drachevskaia and V. V. Stender, Bull. Acad. Sci. Kazak SSR, chem. ser., vol. 2, 20 (1948); M. A. Kalinin and V. V. Stender, J. Appl. Chem. 19, 10, 1045 (1946).

[6] R. Brdicka, Chem. Zvesti 8, 10, 670 (1954).

[7] J. Koruta, Chem. Zvesti 8, 10, 723 (1954).

[8] J. Koruta and J. Koutecky, Coll. Czech. Chem. Comm. 20, 2, 423 (1955).

[9] J. Koutecky, Coll. Czech. Chem. Comm. 20, 1, 116 (1955).

[10] G. Gilbert and E. Rideal, Trans. Farad. Soc. 47, 396 (1951).

[11] A. G. Stromberg and T. M. Markacheva, J. Phys. Chem. 28, 4, 671 (1954).

The F. E. Dzerzhinskii Chemicotechnological Institute, Dnepropetrovsk

Received April 11, 1958

THE ANODIC PROTECTION OF TITANIUM IN SULFURIC ACID

N. D. Tomashov, R. M. Al'tovskii and A. G. Arakelov

(Presented by Academician P. A. Rebinder, April 11, 1958)

Titanium does not exhibit a high enough resistance to corrosion in sulfuric acid of concentrations greater than 10% [1-3]. Anodic protection is not one of the methods most widely applicable to the protection of metals from corrosion, since in the case of the majority of metals, anodic polarization leads, in addition to the suppression of the operation of the microcells on the metal surface (the positive difference effect), to the continuation of anodic dissolution of the metal by means of the applied current. For metals with a distinct tendency to undergo passivation, however, (stainless steel, iron) under conditions where a low anodic current density can lead to the production of a stable passive state, anodic polarization by means of an external current may produce an over-all protective effect. The possibility of using anodic polarization for the protection of stainless steels and iron from corrosion in sulfuric acid has been pointed out in a number of works [4-6]. Titanium has a much greater tendency to undergo passivation than stainless steels or iron. Thus, for example, a passive state is produced on 1X18H9 steel by anodic polarization in 30% H_2SO_4 solution at a current density of approximately 1.5 milliamps/cm^2 [4], whereas anodic passivity is produced in titanium in 45% H_2SO_4 solution at a current density of 0.32 milliamps/cm^2, approximately one fifth. Taking this into account we may be led to the conclusion that the use of anodic polarization for the protection of titanium should be even more effective than for stainless steel and iron. In this connection the present study was devoted to a study of the processes of oxide film formation during the spontaneous passivation of titanium in sulfuric acid solutions and of the processes taking place on the metal surface during anodic polarization. The studies were carried out using titanium of grade VT-1D (O 0.23–0.26%, H 0.022–0.023%, N 0.017%, Fe 0.12%, Si 0.05%) in sulfuric acid solutions at room temperature.

Studies on the cleaning of the metal surface under the solution were carried out using an apparatus specially constructed by ourselves [7, 8]. When a constant potential had been established for the metal whose surface was being cleaned, the cleaning process was stopped and the change of potential with time was recorded.

Figure 1 shows the results of the study of the behavior of titanium when the surface is cleaned in sulfuric acid. As can be seen from the figure, the titanium goes back to the passive state after the surface has been cleaned in 5% H_2SO_4 solution, as is indicated by the fact that the potential of the titanium returns to values of approximately + 0.3 volt, corresponding to the passive state of titanium in sulfuric acid. The potentials in the present article are all given on the hydrogen scale. When the 5% H_2SO_4 solution is stirred, the restoration of the passivity takes place more readily. In 10% H_2SO_4 the titanium remains in active state after the cleaning process. The potential of the titanium in the active state in sulfuric acid was equal to approximately 60.3 volt.

It follows from Fig. 1 that the principal role in the preservation of the stability of the passive state of titanium in dilute sulfuric acid solutions is played by the atmospheric oxygen dissolved in the electrolyte, since in an atmosphere of hydrogen, i.e., when no oxygen is present in the electrolyte, the titanium remains in the active state in 5% H_2SO_4 solution after the surface has been cleaned. If, however, the atmosphere of hydrogen is replaced by an atmosphere of air (Point A on Fig. 1) the titanium rapidly returns to the passive state, as can be seen from the sharp downward displacement of its potential.

In addition, if the cleaning of the titanium surface is carried out in a 10% H_2SO_4 solution under an atmosphere of oxygen, then the titanium again returns to the passive state after the cleaning process is interrupted.

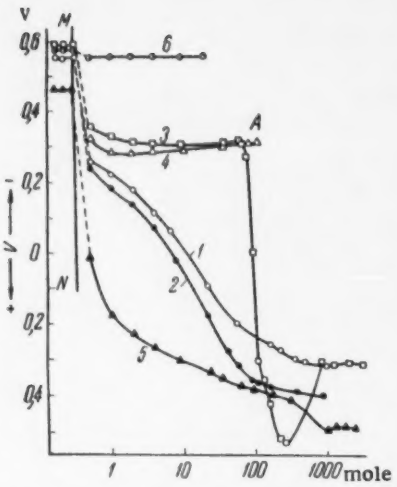

Fig. 1. The change in the potential of Ti with time after the surface had been cleaned in H_2SO_4 solution. 1) 5% H_2SO_4 (atmosphere of air); 2) the same, with stirring of the solution; 3) 5% H_2SO_4 (atmosphere of hydrogen); 4) 10% H_2SO_4 (atmosphere of air); 5) 10% H_2SO_4 (atmosphere of oxygen); 6) 5% H_2SO_4 + + 2% NaF (atmosphere of air). The line MN indicates the moment when the cleaning process was switched off. The point A indicates the moment when the atmosphere of hydrogen was replaced by an atmosphere of air.

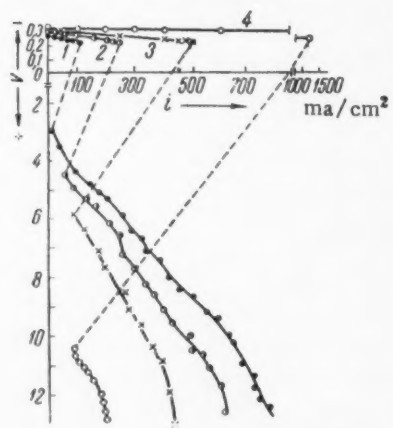

Fig. 2. The anodic polarization of Ti in H_2SO_4. 1) 27% H_2SO_4; 2) 40% H_2SO_4; 3) 50% H_2SO_4; 4) 64% H_2SO_4.

The restoration of the passive state of titanium in 10% H_2SO_4 solution may also be achieved in an atmosphere of air if the electrolyte is stirred after the cleaning process is stopped. It should be noted that the difference between the potential of the titanium during the surface cleaning process and the potential of the titanium in the passive state amounts to approximately 0.85 volt. This provides evidence that in the passive state the surface of the titanium is covered by a stable protective oxide film which is responsible for the passivity. It follows from Fig. 1 that the potential of the titanium in the active state in 10% H_2SO_4 solution also differs considerably (by 0.3 volt) from the potential of titanium during the process of surface cleaning in the same solution. Thus even in the active state, the surface of the titanium is partly covered by an oxide film. It also follows from Fig. 1 that water, as well as the oxygen dissolved in the electrolyte, also takes part in the formation of the oxide film on the surface of the titanium, since even under an atmosphere of hydrogen in a 5% H_2SO_4 solution, the potential of titanium in the active state is 0.3 volt more positive than the potential during the process of surface cleaning. The reaction between titanium and water may take place, for example, according to the reaction [10]:

$$Ti + 2H_2O = TiO_2 \text{ (hydrated)} + 4H^+ + 4e - 0.86 \text{ volt} \quad (I)$$

It is well known that hydrofluoric acid and acidic electrolytes containing fluoride ions are more agressive towards titanium, and in these solutions no oxide film formation is observed on the titanium surface even with anodic polarization [1]. The explanation given for the difference between the potential of the titanium in the active state and its potential during the surface cleaning process, namely that an oxide film is formed on the surface of the titanium, may also be confirmed by the fact that in a solution of 5% H_2SO_4 + 2% NaF, i.e., in a solution in which the oxide layer on the titanium surface is readily soluble, the potential of the titanium during the cleaning process and the potential of the active state are practically the same. The passivation of the titanium after the surface cleaning process in sulfuric acid is stopped may be taken as proceeding in two stages. At first the surface of the metal reacts for the most part with water (according to reaction (I)), whose concentration is of course considerably greater than the concentration of oxygen. In sulfuric acid solutions with a concentration greater than 10%, in which titanium is unstable, the adsorption of oxygen on the titanium surface is hindered, as a result of which the formation of the protective film stops at this stage, which is not capable of producing complete passivation. Confirmation of this idea is provided by the fact that the potentials of titanium in the active state in 10% H_2SO_4 solutions (atmosphere of air) and in 5% H_2SO_4 (atmosphere of hydrogen) are equal. At lower sulfuric acid concentrations (5% and less), immediately after the formation of the oxide film produced by the interaction of the titanium with water, further adsorption of oxygen on the

titanium surface takes place leading to the formation of a stable oxide film which produces complete passivation.

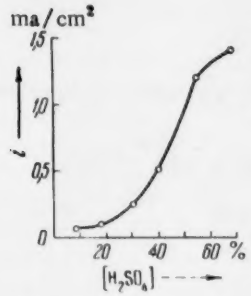

Fig. 3. The relationship between the minimum current density necessary to produce anodic passivation of Ti and the concentration of H_2SO_4.

Figure 2 gives the anodic polarization curves for titanium in sulfuric acid solutions of different concentrations. It can be seen from the figure that the anodic polarization in the region of active dissolution of the titanium increases with decrease in the concentration of the sulfuric acid. This may be explained by the fact that with increase in the concentration of the acid, the solubility of oxygen in the acid decreases [11] while the solubility of the titanium oxides, of which the protective oxide film consists and which partly cover the titanium surface in the active state, increases [12]. After the region of active anodic dissolution, the magnitude of which increases with increase in the acid concentration, the region of anodic passivity follows, accompanied by a sharp jump in potential to values of from + 3 to + 10 volts with a simultaneous appreciable fall in the current. This is related to the formation of anodic films with high ohmic resistance on the electrode surface, while evolution of oxygen also takes place at the electrode simultaneously. In the region of the passive state of the titanium, the anodic polarizability increases with increase in the concentration of the acid, which contrasts with the region of active dissolution of the titanium.

The formation of oxide films with high ohmic resistance on the surface of titanium, which hinders the anodic process taking place during anodic polarization of titanium in sulfuric acid solutions has also been shown in a number of other works [2, 3].

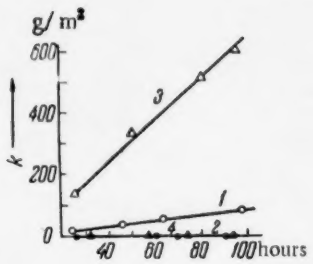

Fig. 4. The corrosion of Ti in H_2SO_4 with and without anodic protection. 1) 40% H_2SO_4 (without protection); 2) 40% H_2SO_4 (with anodic protection); 3) 78% H_2SO_4 (without protection); 4) 78% H_2SO_4 (with anodic protection).

The short period of active anodic dissolution of titanium in sulfuric acid, the considerable fall in current after anodic passivity is achieved (Fig. 2) and the ability of titanium to form strong, stable protective oxide layers both by spontaneous passivation (Fig. 1) and also during anodic polarization (Fig. 2) give grounds for considering it possible to achieve anodic protection of titanium in sulfuric acid. The possibility of anodic protection has been studied in the regions of maximum rate of corrosion of titanium in sulfuric acid (40 and 78%) [2, 3]. An electrode was placed in the solution with an anode current equal to the minimum current necessary to produce anodic passivity of the titanium in the given sulfuric acid solution or slightly greater (by 5-10%) than this current value. The magnitude of this current may be determined from the data given in Fig. 3. As soon as the onset of anodic passivity caused the potential of the titanium to reach a value of the order of + 2 − + 3 volts, and oxygen began to be liberated on the specimen, the polarizing current was reduced so that the potential of the titanium was brought into a range of values somewhat greater than the potential of its passive state, i.e., the potential was maintained approximately within the range from + 0.5 to + 1.0 volt. Lower potential values may be dangerous as a result of incomplete passivation and the possibility of conversion of the titanium to the active state by the action of chance factors capable of destroying the passive state. Potential values greater than 1 volt are not in danger of destroying the passive state, but in order to maintain a higher potential it is necessary to use a higher protective current density, which is an economic disadvantage. In order to maintain the potential of the titanium in the range of values from + 0.5 to + 1 volt in 78% H_2SO_4 solution after the passive state has been established, it was found necessary to use a current density of only 0.5 − 1.0 μ amps/cm^2. For 40% H_2SO_4 an even smaller current was required, equal to 0.1 − 0.2 μ amps/cm^2.

Figure 4 gives the results of corrosion tests carried out on titanium specimens with and without anodic protection. The corrosion losses (determined gravimetrically) of the unprotected specimens increased linearly with time. With anodic protection of the titanium in both the sulfuric acid solutions studied, practically no corrosion losses were observed. The slight losses in weight may be related to the first period of active dissolution

of the titanium before anodic passivation has been established. Anodic protection of titanium may undoubtedly be used for other solutions besides sulfuric acid, if the ready establishment of a passive state of the titanium is possible by means of anodic polarization in these solutions.

LITERATURE CITED

[1] M. E. Straumanis and P. C. Chen, Corrosion, 7, No. 7, 229 (1951).

[2] V. V. Andreeva and V. I. Kazarin, The Corrosion Resistance of Titanium in Agressive Solutions, Inst. Tech. Econ. Inform. AN SSSR, No. N-56-159 (1956).*

[3] L. B. Golden, I. Roy Lane and W. L. Acherman, Ind. and Eng. Chem. 44, No. 8, 1930 (1952).

[4] N. D. Tomashov and G. P. Chernova, Proc. Acad. Sci. 104, No. 1, 104 (1955).

[5] V. M. Novakovskii and A. I. Levin, Proc. Acad. Sci. 99, No. 1, 129 (1954).

[6] R. Edeleanu, Nature, 17, 739 (1954).

[7] N. D. Tomashov, G. P. Chernova, R. M. Al'tovskii and G. K. Blinchevskii, Factory Labs. No. 3 (1958).

[8] N. D. Tomashov, R. M. Al'tovskii and G. P. Chernova, Inst. Tech. Econ. Inform. AN SSSR, subject No. 13, No. M-5894/7 (1958).

[9] G. V. Akimov and G. B. Klark, Proc. Acad. Sci. 45, No. 9, 399 (1944).

[10] W. Latimer, The Oxidation States of the Elements and Their Potentials in Aqueous Solution, IL, 1954.**

[11] The Chemist's Reference Book, 3, 1952.*

[12] O. N. Morozova, The Chemistry of the Rare Elements, 1938.*

Institute of Physical Chemistry,
USSR Academy of Sciences

Received April 8, 1958

*In Russian.

**Russian translation.

THE RATE OF ABSORPTION OF ETHYLENE AND PROPYLENE BY SULFURIC ACID OF DIFFERENT CONCENTRATIONS

G. V. Korovina, S. G. Entelis and N. M. Chirkov

(Presented by Academician V. N. Kondrat'ev, April 24, 1958)

The absorption of olefins by sulfuric acid, as is well known [1, 9], is a complex acid-catalysis reaction in the course of which the simultaneous formation of an alcohol and the alkyl acidtakes place [2]. In the case of the absorption of propylene by sulfuric acid, a number of facts indicate that these processes take place in parallel [3]. The problem of the order of both the reactions has not yet been solved. The hydration of olefins, according to Taft [4], is a monomolecular reaction and the order relative to water is zero; according to the data of Tsvetkova [5] this reaction is of the second order – first order relative to water and relative to propylene.

The difficulty of determining experimentally the order of the alkylation reaction is related to the fact that the examination is always made in the presence of excess acid, which functions as both reagent and catalyst. Information regarding the order of the alkylation reaction may be obtained by studying the relationship between the rate of reaction and the acidity of the medium.

If the relationship between reaction rate and the acidity h_0 is the same for both reactions, then the relationship between the initial rate of total absorption w_0 ($w_0 = w_{alk} + w_{alc}$) and the acidity will also be the same.

If,however,it is different, then the relationship between w_0 and h_0 will in addition be determined by the ratio of the absolute magnitudes of these terms, which vary with the concentration of the acid, and the observed relationship between log w_0 and H_0 may acquire a complex character.

A knowledge of the relationship between w_0 and H_0 makes it possible to compare the rates of absorption of different olefins under identical conditions, while these rates differ considerably in magnitude.

Since the question of the quantitative difference in the true rates of absorption of olefins has been little studied, it seemed to be of interest to carry out a comparative study of the rates of absorption of propylene and ethylene by acids over a wide range of concentrations. A knowledge of the true rates of absorption of propylene and ethylene by aqueous sulfuric acid has, in addition to its theoretical interest, considerable practical importance in connection with the process for the preparation of ethyl and isopropyl alcohols with sulfuric acid.

The data available in the literature on the rates of absorption of ethylene and propylene by aqueous sulfuric acid [6] are of no value in this connection, since they were obtained in the diffusion region where the difference in the rates of absorption is leveled out. One exception is a paper by Gel'bshtein and Temkin [9], in which the authors, by making a number of assumptions, used the diffusion kinetics to obtain rate constants for the chemical interaction of ethylene and propylene with H_2SO_4.

The study of the true kinetics of the absorption of propylene and ethylene by sulfuric acid was carried out at 70° in the circulatory glass apparatus which we have already described [3], with the addition of a 500 cc gas buret. The gas pressure during the course of the experiment was kept constant and equal to the atmospheric pressure. The rate of absorption was measured by observing the quantity of gas removed from the gas buret.

If we limit ourselves to the initial part of the kinetic curve for the total absorption, then, neglecting the reversibility, we may use the following equation in the calculations:

$$\frac{d\Delta v}{dt} = k'P, \quad (1)$$

where Δv – change in the volume of the gas phase, reduced to normal conditions; P – pressure of gas in the system and

$$k' = 22.4 \cdot 10^3 kqv_a. \quad (2)$$

The specific rate k' was calculated using Equation (1) from the average rate of absorption of the first 400 cc of gas under the conditions of the experiment, afterwards reduced to normal. The rate constant $\underline{k}$ was calculated from Equation (2), where $\underline{q}$ – the Henry constant in moles/liter·mm; v_a – volume of acid in cc. The Henry constant was found by extrapolating the literature data on the solubility of propylene in water [7] to high temperatures (at 70°, $q = 3.11 \cdot 10^{-6}$ moles/liter·mm). The same value was taken for ethylene.

TABLE 1

The Results of Experiments on the Absorption of Propylene and Ethylene by Sulfuric Acid of Different Concentrations at 70°

H_2SO_4, % by weight	H_0	v_a, cc	W_{aver}, cc/minute	P, mm mercury	$k' \cdot 10^3$, cc/minute·min	k, min^{-1}	lg k	$\lg k + nH_0$***
				Propylene				
56,57	—3,70	4,8	0,49*	691,0	0,70	2,11	0,325	—3,24
60,34	—4,18	4,9	1,47	707,0	2,09	6,09	0,785	—3,25
64,92	—4,75	4,6	5,22	710,0	7,36	22,90	1,360	—3,22
67,70	—5,15	4,4	11,80	731,0	16,15	52,30	1,718	—3,25
70,04	—5,45	4,4	18,78	729,0	25,80	84,30	1,926	—3,24
				Ethylene				
79,51	—6,78	4,1	0,11**	745,5	0,14	0,5	—0,311	—7,91
86,05	—7,69	4,6	1,78	750,5	2,37	8,1	0,908	—7,71
89,39	—8,13	4,3	4,57	741,0	6,17	20,8	1,318	—7,79
91,46	—8,35	3,8	8,58	754,0	11,38	42,7	1,630	—7,72
95,41	—8,83	3,5	28,08	752,0	37,40	151,3	2,180	—7,70

*The value of w_{aver} was calculated for the time of absorption of the first 200 cc C_3H_6.
**The value of w_{aver} was calculated for the time of absorption of the first 40 cc C_2H_4.
***For propylene, n = 0.97, for ethylene, n = 1.1.

Table 1 gives the experimental data for the absorption of propylene and ethylene by sulfuric acid of different concentrations. The values of H_0 for sulfuric acid at 70° were taken from the paper by Temkin and coworkers [8]. The change in the value of H_0 for sulfuric acid when an olefin is dissolved in the acid was not taken into account, since the degree of saturation of the acid in the initial stage of the kinetic curve is small.

From the data given (Fig. 1) it follows that a linear relationship exists between the logarithm of the rate constant for the absorption of olefin and a function of the acidity of the medium;

$$\text{for ethylene, } \log k = -1.1H_0 - 7.77 \quad (3)$$

$$\text{for propylene, } \log k = -0.97H_0 - 3.24. \quad (4)$$

In both cases the proportionality coefficients of H_0 are close to unity; this indicates that in the reactions of alcohol formation and alkylation, of which the process of olefin absorption by the acid is composed, the same process of protonization of the olefin precedes the limiting stage.

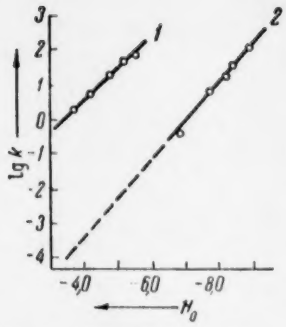

Fig. 1. The relationship between the rate of absorption of propylene (1) and ethylene (2) and a function of the acidity of the medium.

In our case the absorption of ethylene has been studied in conditions where the observed process may be almost entirely related to the formation of ethylsulfuric acid and the relationship obtained between the rate constant for the absorption and the acidity (Equation (4)) reflects the relationship between the constant for the alkylation of sulfuric acid and the acidity.

The proportionality between the observed constant and the acidity indicates that the sulfuric acid particle is not part of the activated complex and the reaction of alkyl acid formation is evidently of the first order, i.e., the expression for the rate of the alkylation reaction is of the form:

$$w_{alk} = k_0 K h_0 C_{eth}$$

Here k_0 – true rate constant for the limiting stage, K – constant for the protonization of ethylene, C_{eth} – molar concentration of ethylene, a_i – activity and f_i – activity coefficient.

The extrapolation of the straight lines log k – H_0 in Fig. 1 into the same region of H_0 values makes it possible to compare the true rates of absorption of propylene and ethylene. It can be seen from Fig. 1 that the rate of absorption of these olefins by sulfuric acid solutions of the same concentration differ by a factor of more than 1000. This considerable difference in the true rates of absorption of propylene and ethylene by sulfuric acid, which is realized in the kinetic region or close to it, makes possible the quantitative separation of C_3H_6 from C_2H_4 and at the same time makes it possible to avoid the uneconomic stage of separation of the gases by fractional distillation, which is at present employed in the production of synthetic alcohol.

LITERATURE CITED

[1] Kh. R. Rustamov and N. M. Chirkov, J. Phys. Chem. 30, 261 (1956); Proc. Acad. Sci. Uzbek SSR, No. 7, 43 (1954).

[2] R. Robey, Ind. and Eng. Chem. 33, 1077 (1941); R. W. Schrage and E. H. Anick, Ind. and Eng. Chem. 42, 2550 (1950).

[3] S. G. Entelis, V. E. Petrakovich, G. V. Korovina and N. M. Chirkov, Proc. Acad. Sci. 114, 848 (1957).*

[4] R. W. Taft, J. Am. Chem. Soc. 74, 5372 (1952).

[5] V. I. Tsvetkova, Degree Dissertation, Inst. Phys. Chem. AN SSSR, 1956.

[6] H. S. Davis and R. Schuler, J. Am. Chem. Soc. 52, 721 (1930); V. V. Pigulevskii and N. V. Rudakova, Cracking and the Chemical Treatment of Its Products, No. 1, 67 (1933); V. G. Moor, ibid., No. 3, 108 (1936); M. A. Kerdivarenko, P. K. Migal' and M. K. Kishinevskii, J. Appl. Chem. 28, 459 (1955); S. A. Nazarov and M. B. Markovich, Cracking and the Chemical Treatment of Its Products, No. 4, part II, 3 (1949).

[7] Internat. Crit. Tables of Num. Data in Phys. Chem. and Technol. 3, p. 260.

[8] A. I. Gel'bshtein, G. G. Shcheglova and M. I. Temkin, J. Inorg. Chem. 1, No. 3, 505 (1956).

[9] A. I. Gel'bshtein and M. I. Temkin, J. Phys. Chem. 31, 2697 (1957).

Institute of Chemical Physics,
USSR Academy of Sciences

Received April 22, 1958

*Original Russian pagination. See C. B. Translation.

THE INFLUENCE OF PRESSURE ON THE SOLUBILITY OF MOLECULAR HYDROGEN IN NIOBIUM AND TANTALUM*

P. S. Perminov

(Presented by Academician A. N. Frumkin, April 14, 1958)

In an article [1] devoted to a study of the influence of pressure on the solubility of molecular hydrogen in the β-phase of the palladium–hydrogen system, it was shown that a linear relationship exists between the quantity of dissolved hydrogen and the logarithm of the pressure up to concentrations of 0.92 g-atoms H per g-atom of Pd. The suggestion was put forward that in all probability a logarithmic relationship also exists in the case of other solutions of gases in metals in the regions of extensive filling of the lattice.

TABLE 1

The Relationship Between the Pressure and the Solubility of Hydrogen in Powdered Niobium and Tantalum Metal Sheet (thickness 0.1 mm)

P, atm	Solubility			P, atm	Solubility		
	g-atoms of H per g-atom of Nb at 673°	g-atoms H per g-atom Ta			g-atoms of H per g-atom of Nb at 673°	g-atoms H per g-atom Ta	
		at 622°	at 679°			at 622°	at 679°
1	0,126	0,0759	0,0605	100	0,643	0,5118	0,4673
2,5	—	0,15	—	200	—	—	0,5262
3	—	—	0,1540	300	0,690	—	0,5622
5	0,534	—	0,1955	400	—	0,6350	0,5860
10	0,558	—	0,2508	500	0,715	—	0,5870
11,5	—	0,3324	—	550	—	—	0,6056
20	0,593	—	—	600	—	0,6714	—
25	—	0,3950	0,3360	610	0,721	—	—
30	0,595	—	—	750	—	—	0,6110
50	0,620	—	0,3812	800	0,728	—	—
80	—	0,4902	—	1000	0,732	0,7186	—

In order to check this suggestion, a study was made of the Ta – H and Nb – H systems, in which, as is well known, the concentration of hydrogen reaches values corresponding to an atomic ratio of 1 : 1. For a number of reasons the present study was limited to the measurement of the solubility of hydrogen only at high temperatures of 620-680°, at which the equilibrium saturation values are quickly established and at which no hysteresis loops are observed when measurements are made with increase and decrease in the pressure.

The studies were carried out using chemically pure powdered niobium and tantalum metal in the form of a sheet 0.1 mm thick. Both metals were given a preliminary treatment (activation) with hydrogen at a temperature of 700° by alternately raising and lowering the pressure repeatedly between values of 500-600 atmospheres and a value of 1 atmosphere. This process was repeated until the quantity of hydrogen evolved when the pressure was reduced had reached a constant value.

The determination of the solubility of the hydrogen was carried out according to the method used for the

*The experimental part of the work was carried out with A. A. Orlov.

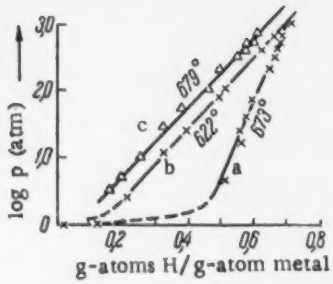

Fig. 1. The relationship between the logarithm of the pressure and the atomic concentration of hydrogen in (a) niobium and (b, c) tantalum.

study of the system Pd–H. The small bombs used for the work were prepared from special chromium–nickel–molybdenum–silicon valve steel, which retains fairly high mechanical properties at a temperature of 700-800°. Three bombs, each with a volume of 15 cc, were used in the experiments. One of the bombs contained 56.790 g niobium, another contained 74.119 g tantalum, while the third contained a copper calibration specimen of the same volume as the niobium or tantalum specimens. As in the case of the studies carried out on the Pd–H system, each experimental point was determined 3-4 times from both directions during the processes of raising and of lowering the pressure. The experimental data obtained are given in Table 1 and Fig. 1.

It can be seen from Fig. 1 that in both the systems studied, as the pressure is raised to values greater than the atmospheric pressure, there is observed at first a comparatively sharp increase in the solubility, which possibly corresponds to the formation of new hydrogen-rich phases, after which there is a slow increase in the solubility according to the logarithmic relationship.

For the Nb–H system, the logarithmic relationship is observed within the concentration range from 0.53 to 0.73 g-atoms H per g-atom Nb. In the Ta–H system, the range over which the logarithmic law is obeyed is more extensive – from 0.2 to 0.72 g-atoms H per g-atom Ta. The absolute values of the solubility at atmospheric pressure in the case of the Ta–H system correspond to the known data of Sieverts and Brunning [2]. The values for the solubility of hydrogen in niobium, which we have obtained under the same conditions, agree with the old measurements of Crüss and Nilson [3] and Bolton [4] and are approximately twice the values obtained more recently by Hagen and Sieverts [5], which is probably related to the difference in the pretreatment of the specimens studied.

For technical reasons we were unable to extend the studies to the region of higher pressures and lower temperatures. However, the analogy with the Pd–H system, for which the logarithmic law holds up to a concentration of 0.92 g-atoms H/g-atom Pd, gives grounds for assuming that further saturation of the Nb and Ta lattice will also take place according to the logarithmic law.

The experimental data obtained seem to us to provide convincing proof of the suggestions put forward at the beginning of the article that the logarithmic relationship is applicable over a wide range of pressures and is characteristic for metal–gas systems in the regions where the lattice is extensively filled.

LITERATURE CITED

[1] P. S. Perminov, A. A. Orlov and A, N. Frumkin, Proc. Acad. Sci. 84, 749 (1952).

[2] A. Sieverts and H. Brünning, Zs. phys. Chem., (A), 174, 365 (1935).

[3] G. Crüss and L. F. Nilson, Ber. 20, 1691 (1887).

[4] W. Bolton, Zs. Elektrochem. 13, 145 (1907).

[5] H. Hagen and A. Sieverts, Zs. anorg. Chem. 185, 225 (1930).

Received February 5, 1958

A CONTRIBUTION TO THE THEORY OF THE TEMPERATURE DEPENDENCE OF THE COORDINATION NUMBERS OF IONS IN AQUEOUS SOLUTIONS

O. Ia. Samoilov

(Presented by Academician I. I. Cherniaev, April 21, 1958)

The mean coordination number of the particles is one of the fundamental quantitative characteristics of a liquid. The coordination number is of great significance in investigating the structures and many of the properties of liquid solutions [1]. The special significance of the coordination number in studies on liquids is due to the fact that its value depends in a large measure on the thermal movement and especially on the translational movement of the particles [2]. This, in particular, gives rise to the large fluctuations in the coordination numbers in liquids [3].

The coordination number of an ion in dilute aqueous solution will be understood as designating the mean number of water molcules composing the immediate neighborhood of the ion. To a considerable degree, the coordination number characterizes the state of the ion in solution. The present work will briefly consider the question of the temperature dependence of the coordination numbers of the particles in liquid solutions, using the aqueous electrolytic solutions by way of example.

The particles of a liquid, and the water molecules in aqueous electrolytic solutions, in particular, are in continual translational motion and continually executing activating jumps and exchanging their nearest neighbors. The observed value of the coordination number results from two opposed processes: there are, on the one hand, activating jumps which lead to the passage of particles out of the immediate neighborhood of the selected individual, and on the other hand, activating jumps which lead to the entrance of particles into the immediate neighborhood of this particle. The first of these processes results in a decrease and the second to an increase in the coordination number. The coordination number of the selected individual is determined by the equilibrium in the exchange of particles which constitute its immediate neighborhood.*

The equilibrium condition can be written down for the case of an aqueous solution of an electrolyte which contains, let us say, ions of the type i. Just as earlier [2], consideration of the coordination numbers will be carried out for the field of dilute solutions and it will be supposed that the immediate neighborhood of the selected individual consists exclusively of water molecules. Let us now select some water molecule and some ion. In terms of their water molecule environment, the equilibrium between these two particles of the solution is naturally characterized by the condition that the number of molecules constituting the immediate neighborhoods of these particles does not change with time, so that the continual interchange does not lead to a displacement of water from the selected ion to the selected water molecule, or inversely. This equilibrium condition can take the form of an equality between the mean number of activating jumps of water molecules (per second, for example) out of the immediate neighborhoods of the selected particles

$$n_i j_i = n j, \tag{1}$$

*In considering the question of the temperature dependence of the coordination numbers, it can be assumed that the activating jumps which occur in the liquid involve only individual particles; for this problem, it is likely that collective displacements are of less significance.

where n_i is the coordination number of the ion, j_i is the mean number of activating jumps per second of the water molecules constituting the immediate neighborhood of the ion, and $\underline{n}$ and $\underline{j}$ are, respectively, the coordination number and the mean number of activating jumps per second of the water molecules in the water. For the quantities $\underline{j}$ and j_i there can be written the relations: $j = j_0 e^{-E/RT}$ and $j_i = j_{0i} e^{-(E+\Delta E)/RT}$, where j_0 and j_{0i} are the coefficients of the exponential terms, and E and E+ΔE are the values of the corresponding potential barriers [2]. Setting these relations into Equation (1), we have $n_i j_{0i} e^{-(E+\Delta E)/RT} = n j_0 e^{-E/RT}$, and from this it follows that

$$\frac{n_i}{n} = \frac{j_0}{j_{0i}} e^{\Delta E/RT}. \tag{2}$$

The relation (2) determines the temperature dependence of $\frac{n_i}{n}$, and of n_i as well, since the temperature dependence of $\underline{n}$ is known from x-ray investigations on water [2]. Differentiating (2) with respect to temperature gives:

$$\frac{d}{dT}\left(\frac{n_i}{n}\right) = -\frac{\Delta E}{RT^2} \frac{j_0}{j_{0i}} e^{\Delta E/RT}. \tag{3}$$

Equation (3) gives the sign of the change in the coordination number of the ion with temperature:

$$\frac{d}{dT}\left(\frac{n_i}{n}\right) > 0, \quad \text{if} \quad \Delta E < 0$$
$$\frac{d}{dT}\left(\frac{n_i}{n}\right) < 0, \quad \text{if} \quad \Delta E > 0.$$

Thus, in conformity with (3), the coordination number must increase with rising temperature for an ion with negative hydration (Δ E < 0), and must decrease for an ion with positive hydration (Δ E > 0) (relative to the coordination number of the water molecule). With rising temperature there must be a transfer of water to or from the ion, depending on the sign of ΔE.

This discussion of the relation between the temperature variation of the coordination numbers and the values of the potential barriers which separate neighboring equilibrium positions of the particles, is general for many types of solutions. A manifestation of this relation is the dissociation of compounds in liquids with rising temperature. According to what has been said, this dissociation amounts in many cases to a displacement, with rising temperature of the liquid particles into a region with lower values of the potential barriers (i.e., into such grouping of particles as is characterized by lower values of the potential barriers).

It follows from Equation (3) in which the square of the absolute temperature enters into the denominator, that the coordination numbers of ions change only slightly with temperature. Only in the case of relatively large values of ΔE can the alteration in the coordination numbers be considerable. It is, however, not to be denied that Equation (3) is only qualitative. In particular, no account has been taken of the variation of ΔE with temperature. Attempts should be made to experimentally determine the temperature dependence of the coordination numbers of ions in aqueous solutions. A comparison of the experimental results with the considerations which have been adduced would, in all likelihood, aid in explaining the mechanism of the thermal motion of the particles in aqueous solutions of electrolytes.

LITERATURE CITED

[1] V. K. Semenchenko, J. Inorg. Chem. 1, No. 6, 1131 (1956).

[2] O. Ia. Samoilov, The Structure of Aqueous Solutions of Electrolytes and the Hydration of Ions (in Russian) Acad. Sci. USSR, Press, 1957.*

[3] V. K. Prokhorenko and I. Z. Fisher, J. Phys. Chem. 31, No. 9, 1245 (1957).

The N. S. Kurnakov Institute of General and Inorganic Chemistry of the Academy of Sciences of the USSR

Received April 3, 1958

* In Russian.

A CONTRIBUTION TO THE DIFFUSION THEORY OF THE KINETICS OF BIMOLECULAR REACTIONS IN SOLUTION

B. Ia. Sveshnikov and L. A. Kuznetsova

(Presented by Academician A. N. Terenin, April 23, 1958)

In 1936, the attempt was made by one of us [1] to explain the relationship existing between the rates of certain bimolecular reactions and the solvent viscosity in terms of the fundamental ideas of the theory of the diffusional quenching of the fluorescence of solutions. By simply assuming the diffusion rate to be the basic factor which fixes the rate of reaction in solution, it was shown to be possible to explain the existence of certain, admittedly rather rare cases, in which there is a linear relation between the reaction rate and the viscosity of the solvent. Without special difficulty, the diffusion theory can also explain the more common situation in which the reaction rate diminishes much more gradually than the fluidity of the solution. For this it is only necessary to take into account the singularity in the distribution of collisions between the molecules of the dissolved materials, or, what amounts to the same thing, to suppose the rate of reaction to depend on the time of interaction of two molecules separated from one another by a fixed distance, i.e., to suppose the decrease in the number of encounters between the dissolved molecules in the viscous medium to be compensated for in this case by an increased effectiveness of each encounter.*

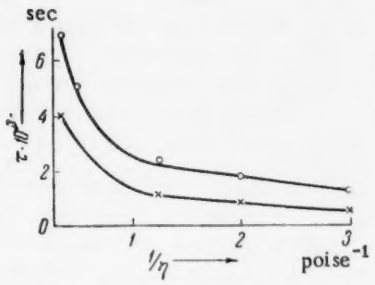

Fig. 1. The persistence of phosphorescence of acridine orange in deaerated and in non-deaerated alcohol-glycerine solutions of various viscosities.

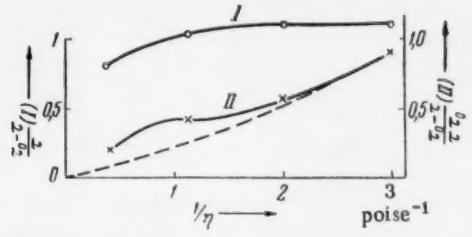

Fig. 2. The effect of the solution viscosity on the quenching of the phosphorescence of acridine orange by oxygen.

However, the case is also possible in which the decrease in the number of encounters per unit time with increasing solution viscosity is compensated for, not only by an increased effectiveness of the encounters, but also by an increase in the duration of the reactive state of the molecules. In such a case, the possibility is not to be excluded that the reaction rate might be independent of the viscosity of the solution, despite the fact that the kinetics of the reaction is largely determined by the diffusion of the dissolved molecules. This effect

*This peculiarity in the distribution of the collisions between the molecules of the dissolved materials, and its significance for the kinetics of bimolecular reactions in solution, has also been noted in the papers of Rabinovich [2], and of Fowler and Slater [3]. These authors introduced the now generally accepted nomenclature of "encounters" and "collisions" (in place of the "primary" and "secondary" collisions of our work).

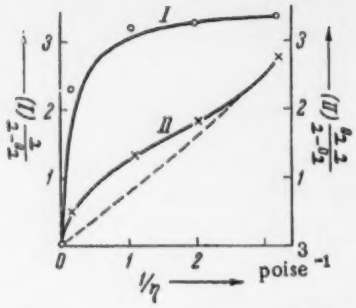

Fig. 3. The effect of the solution viscosity on the quenching of the phosphorescence of acridine orange by potassium iodide.

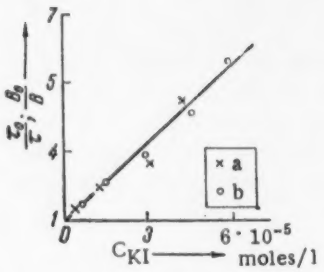

Fig. 4. The dependence of the relative yield (B_0/B), and the persistence of phosphorescence (τ_0/τ) of acridine orange on the concentration of the quencher, a) B_0/B, b) τ_0/τ.

is to be expected, for example, when excited electronic states (singlets or triplets) of the molecule are responsible for the reaction, since the life-times of these states increase with an increase in the solvent viscosity.

In view of the fact that it is the metastable (triplet) states of organic molecules which are responsible, not only for their phosphorescence, but also for their most important chemical and photochemical reactions, we have considered it most expedient to illustrate the above ideas by investigating the quenching by foreign substances of the phosphorescence of liquid solutions of organic compounds. A well-known and convenient subject for such an investigation is a solution of acridine orange, earlier investigations on such solutions having shown that the persistence of phosphorescence increases with increasing viscosity [5] and sharply decreases on the addition of insignificant amounts of such quenchers as analine and hydroquinone [6]. In this work investigation was made of the effect of the viscosity of the solvent on the quenching by potassium iodide and by oxygen* of the phosphorescence of alcohol-glycerine solutions of the above dyestuff. The fundamental characteristic of the quenching was the alteration in the lifetime of the phosphorent state of the molecule; in certain cases, study was also made of the change in the relative phosphorescence yield during quenching.

All of the investigated solutions contained the dye at the fixed concentration of $5 \cdot 10^{-5}$ moles/l. The solution viscosity varied from 0.3 to 5 poises. The highest concentration of potassium iodide was $6 \cdot 10^{-5}$ moles/l.

The apparatus consisted of a super-high pressure mercury lamp, equipped with a stabilizer of the type of V. I. Shirokov [7]; lenses; two filters, one for the adsorption of the thermal radiation, and the other for separating out the 436 mμ mercury line; a two disc phosphoroscope operated from a synchronous motor at 1500 or 2500 rev/sec; a glass cell** with the investigated solution; a photomultiplier tube with a power supply; a cathode follower; and an electron oscillograph of the EO-7 type. In the measurements of the relative yield, this last was replaced by a high-inertia galvanometer.

Through the proper choice of the openings in the discs of the phosphoroscope, a phosphorescence damping curve corresponding to a pronounced alteration in the initial intensity of illumination could be obtained on the oscillograph screen. This curve was copied down and then studied. If certain short segments associated with the opening and closing of the aperture of the phosphoroscope were excluded at the beginning and the end, this curve was approximately exponential. The damping constant for the phosphorescence thus obtained was in good agreement with that obtained through the usual procedure of comparing the intensities of illumination for two positions of the phosphoroscope discs relative to one another.***

With the Becquerel phosphoroscope, the exact determination of the relative phosphorescence yield becomes difficult when the duration of phosphorescence is comparable with the time of rotation of the disc. Account must then be taken of the drop in the intensity of illumination during the time of passage of the disc aperture before the window of the photomultiplier, and consideration given to the possibility that a stationary state may not be reached in the excitation of phosphorescence. Exact calculation for the necessary corrections can be carried out

* We have found that the persistence of the phosphorescence of acridine orange solutions is considerably increased by deaeration.

** This cell was constructed of uviol glass which did not give rise to an afterglow.

*** Here the measurements were carried out with the aid of the inertial galvanometer.

only with difficulty, but in the present case the problem was simplified by the fact that it was not the exact determination of the relative phosphorescence yield itself which was of interest, but the alteration in this relative yield during quenching.

In Fig. 1 there are shown the experimentally determined values of the persistence of the phosphorescent state of deaerated (τ_0) and nondeaerated (τ) solutions of acridine orange and their dependence on the solution fluidity (full curves). On first glancing at these curves, it is difficult to believe that the quenching of phosphorescence by oxygen is due to diffusional processes. But if account is taken of the fact that the diffusional quenching is proportional to the lifetime of the excited state of the molecule, and a graph showing the relation between the quenching and the viscosity is then so constructed that the quenching action is characterized, not by generally accepted quantity $\frac{\tau_0}{\tau}$, but by $\frac{\tau_0 - \tau}{\tau_0 \tau}$, the resulting curve (Fig. 2) is very similar to the well-known curve which relates the phosphorescence yield (duration) and the viscosity of the solvent. A similar curve was obtained in studying the effect of viscosity on the potassium iodide quenching of the phosphorescence of deaerated solutions of this same dyestuff (Fig. 3). Quenching of the phosphorescence was not observed at very high values of the viscosity. Thus, at the temperature of liquid air, the phosphorescence of alcohol-glycerine solutions is quenched according to the same law when there is no potassium iodide present as when it is added to the extent of $6 \cdot 10^{-5}$ moles/l.

The claim that the quenching of the phosphorescence of solutions of acridine orange resembles the quenching the phosphorescence of this dyestuff in that both result from diffusional processes, is in good agreement with the results of a comparison of the alterations in the relative yield, and the persistence, of phosphorescence. From the theory of diffusional quenching [9], it follows that at low concentrations of the quencher and at low effectiveness of the encounters between the quenching, and the excited, molecules (small sphere of action),* the alterations in the yield, and in the duration of the illumination, should be strictly proportional to one another. Figure 4 shows that in the quenching of the phosphorescence of water-glycerine solutions of acridine orange by potassium iodide, the relative yield and the duration of phosphorescence alter similarly.

LITERATURE CITED

[1] B. Ia. Sveshnikov, Proc. Acad. Sci. USSR, 3, 61 (1936).

[2] E. Rabinowitch, Trans. Farad. Soc. 33, 1225 (1937).

[3] R. H. Fowler and N. B. Slater, Trans. Farad. Soc. 34, 81 (1938).

[4] A. N. Terenin, The Photochemistry of Dyestuffs (in Russian) 1947.

[5] B. Ia. Sveshnikov and P. P. Dikun, Proc. Acad. Sci. USSR, 60, 571 (1948).

[6] B. Ia. Sveshnikov and P. P. Dikun, Proc. Acad. Sci. USSR, 60, 791 (1948).

[7] V. I. Shirokov, Bull. Acad. Sci. USSR phys. ser., 10, vol. 5, 605 (1956).

[8] I. M. Frank and S. I. Wawilow, Zs. Phys. 69, 100 (1931); B. Ia. Sveshnikov, Acta Physicochim. URSS, 7, 775 (1937).

[9] L. A. Kuznetsova, B. Ia. Sveshnikov and V. I. Shirokov, Optics and Spectroscopy, 2, vol. 5, 578 (1957).

* A comparison of the concentrations of the quenchers which are required for obtaining a given effect in phosphorescence and in fluorescence, with the lifetimes of the corresponding excited states shows the effectiveness of quenching to be scores, and hundreds, of times greater in the latter case.

THE DIPOLE MOMENTS OF THE HEMIOXANINES OF THE DERIVATIVES OF 3-ETHYLRHODANINE AND 1,3-INDANDIONE

E. A. Shott-L'vova, Corresponding Member, Acad. Sci. USSR,
Ia. K. Syrkin, I. I. L[illegible]koev and M. V. Deichmeister

Applying the heterodyne method to benzene solutions at 25°, dipole moments have been measured for a series of those hemioxanines which contain the 3-ethylrhodanine (I) and the 1,3-indanedione (II) radicals, and differ in the grouping at the nitrogen atom lying outside of the ring, and in the length of the conjugated polymethine chain

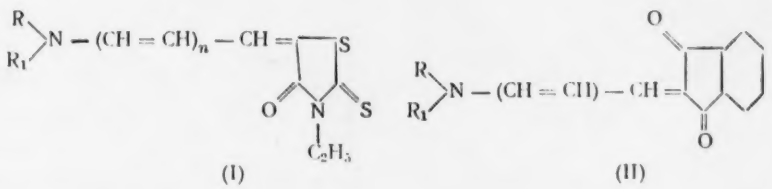

(I) (II)

here R = C_6H_5; R_1 = HCH_3 or CH_3CO; R and R_1 together = $(CH_2)_5$; and n = 0, 1, or 2.

The dyes with the phenylamino- and the phenylacetoamino- groups were prepared by well-known methods [1-5]. The N-piperidine-derivatives were synthesized by treating these compounds with piperidine in alcoholic solution [6]. The methylphenylaminomethylene derivatives were obtained by heating 3-ethylrhodanine, or 1,3-indandione, with ortho-ethyl formate and methyl aniline [7]. These dyes were purified by chromatography on aluminum oxide with subsequent crystallization from ethyl alcohol, and from benzene, and were then dried in vacuum at 70 – 80°.

In Table 1 there are shown in succession the order number, the formula of the compound, the limits of the working concentrations, the total polarization, the electronic polarization, the value of the dipole moment in Debye units, and the position of the absorption maximum (λ_{max}) for alcoholic solutions of the dye as measured on a SF-4 spectrophotometer. The electronic polarizations were determined from the bond refractions. Atomic polarizations were not specifically considered, but this fact could lead to only insignificant variations in the dipole moments since all of the test materials had high orientation polarizations.

In the investigated compounds, the nitrogen lying outside of the ring is joined to three atoms. It is probable, however, that the configuration here is not pyramidal, but planar, as is the case in urea, acetamide, and other compounds, in which the nitrogen is predominantly postively charged (with sp^2 – hybridization and the formation of three σ-, and one π-bond) [8]. The method of dipole moments is inadequate, however, for a unique determination of the configuration.

The data show that compounds differing only in the length of the polymethine chain have markedly different moments. Increasing the number of double bonds between the polar radicals $>C=O$ and $-N<^{R}_{R_1}$ invariably leads to an increase in the moment. Clearly, this is due not only to a change in the configuration, but

TABLE 1

Compound No.	Formula	Mole fraction, f	P_{total}	P_{elec}	Dipole moment $\mu \cdot 10^{18}$ (D)	Max. absorption in C_2H_5OH (mμ)
1	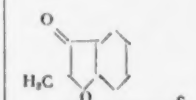 1,3-Indandione	0,00063 0,00325	192,4	38,2	2,72	—
2	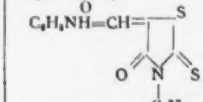	0,00050 0,00062	453,6	74,5	4,27	413
3	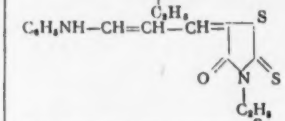	0,00011 0,00019	794,5	82,9	5,85	483
4	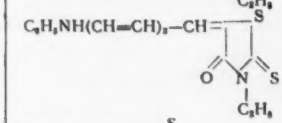	0,000091 0,000094	913,3	91,7	6,28	538
5	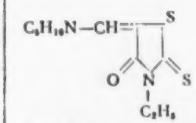	0,00041 0,00138	877,6	71,2	6,23	390
6	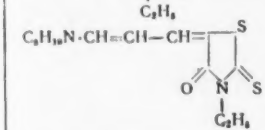	0,00057 0,00088	1470,3	80	8,17	467
7	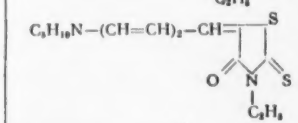	0,00017 0,00031	1770,2	88,8	9,00	553
8	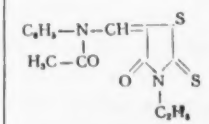	0,00099 0,00307	484,2	83,7	4,39	370
9	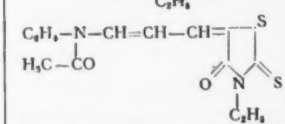	0,00041 0,00055	626,2	92,5	5,06	405
10	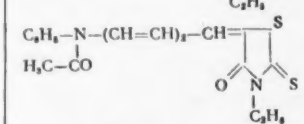	0,00029 0,00094	718,5	101,3	5,44	437
11	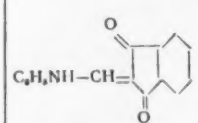	0,00059 0,00132	189,6	70,2	2,40	366
12*	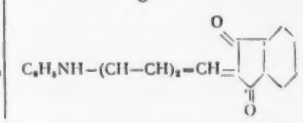	0,000028 0,00003	915,7	87,7	6,31	568

TABLE 1 (continued)

Compound No.	Formula	Mole fraction, f	P_{total}	P_{elec}	Dipole moment $\mu \cdot 10^{18}$ (D)	Max. absorption in C_2H_5OH (mμ)
13	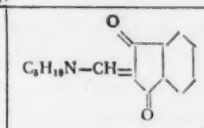	0,00035 0,00092	316,1	67,2	3,46	338
14	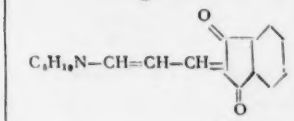	0,00016 0,00061	897	76	6,28	432
15	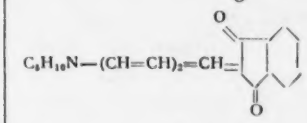	0,00024 0,00034	1289,8	84,8	7,61	535
16	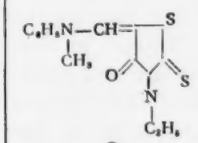	0,00092 0,00277	661,1	79,1	5,29	395
17	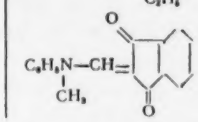	0,00095 0,00124	217,4	75,1	2,62	353

* 2-γ -phenylaminoallylidine indandione(1,3)is very sparingly soluble in benzene. In ethyl alcohol, the maximum absorption of the compound is at 470 mμ. In the earlier work [5] there is a misprint.

also to a rise in the total polarity resulting from the lengthing of the polymethine chain. On introducing one vinylene group, the moment increases to a greater extent than is the case with the introduction of a second such group [9]. This indicates that in these compounds, the conjugation between the oxygen and the extra-ring nitrogen continually diminishes as the polymethine chain is lengthened [4, 10, 11]. Both the magnitude of the change of the moment, and the extent of the decrease in this change, depend on the structures of the radicals from the amine and the ketomethylene compound. These values are much larger with the hemioxanine containing the piperidine radical than with those which contain the phenylamino group (in Table 1, compare Nos. 5, 6, 7, with 2, 3, 4; and 13, 14, 15 with 11 and 12). This is due to the decreased basicity of the nitrogen of the phenylamino group which results from its conjugation with the benzene ring, the electronic displacements from the nitrogen to the carbonyl group being diminished in compounds containing this group. We will compare the dyes which are derivatives of 3-ethylrhodanine and contain the aniline and piperidine radicals. In the case of the methylene derivatives (Nos. 2 and 5) the difference between the moments is equal to 1.96 D. With the allylidene derivatives (Nos. 3 and 6) this difference is 2.32 D, and in the case of the pentadienylidene derivatives (Nos. 4 and 7) it is 2.72 D. Thus in passing from one to two double bonds in the external chain, the difference increases by 0.36, and in passing from two to three double bonds it increases by 0.40, i.e., the difference increases almost linearly with the length of the polymethine chain. In compounds containing the phenylacetoamino group (Nos. 8, 9, 10), the moment increases to a smaller extent on lengthening the polymethine chain. This is due to the fact that the nitrogen atom is conjugated, not only with the benzene ring, but also with the oxygen atom of the acetyl group. As a result, the conjugation through the polymethine chain is diminished.

Although the moment of 1,3 indandione, 2.72 D, is larger than that of 3-ethylrhodanine, 1.75 D [12], the moments are considerably less in the monomethinehemioxanine which are derivatives of the first of these

compounds. This is clearly related to the different directions of the moment vectors in 3-ethylrhodanine and in 1,3-indandione. Calculations are rendered difficult by the absence of data on the spatial configurations of these compounds. However, on lengthening the chain, the values of the moments of the hemioxanine of the derivatives of 1,3-indandione increases considerably more than those of the derivatives of 3-ethylrhodanine. Thus by introducing two vinylene groups into the chain of the dyes with aniline radicals, the increase in the moment is 3.91 D in the first case and only 2.01 D in the second case, whereas with the compounds containing the piperidine radical these increases are, respectively 4.15 and 2.77 D. These data show the electron acceptor properties of the 1,3-indandione radical to be much more pronounced than those of the 3-ethylrhodanine radical [5, 11]. However, even with the derivatives of 1,3-indandione, the conjugation of the nitrogen and oxygen atoms diminishes as the chain is lengthened, so that the introduction of the first vinylene group into 2-piperidylmethylenindandione (1,3) increases the moment by 2.82 D whereas a second group increases it by only 1.33 D.

The changes which result in the absorption spectra of the investigated hemioxanine on increasing the length of the polymethine chain are consistent with those conclusions concerning structures which have been drawn from a consideration of the dipole moments. So, on increasing the chain length, the color depth of compounds containing the acetylphenylamino group is rather slightly increased (by 35 and 32 mμ per vinylene group) and the moment also alters only insignificantly. The largest displacement of the absorption maximum on the introduction of vinylene groups (94-104 mμ) is met with the derivatives of 1,3-indandione which at the same time show an especially marked increase in the moment. In the case of the phenylamino derivatives of 3-ethylrhodanine, the introduction of vinylene groups exerts a greater effect on the displacement of the maximum, and on the change in the moment, than does the introduction of a second group of this same type (70 and 55 mμ; 1.58 and 0.43 mμ). As compared with the introduction of the first vinylene group into the dyes with the piperidine radical, the increase in the bathochromic displacement of the absorption maximum on introducing the second vinylene group into the chain can possibly be explained by the fact that in alcoholic solutions, the structures of the mono- and trimethine compounds of this series are close to the intra-ionic structures. In the less polar pentamethine derivatives there is under the same conditions a more uniform distribution of the electron density in the chromophore, which leads, as in the case of the other intra-ionic dyes, to a displacement of the absorption maximum into the region of long wavelengths [5, 11, 13].

It is interesting to compare the moments of compounds Nos. 2 and 16. In dye No. 16, an intramolecular hydrogen bonding is impossible. In compound No. 2, the hydrogen atom on the nitrogen can give hydrogen bonding with the oxygen of the rhodanine radical, a stable 6-membered ring being thereby formed. The presence of the hydrogen bonding stabilizes one of the spatial configurations.

LITERATURE CITED

[1] Kodak, Ltd. Brit. Pat. 470725, 479970; Chem. Zbl. 2, 4002 (1937); 2, 4271 (1938), Kodak Pathé, French Pat. 49385; Chem. Zbl. 2, 3522 (1939).

[2] I. I. Levkoev, N. N. Sveshnikov and L. V. Rozvadovskaia, USSR Patent 68789.

[3] F. M. Hamer and B. S. Winton, J. Chem. Soc. 1949, 1126.

[4] M. V. Deichmeister, Dissertation, Moscow, 1951; M. V. Deichmeister, Z. P. Sytnik and E. B. Lifshits, J. Gen. Chem. 22, 166 (1952);* M. V. Deichmeister, I. I. Levkoev and E. B. Lifshits, J. Gen. Chem. 23, 1529 (1953).*

[5] V. G. Zhiriakov and I. I. Levkoev, J. Gen. Chem. 24, 710 (1954).*

[6] Kodak Pathé, French Pat. 841632; Chem. Zbl. 2, 3523 (1939).

[7] Fabwerke Hoechst, Pat. FRG** 834104; Chem. Zbl. 7942 (1953).

[8] R. J. Kurland, J. Chem. Phys. 23, 2202 (1955).

[9] L. G. S. Brooker and F. L. White, et al., J. Am. Chem. Soc. 63, 3192 (1941).

[10] L. G. S. Brooker, Frontiers in Chem. N. Y. 3, 63 (1945).

*Original Russian pagination. See C. B. Translation.

**Federal Republic of Germany.

[11] L. G. S. Brooker and G. H. Keyes, et al., J. Am. Chem. Soc. 73, 5332 (1951).

[12] E. A. Shott-L'vova, Ia. K. Syrkin, I. I. Levkoev and Z. P. Sytnik, Proc. Acad. Sci. USSR, 116, 804 (1957).•

[13] A. I. Kiprianov and V. E. Petrun'kin, J. Gen. Chem. 10, 613 (1940); A. I. Kiprianov and E. S. Timoshenko, Ukraine Chem. J. 18, 347 (1952); I. I. Levkoev, N. N. Sveshnikov and E. V. Lifshits, Proc. Acad. Sci USSR, 74, 275 (1950).

Received May 9, 1958

•Original Russian pagination. See C. B. Translation.

SIGNIFICANCE OF ABBREVIATIONS MOST FREQUENTLY ENCOUNTERED IN SOVIET PERIODICALS

FIAN	Phys. Inst. Acad. Sci. USSR.
GDI	Water Power Inst.
GITI	State Sci.-Tech. Press
GITTL	State Tech. and Theor. Lit. Press
GONTI	State United Sci.-Tech. Press
Gosenergoizdat	State Power Press
Goskhimizdat	State Chem. Press
GOST	All-Union State Standard
GTTI	State Tech. and Theor. Lit. Press
IL	Foreign Lit. Press
ISN (Izd. Sov. Nauk)	Soviet Science Press
Izd. AN SSSR	Acad. Sci. USSR Press
Izd. MGU	Moscow State Univ. Press
LEIIZhT	Leningrad Power Inst. of Railroad Engineering
LET	Leningrad Elec. Engr. School
LETI	Leningrad Electrotechnical Inst.
LETIIZhT	Leningrad Electrical Engineering Research Inst. of Railroad Engr.
Mashgiz	State Sci.-Tech. Press for Machine Construction Lit.
MEP	Ministry of Electrical Industry
MES	Ministry of Electrical Power Plants
MESEP	Ministry of Electrical Power Plants and the Electrical Industry
MGU	Moscow State Univ.
MKhTI	Moscow Inst. Chem. Tech.
MOPI	Moscow Regional Pedagogical Inst.
MSP	Ministry of Industrial Construction
NII ZVUKSZAPIOI	Scientific Research Inst. of Sound Recording
NIKFI	Sci. Inst. of Modern Motion Picture Photography
ONTI	United Sci.-Tech. Press
OTI	Division of Technical Information
OTN	Div. Tech. Sci.
Stroiizdat	Construction Press
TOE	Association of Power Engineers
TsKTI	Central Research Inst. for Boilers and Turbines
TsNIEL	Central Scientific Research Elec. Engr. Lab.
TsNIEL-MES	Central Scientific Research Elec. Engr. Lab.– Ministry of Electric Power Plants
TsVTI	Central Office of Economic Information
UF	Ural Branch
VIESKh	All-Union Inst. of Rural Elec. Power Stations
VNIIM	All-Union Scientific Research Inst. of Meteorology
VNIIZhDT	All-Union Scientific Research Inst. of Railroad Engineering
VTI	All-Union Thermotech. Inst.
VZEI	All-Union Power Correspondence Inst.

Note: Abbreviations not on this list and not explained in the translation have been transliterated, no further information about their significance being available to us. – Publisher.